IDENTIFYING THE IMPORTANCE OF PHOSPHORYLATION OF SNAP-25 AT SER187 IN PROTEIN KINASE C-MEDIATED ENHANCEMENT OF EXOCYTOSIS

A Dissertation

Presented to

The Faculty of the Graduate School

University of Missouri-Columbia

In Partial Fulfillment

Of the Requirements for the Degree

Doctor of Philosophy

---

by

YILONG SHU

Dr. Kevin D. Gillis, Dissertation Supervisor

MAY 2007

The undersigned, approved by the Dean of the Graduate School, have examined the thesis entitled

IDENTIFYING THE IMPORTANCE OF PHOSPHORYLATION OF SNAP-25 AT SER187 IN PROTEIN KINASE C-MEDIATED ENHANCEMENT OF EXOCYTOSIS

presented by Yilong Shu

a candidate for the degree of Doctor of Philosophy

and hereby certify that in their opinion it is worthy of acceptance

Andrew G. McClellan, PhD

Tzyh-chang Hwang, MD PhD

Mark A. Milanick, PhD

Mark D. Kirk, PhD

Kevin D. Gillis, DSc

Acknowledgements

First of all, I would like to thank my advisor, Dr. Kevin Gillis, with all my gratitude and admiration. It is Dr. Gillis who gave me the great opportunity to accomplish my Ph.D study in his laboratory. It is also Dr. Gillis who led me into the field of Electrophysiology. I cannot appreciate Dr. Gillis sufficient not only as a great academic mentor for his guidance, inspiration and encouragement, but also as a great friend for his willingness of help, kindness and patience. I am very glad to have this chance to work with Dr. Gillis.

I appreciate the members of my dissertation committee, Drs. Tzyh-Chang Hwang, Adrew McClellan, Mark Milanick and Mark Kirk for their valuable guidance, encouragement, comments and suggestions. I specially thank Dr. Milanick and Min Li from Dr. Hwang's laboratory for their great technical supports during my research.

I also thank all other lab members, particularly Dr. Yang Yan, who taught me the experimental techniques from the scratch. Melton Vanessa, who helped me a lot with the molecular work and cell culture. I thank Xiaohui Chen, Won-chul Shin and Meghana Honnati for their kind help, inspiring talks and suggestions.

My deepest appreciation goes to my parents, Shu Zhongjin and Jiang Zhongfang, and my brother, Shu Gang for their dedication and supporting me for

so long time. I also thank my girlfriend, Xiao Tong, for her great help, understanding and encouragement during my study.

TABLE OF CONTENTS

LIST OF FIGURES

FIGURE **PAGE**

LIST OF TABLES

TABLE **PAGE**

IDENTIFYING THE IMPORTANCE OF PHOSPHORYLATION OF SNAP-25 AT SER187 IN PROTEIN KINASE C-MEDIATED ENHANCEMENT OF EXOCYTOSIS

Yilong Shu

Dr. Kevin D. Gillis, Dissertation Supervisor

ABSTRACT

Protein Kinase C (PKC) activation has been shown to enhance exocytosis in various studies. However, the molecular mechanism for PKC to promote exocytosis is still elusive. A possible target of PKC is SNAP-25 (25 kDa synaptosome-associated protein), which is a key member of the SNARE (soluble *N*-ethylmaleimide-sensitive fusion protein attachment protein receptor) core complex that is essential for exocytosis. Both *in vitro* and *in vivo* experiments demonstrate that activation of PKC results in phosphorylation of SNAP-25 at Ser187. However, the importance of SNAP-25 phosphorylation at Ser187 in PKC-mediated enhancement of exocytosis has not been fully studied. Here, I investigated the importance of SNAP-25 phosphorylation at Ser187 upon activation of PKC by a phorbol ester to stimulate exocytosis in rat insulin-secreting

INS-1 cells. With the transfection of botulinium toxin E (BoNT/E) to disable the endogenous SNAP-25, my results show that SNAP-25 phosphorylation at Ser187 is important for phorbol ester-enhanced exocytosis. However, my results also indicate that SNAP-25 phosphorylation at Ser187 is not the only mechanism involved in phorbol ester-enhanced exocytosis at high $[Ca^{2+}]_i$. This work helps clarify the molecular mechanisms by which phorbol ester and PKC enhance exocytosis. It also contributes to our understanding of the role of SNAP-25 in exocytosis.

CHAPTER 1

INTRODUCTION

Neurotransmitter release from neurons and hormone release from endocrine cells are mediated by a process called exocytosis, which is defined as the fusion of an intracellular trafficking vesicle with the plasma membrane (Jahn, Lang et al. 2003). Exocytosis is a highly conserved process which can be found in various species from bacteria to human. There are two classes of exocytosis, constitutive exocytosis and regulated exocytosis (Kelly 1985). Constitutive exocytosis refers to constant and unregulated vesicle fusion. Thus, this process is not believed to be initiated by specific extracellular or intracellular signals. On the other hand, vesicle release by the regulated exocytosis pathway is “on demand”. Many specific signals, typically second messengers such as Ca^{2+}, cAMP, cGMP, diacylglycerol (DAG), etc, play vital roles in regulating this process. Constitutive exocytosis is thought to provide a continuous maintenance of plasma membrane lipids and proteins and the extracellular environment. However, regulated exocytosis has multiple functions, such as the release of neurotransmitters,

hormones, enzymes and cytokines, etc, as well as controlling the levels of different lipids, receptors and transporters in the plasma membrane (Lin and Scheller 2000). These important activities of regulated exocytosis shape the developing organism, induce and maintain tissues, send signals through the organism and processes and store information (Sollner 2003).

Within the last 50 years, the most extensively studied case of regulated exocytosis is chemical synaptic transmission, the major pathway for cell-to-cell communication in the nervous system. There are several steps including synthesis, docking, priming and fusion involved in the process of exocytosis of synaptic vesicles (figure 1.1). The lipids and membrane proteins are synthesized in the endoplasmic reticulum and then modified in the Golgi apparatus in the soma of neurons. The vesicles are then assembled. Neurotransmitters of neuropetides are also loaded into vesicles at this point. These vesicles will then be transported to the presynaptic terminals, where the small molecular neurotransmitters such as amines are loaded by the specific neurotransmitter transporters locally. The vesicles are then moved close to the plasma membrane and become “docked”. An ATP-dependent process called “priming” makes these docked vesicles competent for release. Once the vesicles receive the trigger signal for releasing, which is an increase in intracellular $[Ca^{2+}]_i$ in excitable cells, the vesicles fuse with the plasma membrane and release neurotransmitters to the outside of the cell. Following exocytosis, the vesicle membrane is recycled

through a process called “endocytosis” for another round of release.

Figure 1.1: The cycle of synaptic vesicles in presynaptic terminal (from figure 5.7D, Neuroscience, 2nd edition, 2001).

There is another type of exocytosis called “kiss-and-run”, in which the vesicles only fuse with the plasma membrane temporarily to allow partial release of the vesicle contents. The vesicles then pinch off the plasma membrane quickly and get reloaded with the vesicle contents locally for another round of release (more details in review by Harata, Aravanis et al. 2006).

1.1 Measurement of membrane capacitance in the whole-cell patch clamp configuration to assay exocytosis

Exocytosis can be assayed with different methods depending on the cell preparation. Three popular techniques are: (1) In neuronal preparations, neurotransmitter release from the presynaptic terminal can be monitored by measuring postsynaptic responses such as the EPSP or EPSC (Excitatory Postsynaptic Potential or Excitatory Postsynaptic Current) or the IPSP or IPSC (Inhibitory Postsynaptic Potential or Inhibitory Postsynaptic Current) (Fatt and Katz 1952; Katz 1969). (2) In cells with a simple electrical equivalent circuit, e.g., dissociated neuroendocrine cells, membrane capacitance measurements using patch-clamp techniques can be used to monitor exocytosis (Gillis 1995). (3) Electrochemical methods such as carbon fiber amperometry can be applied to cells secreting oxidizable materials (see chapter 5 for more details) (Chow and Ruden 1995). In this study, I used a neuroendocrine cell, rat Insuling-secreting INS-1 cell (Asfari, Janjic et al. 1992). Capacitance measurement is the primary method utilized in this thesis to monitor exocytosis.

Even though patch-clamp techniques were originally developed to study ion channels (Neher and Sakmann 1976; Neher, Sakmann et al. 1978), they are also powerful tools to study exocytosis. Figure 1.2A illustrates the “on-cell” patch-clamp configuration. A glass pipette with fire-polished tip (1 - 2 μm in diameter) is touched to the surface of the cell. Usually a suction force is applied through the pipette to form an electrical and mechanical giga-ohm seal between the pipette tip and the cell membrane (Sigworth and Neher 1980). This “giga-seal”

results in low background noise. The “whole-cell” patch-clamp configuration is achieved by rupturing the patch of membrane under the pipette tip (figure 1.2B). Thus, soluble components of the cell, such as ions and ATP, are exchanging with the pipette solution via dialysis. This allows us to control the intracellular environment by delivering materials such as drugs and Ca^{2+} dyes into the cell.

A. **B.**

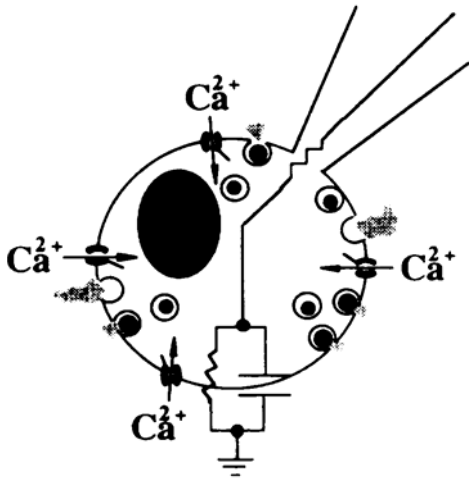

Figure 1.2: Capacitance measurement to assay exocytosis. (A), configuration of patch clamp (after Neher 1992; Sakmann 1992). (B), configuration of whole-cell patch clamp.

Exocytosis can be assayed by monitoring the change in the membrane capacitance (Neher and Marty 1982; Gillis 1995). Membrane capacitance is calculated by measuring the current resulting from a ~ 1 KHz sine wave voltage stimulus applied to the cell (Gillis 1995). In a parallel plate capacitor, the capacitance is proportional to the surface area according to the equation $C=\varepsilon_0 A/d$, where C is capacitance, A is the area of the plate, ε_0 is the dielectric constant, and

d is the distance between the conducting plates. Applying this equation to the cell membrane indicates a specific capacitance (C_m) of ~1 μF/cm^2 (Cole 1968). The fusion of vesicles with the cell membrane increases the plasma membrane surface area and therefore results in an increase in C_m (ΔC_m). One problem with this method is the interference of endocytosis, which results in a decrease in C_m as membrane is internalized into the cell. Thus, the final capacitance change with the whole-cell patch clamp is the net result of exocytosis and endocytosis. However, measurement of membrane capacitance is still powerful to assay exocytosis with high resolution since endocytosis is usually much slower than exocytosis (Gillis 1995) and endocytosis is inhibited in the whole-cell configuration (Smith and Neher 1997).

1.2 Photorelease of caged-Ca^{2+} to study the Ca^{2+}-dependence of exocytosis

As mentioned previously, vesicle fusion with the plasma membrane in the regulated exocytosis is triggered predominantly by Ca^{2+} in excitable cells. The elevation of intracellular Ca^{2+} is triggered by receptor activation or membrane depolarization (Douglas 1968; Katz 1969; Burgess and Kelly 1987). In neuron and other excitable cells, Ca^{2+} influx through the voltage-gated Ca^{2+} channels opened by depolarization is the major source to trigger exocytosis (Augustine, Charlton et

al. 1987). Other Ca^{2+} sources may also contribute to the intracellular $[Ca^{2+}]_i$ elevation, such as ligand-gated ion channel-mediated Ca^{2+} influx (Mollard, Seward et al. 1995; Gray, Rajan et al. 1996) or Ca^{2+} release from intracellular stores (ER and mitochondria) (Berridge 1998). Ca^{2+} not only serves as the trigger for exocytosis, but also plays important roles in other processes such as vesicle priming (Bittner and Holz 1992; Smith, Moser et al. 1998; Dinkelacker, Voets et al. 2000). Thus methods to control and measure $[Ca^{2+}]_i$ are important to study exocytosis.

The spatial distribution of $[Ca^{2+}]_i$ resulting from influx through voltage-gated Ca^{2+}channel is complex (Pumplin, Reese et al. 1981; Roberts, Jacobs et al. 1990; Robitaille, Adler et al. 1990; Bennett, Calakos et al. 1992; Burns and Augustine 1995). Figure 1.3 illustrates the spatio-temporal dynamics of $[Ca^{2+}]$ in the cell caused by the Ca^{2+} influx through the Ca^{2+} channel. In the vicinity of the Ca^{2+} channel, $[Ca^{2+}]$ forms a local microdomain and is high enough to trigger exocytosis of nearby vesicles. $[Ca^{2+}]_i$ is estimated to be around 100 μM at a 20 nm distance from a Ca^{2+} channel. $[Ca^{2+}]$ decreases to about 5 μM at the place 200nm from the Ca^{2+} channel (Neher 1998). Therefore, the vesicles are exposed to different values of $[Ca^{2+}]$, which imposes difficulties in studying the Ca^{2+}-dependence of exocytosis precisely. Over the last decade, photorelease of caged-Ca^{2+} [primarily DM-Nitrophen and Nitrophenyl-EGTA (NP-EGTA), (Ellis-Davies, Kaplan et al. 1996)] has been successfully applied in different

systems to resolve this problem (Neher and Zucker 1993; Thomas, Wong et al. 1993; Heidelberger, Heinemann et al. 1994; Heinemann, Chow et al. 1994; Eliasson, Renstrom et al. 1997; Yang, Udayasankar et al. 2002; Yang and Gillis 2004) (figure 1.4). This method elevates $[Ca^{2+}]_i$ uniformly throughout the cell in a very short time (usually within 1 ms). Therefore, all the vesicles are exposed to the same $[Ca^{2+}]_i$, which makes it possible to directly probe the relationship between $[Ca^{2+}]_i$ and exocytosis.

Figure 1.3: Dynamics of Ca^{2+} distribution following the Ca^{2+} influx through the Ca^{2+} channel (from figure 1, Neher E, Neuron, 1998).

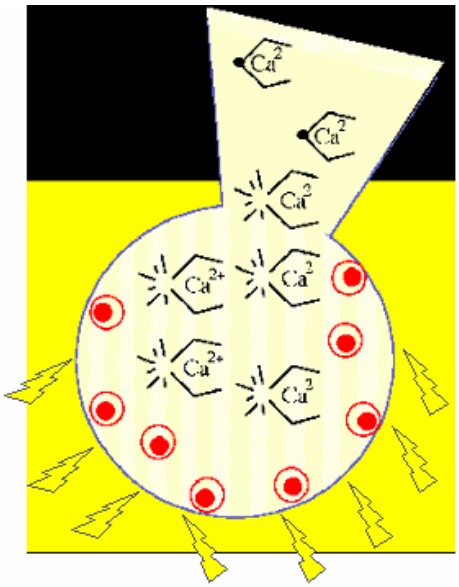

Figure1.4: Schematic demonstration of caged-Ca^{2+} experiment. The caged-Ca^{2+} and Ca^{2+} fluorescent dyes are delivered into cells through the patch clamp pipette. Usually the UV flash is limited to the cell body.

1.3 The dynamics of exocytosis reveals multiple vesicle "pools"

Many studies performed in diverse cell preparations show exocytosis proceeds with multiple kinetic components upon stimulation, upon photoelevation of Ca^{2+}, typically. There is an initial burst followed by much slower phases of secretion interpreted as the combined sequence of mobilization and release of secretory granules (Neher and Zucker 1993; Thomas, Wong et al. 1993; Heinemann, Chow et al. 1994; Eliasson, Renstrom et al. 1997). Figure 1.5 depicts such an experiment performed in bovine adrenal chromaffin cells with the

Figure 1.5: A typical capacitance trace (Middle trace) induced by photorelease of caged-Ca^{2+} (upper trace) in bovine adrenal chromaffin cells. The corresponding vesicle pools for each component of the capacitance trace are also demonstrated in the right part. The cytosolic [Ca^{2+}] was elevated from a basal level of about 300 nM to 20 μM. The amperometric signal measured with a carbon fiber electrode is also present (bottom trace) (after figure 1, Rettig and Neher, Science, 2002).

photorelease of caged-Ca^{2+}(Rettig and Neher 2002). An interesting observation is that the rate of release (slope of Cm curve) declines despite the continuous elevation of $[Ca^{2+}]_i$. The usual explanation for the declining rate is depletion of a release-ready pool of vesicles. If $[Ca^{2+}]_i$ is elevated to levels of ~20 μM, close examination of the time course of release reveals at least three kinetic components. Immediately following flash elevation of $[Ca^{2+}]_i$, there is a fast burst,

which may reflect exocytosis of the vesicles already primed for release. This component is believed to result from depletion of a “readily releasable pool" (RRP) of vesicles. The second slow component is attributed to a "slowly releasable pool" (SRP) of vesicles. The third phase of release is an approximately constant “sustained component” which is believed to correspond to a refilling step where vesicles are released as soon as they are mobilized into the SRP or RRP (Rettig and Neher 2002).

A quantitative analysis of putative pool release dynamics can be made by fitting the capacitance trace with a sum of exponentials according to the following equation. Usually, the capacitance of the RRP and the SRP can be fitted with exponentials. The release of the sustained component is too slow to be considered as an exponential process (figure 1.6):

$$C_{m(t)}=C_{m,0} + A_1(1-e^{k_1 t}) + A_2(1-e^{k_2 t}) + A_3 t$$

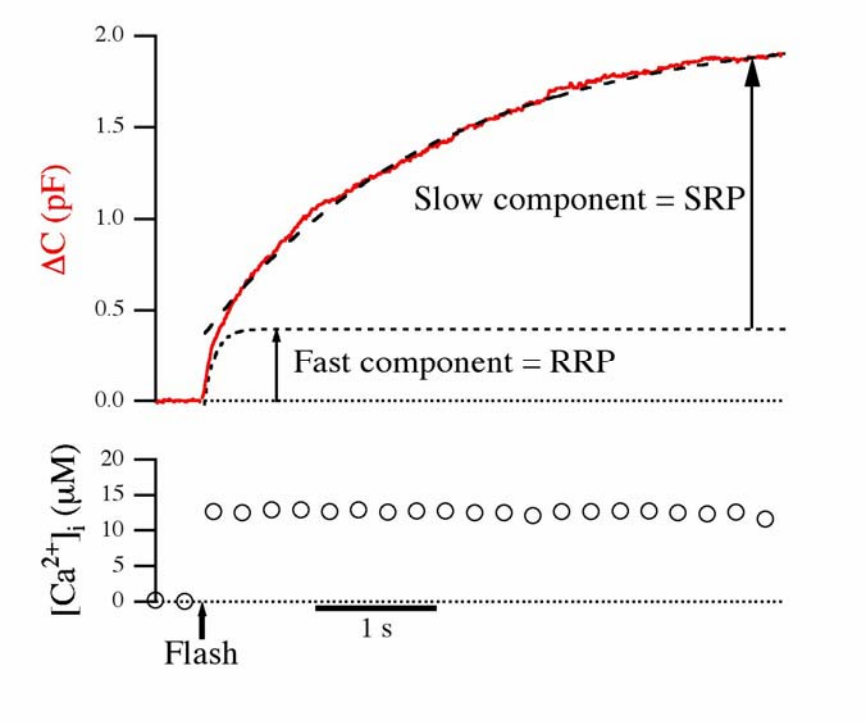

Figure 1.6: Analysis of capacitance trace with e*xponential fits*. *Only the fits of the RRP and the SRP are shown here.*

The amplitude ($A_1$and A_2) of the exponential components indicates the size of the vesicle pool. A_3 is the size of the sustained component which may be calculated by subtracting the RRP and the SRP from the whole release. The rate constants of the exponential function (K_1 and K_2, inverse of time constants) are the Ca^{2+}-dependent rates of exocytosis. Many studies have shown that these rate constants are strongly dependent on the concentration of Ca^{2+} reached after the flash (Thomas, Wong et al. 1993; Heinemann, Chow et al. 1994; Voets 2000), confirming that the burst represents Ca^{2+}-dependent triggering of release. On the

other hand, the amplitude of the responses (A1 and A2) are not strong functions of post-flash $[Ca^{2+}]_i$, supporting the pool depletion hypothesis. For example, even though post-flash $[Ca^{2+}]_i$, varies, the amplitude of the RRP does not change too much (Rettig and Neher 2002).

In neuronal preparations, a similar exocytotic response pattern was also observed: a fast component that is synchronous with the action potential accounts for >90% of total release, and a slow component asynchronous with the action potential mediates <10% of total release (Geppert, Goda et al. 1994; Goda and Stevens 1994; Atluri and Regehr 1998). Both components exhibit a high degree of Ca^{2+} cooperativity but different Ca^{2+} affinities (Dodge and Rahamimoff 1967; Goda and Stevens 1994). This phenomenon is observed in a number of synapses (Hessler, Shirke et al. 1993; Rosenmund, Clements et al. 1993; Dobrunz and Stevens 1997; Murthy, Sejnowski et al. 1997).

This complex kinetics of exocytosis indicates that vesicles exist in at least several discrete states of fusion competence. Actually, the concept of functionally distinct vesicle pools emerged soon after formulation of the quantal release hypothesis (Del Castillo and Katz 1954; Neher 1998). Heterogeneous release probability is a property of both synaptic transmission and secretion of hormones of neuroendocrine cells. Other than the two pools (RRP and SRP) described above, several others have been identified such as Immediately Releasable Pool (IRP) and Reserve Pool (RP)(for more detailed information, see review by (Rizzoli

and Betz 2005). Many studies have been quite successful in associating short term plastic changes, such as paired pulse facilitation, frequency facilitation, or depression with these pools (Zucker 1996; Neher 1998).

1.4 A Highly Ca^{2+}-Senstive Pool of vesicles (HCSP)

Most previous studies focused on the exocytotic response at high $[Ca^{2+}]_i$. At neuronal synapses, high $[Ca^{2+}]_i$ has been shown to be required to trigger fast exocytosis. For example, in experiments using photorelease of caged-Ca^{2+}, $[Ca^{2+}]_i$ needs reach levels of ~50μM to trigger exocytosis at similar rates achieved by depolarization in goldsfish retinal bipolar neurons and the crayfish neuromuscular junction (Heidelberger, Heinemann et al. 1994; Lando and Zucker 1994). However, exocytosis evoked by low $[Ca^{2+}]_i$ levels such as less than several μM is not as well studied. Exocytosis triggered by low μM levels of $[Ca^{2+}]_i$ occurs in cells under a variety of conditions, such as during spontaneous vesicle release, from vesicles located at a distance from Ca^{2+} channel, and release due to Ca^{2+} release from intracellular Ca^{2+} stores, etc. Understanding the kinetics of exocytosis evoked by low $[Ca^{2+}]_i$ levels is particularly helpful in understanding the secretion of vesicles under these conditions.

In 2002, using photorelease of caged-Ca^{2+} to elevate $[Ca^{2+}]_i$ to several μM level in bovine adrenal chromaffin cells, a highly Ca^{2+}-sensitive pool (HCSP) of

vesicles was first reported (Yang, Udayasankar et al. 2002) (figure 1.7). The characteristics of the HCSP are a small size (about 25 fF measured by change in membrane capacitance, approximately equal to a dozen vesicles) and lower triggering $[Ca^{2+}]_i$ required (lower than 10 μM). This HCSP is particularly sensitive

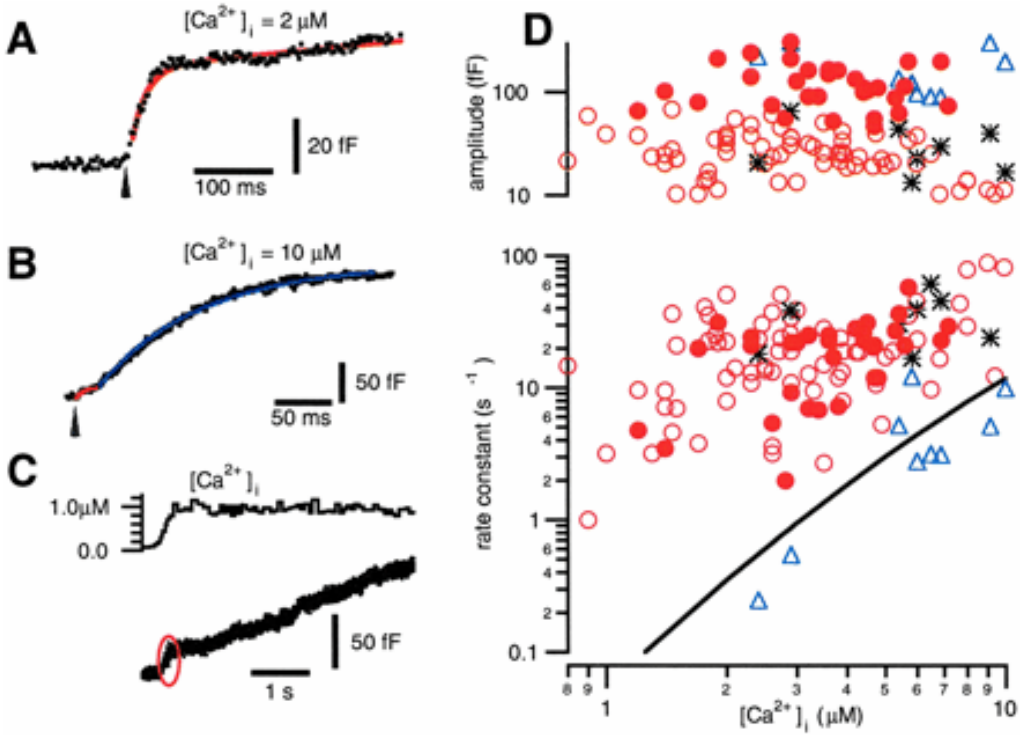

Figure 1.7: Photorelease of caged-Ca^{2+} to several μM to elicit the HCSP in bovine adrenal chromaffin cells. (A), (B) and (C), Three sample traces from three different cells. The HCSP are marked with red lines or circle. (D), The rate constants and amplitudes of the HCSP obtained from exponential fits are plotted against the $[Ca^{2+}]_i$ that follows photorelease of caged-Ca^{2+}. Unfilled circles are from single-exponential fits of the HCSP. The triangles and asterisks represent the slow and fast components, respectively, of double exponential fits to the data. The solid line is the rate constant of release for the RRP from the model in a previous study (Voets 2000) (from figure 1, Yang Y et al., PNAS, 2002)

to the modulation by intracellular signaling molecules such as protein kinase C (PKC) and protein kinase A (PKA), both of which are well known to modulate the RRP. The inhibition of the HCSP by overexpression of truncated SNAP-25 (a dominant-negative form of a “SNARE” protein know to be essential for exocytosis) suggested that this pool is regulated by the SNARE complex. A HCSP with similar characteristics has also been observed in other preparations, including the rat insulin-secreting INS-1 cell line (Yang and Gillis 2004) and isolated rat pancreatic beta cells (Wan, Dong et al. 2004). A similar Ca^{2+}-dependence has been reported in gonadotropes (Yang, Liu et al. 2005) and rod photoreceptor synapses (Thoreson, Rabl et al. 2004). All these results indicate that the HCSP is a common kinetic feature of exocytosis overlooked by previous studies.

1.5 Activation of PKC promotes exocytosis

PKC is a ubiquitous enzyme family involved in cell regulations. The physiological intracellular activator of PKC is diacylglycerol (DAG) together with Ca^{2+} (Asaoka, Nakamura et al. 1992; Nishizuka 1992; Nishizuka 1995). Non-metabolized phorbol ester drugs, especially PMA (Phorbol **12**-myristate **13**-acetate), have been successfully used as potent DAG analogues to activate PKC in laboratory studies (Newton 1995). As shown in Figure 1.8, PKCs are zinc

finger-like C1 domain enriched proteins which have a very high binding affinity for phorbol esters and DAG. There are three distinct groups of isozymes in the PKC family: (1) the conventional PKCs (α,β,γ), (2) the novel PKCs (δ,ε,η, and μ) and (3) the atypical PKCs (Newton 1995; Silinsky and Searl 2003).

Figure 1.8: Schematic demonstration of PKC (conventional) and Phorbol ester. C shows another substrate for phorbol ester, Munc13 (from figure 2, Silinsky and Searl, Br J Pharmacol).

Mammalian model studies demonstrated the involvement of PKC in short-term learning and memory (Kullmann and Siegelbaum 1995; Nicoll and Malenka 1995). Presynaptic activation of PKC shapes post-tetanic potentiation and short-term plasticity of synapses (Brager, Capogna et al. 2002; Brager, Cai et al. 2003). Activation of PKC with phorbol esters results in a profound enhancement of Ca^{2+}-triggered exocytosis in both neurons and endocrine cells.

A variety of studies with pharmacological PKC inhibitors concluded that PKC mediates phorbol esters-enhanced exocytosis. PKC regulates exocytosis mainly through increasing the size of the readily releasable pool or the release probability (Malenka, Madison et al. 1986; Yamamoto, Higashima et al. 1987; Gillis, Mossner et al. 1996; Stevens and Sullivan 1998; Waters and Smith 2000; Wu and Wu 2001). In both bovine adrenal chromaffin cell and rat insulin-secreting INS-1 cell, the PKC inhibitor bisindolylmaleimide (Bis) completely blocked the PMA-mediated enhancement of exocytosis of the HCSP and the RRP (Yang, Udayasankar et al. 2002; Yang and Gillis 2004).

However, the molecular mechanisms for PKC to regulate exocytosis are still elusive. PKC is capable of modulating intracellular proteins by phosphorylation of serine and threonine residues (Kennelly and Krebs 1991). Even though PKC has been shown to activate various proteins, I have focused on studying SNAP-25 as a PKC substrate because this protein is known to have an important function in exocytosis.

1.6 SNAP-25 is a possible substrate for PKC to enhance Ca^{2+}-triggered exocytosis

SNAP-25 is one of three proteins constituting the SNARE core complex. Formation of the SNARE complex has been popularly hypothesized to underlie

multiple membrane fusion steps in the cell (Sollner, Bennett et al. 1993). The three components of the SNARE complex are SNAP-25, syntaxin and synaptobrevin (or VAMP2) (figure 1.9A). Both SNAP-25 and syntaxin are associated with the plasma membrane, and are referred to as “target”, or t-SNAREs. Synaptobrevin is located in the vesicle membrane. Therefore, it is also called v-SNARE (vesicle SNARE). These three SNARE proteins bind together with high affinity to form the SNARE core complex (Lin and Scheller 1997; Sutton, Fasshauer et al. 1998)(figure 1.9B). This core complex is a protein bundle containing four helices, of which SNAP-25 contribute two helices and the other two are from syntaxin and synaptobrevin, respectively (Sutton, Fasshauer et al. 1998; Chen and Scheller 2001; Jahn, Lang et al. 2003). It has been proposed that the formation of the SNARE complex drives membrane fusion between the vesicle and the target membrane. Strong evidence for the important role of SNARE proteins in exocytosis is that they are the only known targets for botulinum and tetanus toxins that act by inhibiting transmitter release (Link, Blasi et al. 1994; Jahn, Hanson et al. 1995).

A. **B.**

Figure 1.9: SNARE complex. A. Localization of three SNARE proteins. B. Three SNARE proteins form the SNARE core complex (from figure 5, Sutton RB, Fasshauer D et al., Nature, 1998)

SNAP-25 is highly expressed in axons and nerve terminals. Cytoplasmic vesicular membranes also contain SNAP-25 (Walch-Solimena, Blasi et al. 1995). SNAP-25 associates with the membrane through the palmitoylation of four cysteine residues (Sollner, Whiteheart et al. 1993; Vogel and Roche 1999). The critical role of SNAP-25 in regulating fast Ca^{2+}-dependent exocytosis has been well demonstrated (Wei, Xu et al. 2000; Sorensen, Matti et al. 2002; Washbourne, Thompson et al. 2002; Sorensen, Nagy et al. 2003). In particular, the C-terminus of SNAP-25 is important for fast Ca^{2+}-triggered exocytosis because cleavage of the C-terminus of SNAP-25 by BoNT/E or /A inhibits or slows exocytosis (Blasi, Chapman et al. 1993; Schiavo, Rossetto et al. 1993; Gutierrez, Canaves et al. 1995; Gerona, Larsen et al. 2000). Besides its essential role in mediating

exocytosis, SNAP-25 has been suggested to play multiple roles in synapses, such as regulating neurite extension and sprouting (Osen-Sand, Catsicas et al. 1993; Bonner, Friedli et al. 1994) and ion channel functions (Wiser, Bennett et al. 1996; Yao, Ferrer-Montiel et al. 1999; Ji, Tsuk et al. 2002; Ji, Yang et al. 2002; MacDonald, Wang et al. 2002).

1.7 The importance of SNAP-25 phosphorylation at Ser187 by PKC is controversial

Within the C-terminal of SNAP-25, Serine187 (Ser187) is the only known PKC phosphorylation site (Shimazaki, Nishiki et al. 1996; Kataoka, Kuwahara et al. 2000; Morgan, Burgoyne et al. 2005). Both *in vitro* and *in vivo* experiments demonstrate SNAP-25 phosphorylation in response to phorbol esters application, PKC addition and physiological stimuli (Shimazaki, Nishiki et al. 1996; Genoud, Pralong et al. 1999; Kataoka, Kuwahara et al. 2000; Gonelle-Gispert, Costa et al. 2002; Nagy, Matti et al. 2002). A recent study in rat brain and cultured hippocampal neurons also showed that both development and neuronal activity could mediate SNAP-25 phosphorylation at Ser187 (Kataoka, Kuwahara et al. 2006).

Even though SNAP-25 phosphorylation at Ser187 is an attractive

hypothesized candidate to mediate the PKC-mediated enhancement of exocytosis, decisive evidence is still lacking. In bovine adrenal chromaffin cells, a phosphomimetic mutation of SNAP-25 at Ser187 (Ser187 to Glu or Asp, see detailed description in chapter 2) potentiated vesicle recruitment and highly Ca^{2+}-senstive exocytosis in bovine adrenal chromaffin cell (Nagy, Matti et al. 2002; Yang, Craig et al. 2007). Transmitter release from PC12 cells was also shown to be regulated by SNAP-25 phosphorylation at Ser187 through recruiting more vesicles to the plasma membrane (Shoji-Kasai, Itakura et al. 2002). SNAP-25 phosphorylation may enhance the formation of the SNARE core complex (Xu, Yu et al. 2004; Yang, Craig et al. 2007). On the other hand, several studies also suggest SNAP-25 is not very important for PKC-mediated enhancement of exocytosis (Iwasaki, Kataoka et al. 2000; Gonelle-Gispert, Costa et al. 2002; Finley, Scheller et al. 2003). A study in hippocampal neurons showed that phorbol esters work on the Munc-13 protein to promote neurotransmitter release in a PKC-independent manner(Rhee, Betz et al. 2002). Other than SNAP-25, targets such as Munc-18 and GAP-43 were also suggested to be the downstream substrate for PKC to enhance exocytosis (DeGraan, Hens et al. 1994; Fujita, Sasaki et al. 1996; Nicoletta, Ross et al. 2004). A possible explanation is that different types of cells use different mechanisms for PKC or PKC-activating agents to modulate exocytosis (Kataoka, Kuwahara et al. 2006). Thus, further study of the role of SNAP-25 phosphorylation at Ser187 in mediating the

enhancement of exocytosis by phorbol esters/PKC is required.

1.8 Expression of non-phosphorylatable mutation of SNAP-25 in bovine adrenal chromaffin cells did not block the enhancement of exocytosis by phorbol ester

As mentioned above, phosphomimetic mutations of SNAP-25 at Ser187 have been shown to enhance the HCSP and the RRP in bovine chromaffin cells (Yang, Craig et al. 2007) (figure 1.10). The HCSP and the RRP are assayed using a “hybrid” protocol developed in Gillis lab. This protocol combining the photorelease of caged-Ca^{2+} and membrane depolarization has been successfully applied to demonstrate the HCSP and the RRP in previous studies (Yang, Udayasankar et al. 2002; Yang and Gillis 2004) (figure 1.10A). The whole-cell patch-clamp configuration is used for this approach. The calcium-cage Nitrophenyl-EGTA (NP-EGTA) ~ 80% loaded with Ca^{2+} and a mixture of two calcium sensitive fluorescent dyes (Bis-fura1 and Fura-2FF) are delivered into the cells through the patch-clamp pipette. The cells are given about 2 minutes after the membrane “break-in” for the contents of the pipette to equilibrate with the cell. An ultra violet (UV) flash is then given to photorelease the caged-Ca^{2+} and elevate $[Ca^{2+}]_i$ from the basal level (around 500 nM) to several μM, which causes an

exponential, burst-like increase in C_m over the following 300 ms. The amplitude of an exponential fit to the C_m response is defined as the size of the HCSP. A train of 10 consecutive membrane depolarizing pulses (30 ms in duration to +20 mV) is applied to further increase the $[Ca^{2+}]_i$ and stimulate exocytosis of the less Ca^{2+}-sensitive RRP. The capacitance response to the 10 depolarizing pulses is defined as ΔC_{10}, which serves as a crude measure of the RRP size. $[Ca^{2+}]_i$ and the Ca^{2+} current I_{Ca} resulting from membrane depolarization are also simultaneously recorded (figure 1.10A).

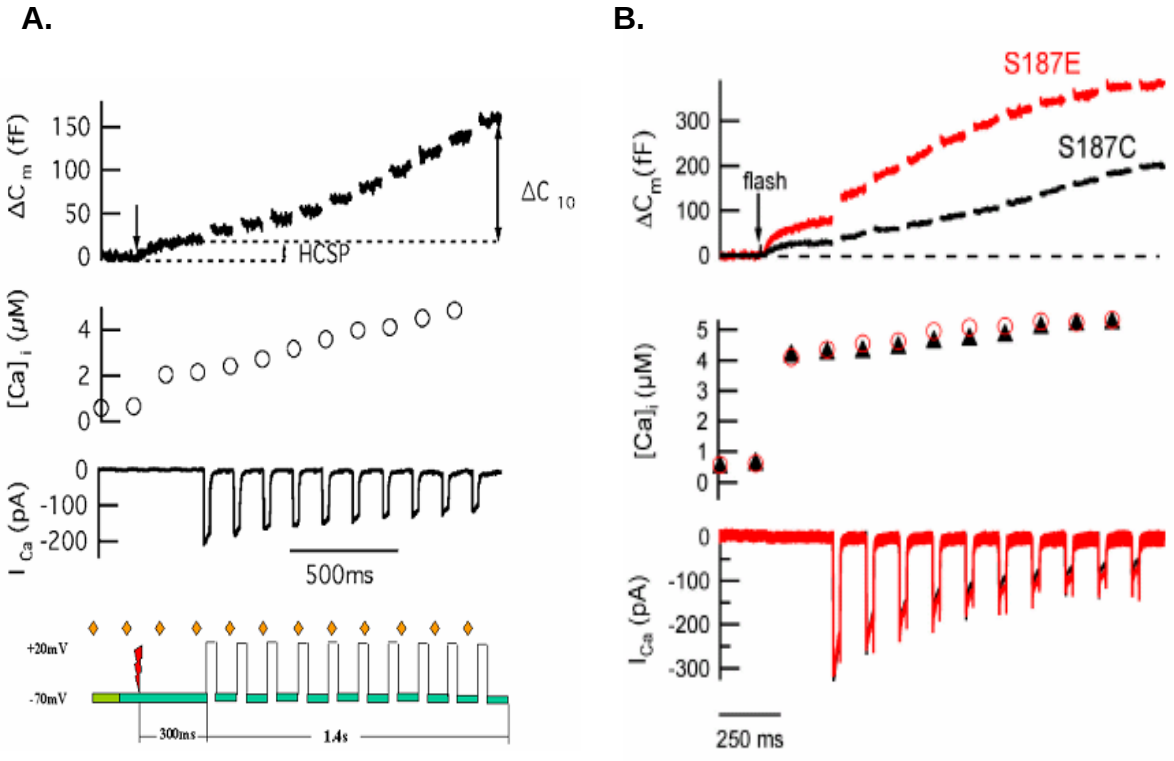

Figure 1.10: Phosphomimetic mutant S187E enhances exocytosis of the HCSP and the RRP in bovine chromaffin cells with the "Hybrid" protocol. (A), "Hybrid" protocol to elicit the HCSP and the RRP (ΔC_{10}) (after Yang and Gillis 2004). A stimulation protocol is present at the bottom. The filed marker indicates the time point for $[Ca^{2+}]_i$ measurement. The corresponding capacitance trace

(ΔCm), $[Ca^{2+}]_i$ measurement and the Ca^{2+} current(I_{Ca}) from the train of 10 membrane depolarization pulses are shown in the top panel. (B), Sample traces from bovine adrenal chromaffin cells expressing S187E and S187C with the "hybrid" protocol (Yang, Craig et al. 2007).

In the study by Yang et al. (2007), the phosphomimetic mutant S187E (Ser to Glu) and the nonphosphomimetic control S187C (Ser to Cys) were expressed in bovine chromaffin cells using the Semiliki Forest Virus (SFV) (see figure 3.1 in **Chapter 3** for detailed description about the phosphomimetic mutation strategy). S187E enhanced exocytosis compared to S187C (figure 1.10B). Based on this result, the Gillis lab tested the importance of SNAP-25 phosphorylation at Ser187 in the enhancement of exocytosis by the PKC-activator PMA (figure 1.11, data not published). Both S187E and S187C cannot be further phosphorylated by PMA/PKC. If Ser187 of SNAP-25 is critical for PKC to enhance exocytosis, overexpression of these non-phosphorylatable mutants of SNAP-25 at Ser187 (S187E or S187C) should block the stimulatory effect of PMA. However, this is not the case. Application of PMA still enhanced exocytosis of both the HCSP and the RRP dramatically in cells expressing S187E or S187C (figure 1.11A). The amplitudes of the HCSP and the ΔC_{10} from cells expressing either wild-type SNAP-25 or the SNAP-25 mutations are summarized in figure 1.11B. Q_{Ca} indicates the integral of the Ca^{2+} current resulting from the 10 membrane depolarization pulses. This value is not modulated significantly by mutations or application of PMA. These results demonstrate that expression of the

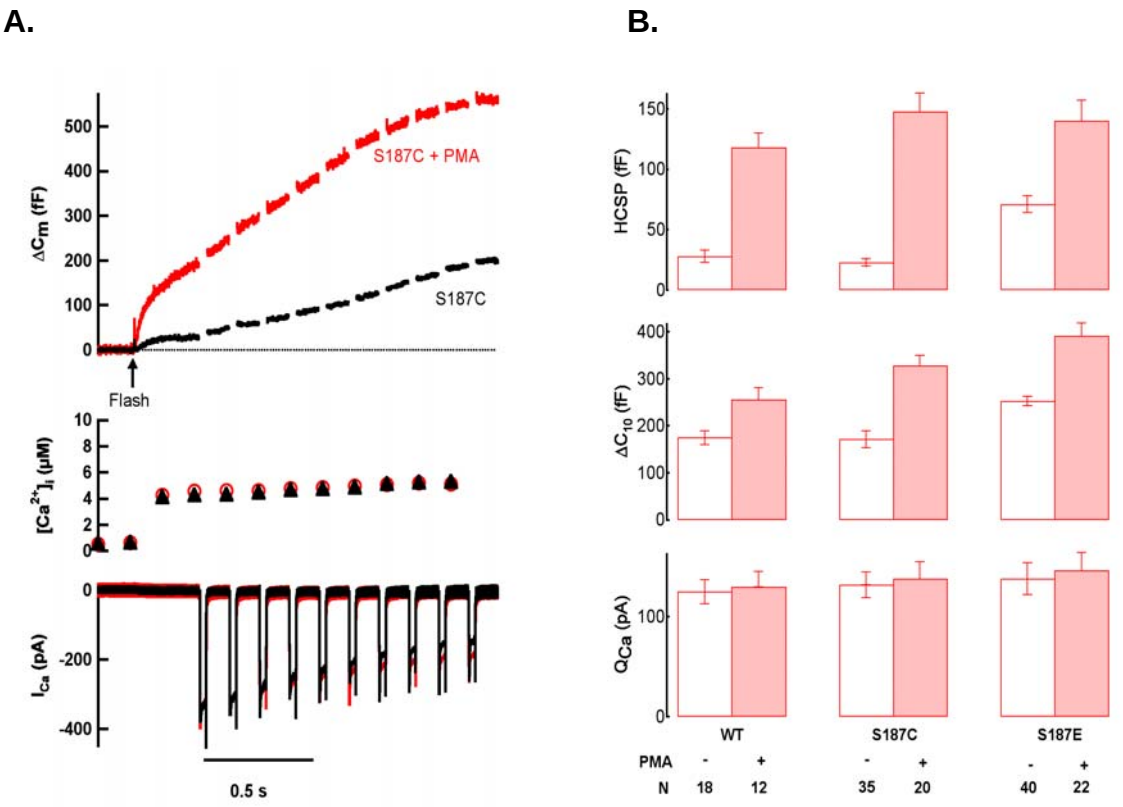

Figure 1.11: PMA still enhances exocytosis in cells expressing the non-phosphorylatable SNAP-25 at Ser187. (A), Sample traces from cell expressing S187C treated with or without PMA. (B), Summary of results from bovine adrenal chromaffin cells with the number of cells given by "N" value in the figure. The data is expressed as mean ± SEM. WT stands for GFP-SNAP-25 (WT), in which the green fluorescent protein (GFP) is fused to the N-terminus of SNAP-25. Both S187C and S187E also contain GFP fragment (see figure 3.1 in chapter 3 for details).

non-phosphorylatable SNAP-25 mutants does not diminish the enhancement of the HCSP or the RRP by PMA.

Why does PMA still promote exocytosis in cells expressing S187E or S187C? There are at least two explanations for these observations:

(1) The endogenous wild-type SNAP-25 is still present and

presumably can be phosphorylated by PMA/PKC and then promotes exocytosis. A previous study estimated that SFV-expressed SNAP-25 is present at levels ~20 times that of the endogenous protein (Wei, Xu et al. 2000). So it is usually assumed that the exogenous protein will effectively compete with the endogenous SNAP-25 for protein-protein interactions. However, it is not known if this is actually the case. Even though we think that overexpression of an extrinsic protein should overwhelm the endogenous one, we still consider this as a potential problem if unexpected results are observed.

(2) PMA may act on other targets to enhance exocytosis. As discussed above, several other proteins such as Munc13 (figure 1.8), Munc18 or GAP43 have been suggested to mediate phorbol esters/PKC-enhanced exocytosis (DeGraan, Hens et al. 1994; Fujita, Sasaki et al. 1996). Studies also suggest that phorbol esters mediate exocytosis through Munc-13 in a PKC-independent manner(Rhee, Betz et al. 2002).

An important step to distinguish these two possibilities is to disable the endogenous SNAP-25 and then test the effect of PMA on exocytosis with SNAP-25 Ser187 mutants.

1.9 Objectives and overviews of this thesis

The overall objective of this thesis is to explore a molecular mechanism for the regulation of exocytosis. In particular, I set out to gain more insight into Protein Kinase C-mediated enhancement of Ca^{2+}-triggered exocytosis, especially the importance of SNAP-25 phosphorylation at Ser187. The results from this study contribute to our further understanding of synaptic transmission and modulation of this process such as during memory formation and learning.

Chapter 2 describes the Materials and Methods used in this thesis.

Chapter 3 contains the main experiments. An insulin-secreting cell line, the rat insulin-secreting INS-1 cell, was employed for my experiments. BoNT/E was transfected into cells to cleave the endogenous SNAP-25. After I got a clean background, I further tested the importance of SNAP-25 phosphorylation at Ser187 in PMA-enhanced exocytosis by expressing BoNT/E-resistant SNAP-25 mutants. The results indicated that SNAP-25 phosphorylation at Ser187 is important for PMA to enhance exocytosis by increasing the size of both the HCSP and the RRP elicited.

Chapter 4 demonstrates the cleavage of SNAP-25 by BoNT/E in INS-1 cells. I took advantage of a specific anti-Pi-SNAP-25 antibody which recognizes the phorphosrylated Ser187 in the C-terminal of SNAP-25. With Immunoblot

assay, I showed that BoNT/E successfully cleaved the GFP-SNAP-25 (WT) and the endogenous SNAP-25 in transfected cells. However, BoNT/E had no effect on the toxin-resistant SNAP-25. These experiments confirmed that BoNT/E is a powerful tool to disable the endogenous SNAP-25 and are important controls for my experiments described in Chapter 3.

Chapter 5 describes experiments that test the importance of SNAP-25 phosphorylation at Ser187 in PMA-enhanced exocytosis at high $[Ca^{2+}]_i$. Exocytosis was stimulated with high $[Ca^{2+}]_i$ (>20 μM) induced by photorelease of caged-Ca^{2+}. The results show that SNAP-25 phosphorylation at Ser187 is responsible for most of PMA-enhanced exocytosis. However, some other mechanisms might be also involved when $[Ca^{2+}]_i$ is high.

Chapter 6 describes the preliminary study in rat hippocampal neurons to explore the importance of SNAP-25 phosphorylation at Ser187 in phorbol esters/PKC-enhanced exocytosis in neuronal cells. I succeeded in culturing the hippocampal neurons on patterned microislands. Transfection of the hippocampal neurons was also tested even though the protocols still need to be optimized.

Chapter 7 contains a summary of this thesis and some possible future directions based on the current study.

Chapter 8 is an appendix documenting my efforts to apply carbon fiber amperometry to measure exocytosis in INS-1 cells. I tried to use the customized 10 μm-diameter carbon fiber electrodes (CFEs) to directly measure the insulin

secretion from INS-1 cells. However, the preliminary results showed there is a dysfunction of this 10 μm-diameter CFE. I then tried to figure out the problems by testing the basic characteristics of the CFEs.

CHAPTER 2

MATERIALS AND METHODS

2.1 Materials

All cell culture reagents were from Gilbco (Invitrogen, Carlsad, CA) unless otherwise stated. The rabbit anti-Pi-SNAP-25 antibody(Kataoka, Kuwahara et al. 2000) was a kind gift from Dr. Masami Takahashi (Department of Molecular Medicine,Kitasato University School of Medicine, Kanagawa, Japan). All other antibodies used in immunoblot analysis were from Santa Cruz Biotechnology, Inc. (Santa Cruz, CA). All other reagents were from Sigma (St. Louis, MO) except as indicated.

2.2 Cell Culture

INS-1 cells culture: Rat insulin-secreting INS-1 cells (provided by C. Wollheim,

University of Geneva, Geneva, Switzerland) were maintained and prepared as described (Asfari, Janjic et al. 1992; Yang and Gillis 2004). Briefly, the cells were maintained in culture media consisting of RPMI 1640 medium supplemented with 50 μM 2-mercaptoethanol, 2 mM L-glutamine, 10 mM HEPES, 100 U/ml penicillin, 100 g/ml streptomycin, 1 mM sodium pyruvate, and 10% FBS. Cells were kept in a humidified 37^{o}C incubator with 5% CO_2 and were subcultured once per week. In patch-clamp experiments, INS-1 cells were plated onto glass coverslips (25mm OD) in 35mm dishes at the density of 5 X10^{5} cells per dish. In Immunoblot experiments, INS-1 cells were plated into 60mm dishes at the density of 2.5 X10^{6} cells per dish. Cells were used 3 to 4 days after plating.

Hippocampal neuron culture on micropatterned coverslips: The experimental protocols used are in accordance with the guidelines of the Institutional Animal Care and Use Committees of the University of University of Missouri-Columbia. Microisland cultures of hippocampal neurons were prepared and maintained as described previously (Bekkers and Stevens 1991; Nishiki and Augustine 2004).Briefly, 1- to 3-d-old postnatal Sprague Dawley rats were anesthetized with halothane. The hippocampi were isolated on iced dissection medium (Hanks without Ca^{2+} and Mg^{2+}, 10mM HEPES, 1mM Na-Pyruvate). The hippocampal neurons were harvested with the enzymatic treatment of 1 mg/ml papain (Worthington Biochemical Corporation, Lakewood, NJ) in oxygenated Leibovitz's

L-15 medium for 15-20 min. The dissociated cells were plated at different concentrations according to experiments in neurobasal A media supplemented with 5% FBS, 2% B-27, 2mM glutamax I, 25 μM L-glutamate (sigma), 0.5 mM Na-Pyruvate, 1 μg/ml gentamycin. This medium was exchanged 24 hr after plating with serum and antibiotics-free medium.

2.3 DNA Constructs

The constructs of BoNT/E light chain and the toxin-resistant human SNAP-25a (TR-SNAP-25a) were kindly provided by Dr. Sadoul and Dr. Halban(Laboratories de Recherche Louis Jeantet, Centre Medical University, Geneva, Switzerland) (Gonelle-Gispert, Halban et al. 1999; Gonelle-Gispert, Costa et al. 2002). The cDNAs of BoNT/E light chain and TR-SNAP-25a were cloned into the pCMV5 vector and pcDNA3 vector respectively. The cDNA coding green fluorescent protein (GFP) was fused to the N-terminus of SNAP-25a sequence. The pcDNA3-GFP-TR-SNAP-25a was used as a template for both a phosphomimetic mutation (S187E) and a non-phosphomimetic mutation (S187C) with using the the QuickChangeTM Site-Directed Mutagenesis kit (Stratagene, La Jolla, CA, U.S.A.), according to the manufacturer's instructions (Gonelle-Gispert, Costa et al. 2002). The primers used were: S187E mutation, 5’-CATGGAGAAGGCTGATGAGAACAAAACCAGAATTG-3’; S187C mutation,

5’-CATGGAGAAGGCTGATTGCAACAAAACCAGAATTG-3’. The sequences of all constructs were confirmed by DNA-sequencing.

2.4 Transfection of Cells

Transfection of INS-1 Cells: On the day following plating, INS-1 cells were transfected with SNAP-25 and/or BoNT/E DNA using LipofectAMINE 2000 (Invitrogen) according to the manufacturer’s instructions. Transfection medium was changed 6 hours later to fresh cell culture medium. Cells were used for experiments 2 days after transfection. For co-transfection of BoNT/E with SNAP-25 constructs, the ratio of BoNT/E to SNAP-25 DNA was 3:1 to make it more likely that cells identified from fluorescence of GFP-SNAP-25 also express the toxin. The transfection efficiency was estimated to be about 10% from GFP fluorescence measurements.

Transfection of neurons: The transfection of hippocampal neurons were performed as described previously (Nishiki and Augustine 2004). Briefly, neurons will be transfected 3 or 4 d after plating using Lipofectamine 2000 (Invitrogen, Carlsbad, CA) according to the manufacturer's instructions. Before transfection, 1 ml of Neurobasal-A medium (Invitrogen) supplemented with GlutaMax-I (Invitrogen) and B-27 (Invitrogen), wereadded into the dishes containing neurons,

and the same volume of the medium wereremoved and set aside for later use. DNA plasmid (0.4 μg) and Lipofectamine 2000 reagent (1 μl) were diluted separately with 25 μl of Opti-MEM I (Invitrogen), mixed, and then incubated with cells at 37°C for 3-4 hr in a CO_2 incubator. In the co-transfection of BoNT/E with SNAP-25 constructs, 3 fold of BoNT/E DNA were used to ensure co-transfection efficiency.

2.5 $[Ca^{2+}]_i$ Calibration in Cells

A combination of the low affinity Ca^{2+} indicator fura2-ff (Teflabs, 100 μM) and the high affinity indicator bisfura-2 (Molecular Probes, 100 μM) was used to measure $[Ca^{2+}]_i$ over a wide dynamic range. The Ca^{2+} indicator combination was calibrated in cells as described before(Yang and Gillis 2004). Briefly, eight solutions with free $[Ca^{2+}]_i$ of, 0.31, 1.2, 3.6, 7.2, 28, 127 μM and 10 mM were prepared using Ca^{2+} buffers EGTA (K_D=150 nM at pH 7.2, total concentration 10 mM), *N*-hydroxyethylethylenediaminetriacetic acid (K_D=3.6μM, concentration 10 mM), or 2-ol-*N*,*N'*-tetraacetic acid (K_D=81μM, concentration 30 mM). Dissociation constants for the buffers were obtained from (Maertell and Smith 1974-1989). Whole-cell recordings were made using each of the calibration solutions in the pipette, and the ratio of fluorescence emission (535 $\pm$ 25 nm) for 340 and 365 nm excitations were recorded after allowing 2 min for the pipette solution to diffuse

into the cell. Three to five recordings were made for each calibration solution. The following equation was fit to the eight measured ratio values (R) to find the five unknown parameters (Voets, 2000):

$$R = R_0 + R_1 \frac{[Ca^{2+}]_i}{[Ca^{2+}]_i + K_1} + R_2 \frac{[Ca^{2+}]_i}{[Ca^{2+}]_i + K_2}.$$

2.6 Electrophysiology and Photometry

All the electrophysiological experiments were performed at room temperature (~22^{o}C). Whole-cell patch-clamp measurements were performed using an EPC-9 patch-clamp amplifier and PULSE acquisition software (HEKA). Pipettes (2–4 MΩ resistance) were pulled from Kimax glass capillaries, coated with dental wax at the tips, and fire polished. The pipette potential was held at a dc value of -70 mV. Capacitance measurements were performed using the “sine + dc” software lock-in amplifier method implemented in PULSE software (Pusch and Neher 1988; Gillis 2000). The assumed reversal potential was 0 mV and the sinusoid had amplitude of 25 mV and a frequency of 1.5 kHz. The sampling frequency is 16.7 kHz and filtered with two built-in Bessel filters (10 kHz and 2.9 kHz, respectively).

A monochromator (Polychrome IV, TILL/ASI) coupled to the

epifluorescence port of an Olympus IX-50 microscope with a fiber-optic cable were used to excite the Ca^{2+} indicators at 340 and 365 nm. A two-port condenser (TILL/ASI) combined the monochromator excitation path with that of a flash lamp (TILL/ASI). A 40X 1.15 NA water immersion lens (U-APO; Olympus) focused the excitation light and collects fluorescent light. The fluorescent light (535$\pm$25 nm) was measured using a photodiode mounted in a viewfinder (TILL/ASI).

The standard bath solution consisted of (in mM) 140 NaCl, 5.5 KCl, 1 $MgCl_2$, 5 $CaCl_2$, 10 HEPES titrated to pH 7.2 with NaOH. The bath solution also contained 2.6 mM glucose. Standard pipette solution consisted of (in mM) 130 L-glutamic acid, 1 $MgCl_2$, 2 Na_2-ATP, and 40 HEPES titrated to pH 7.2 with CsOH. The Ca^{2+} indicator dyes fura-2FF (K^+ salt; Teflabs) and bisfura-2 (K^+ salt; Molecular Probes) were included in the pipette solution at an equimolar ratio (0.1 mM). In caged-Ca^{2+} experiments, 0.3 – 1.5 mM NP-EGTA (Ellis-Davies and Kaplan 1994), about 80% loaded with $CaCl_2$ was added to the pipette solution. Basal $[Ca^{2+}]_i$ of the pipette solution was adjusted to ~500 nM by adding additional $CaCl_2$ or NP-EGTA as needed.

2.7 Immunoblot Analysis

After INS-1 cells were incubated in test solution, they were lysed with

ice-cold RIPA buffer (50 mM Tris HCl, pH=8; 150 mM NaCl; 1% NP-40; 0.5% sodium deoxycholate; 0.1% SDS; 2 mM EDTA). Protease inhibitors (protease cocktail; 1mM PMSF; 1mM Na_3VO_4) were added freshly. The lysates were harvested and centrifuged at 12000 rpm for 20 min at 4^0C. The supernatants were collected and the protein concentrations were measured by using the DCA method (Bio-Rad). Equal amounts of samples (15 μg of protein unless otherwise stated) were separated with a 12% SDS-polyacrylamide gel at 100 V for about 45 min and then transferred onto a nitrocellulose membrane. The membranes were incubated with primary antibodies (rabbit anti-Pi-SNAP-25 antibody, 1:250; goat anti-SNAP-25 antibody, N-terminal, 1:250) for 2 h at room temperature, followed by 1hr incubation with corresponding secondary antibodies (goat anti-rabbit IgG-HRP and bovine anti-goat IgG-HRP, 1:2000, respectively) for 1 h at room temperature. The ECL Western blotting detection reagents (Pierce, Rockford, IL) were used to develop the membranes and the proteins bands were visualized with Hyperfilm ECL (Amersham Biosciences, Buckinghamshire, UK). To normalize the signals in some experiments, the membranes were stripped in the stripping buffer [1.5% glycine (W/V), 0.1% SDS (W/V), 1% Tween20 (V/V), pH 2.0] for 30 min at room temperature. After being washed with PBS, the membranes were blotted with another pair of primary antibody and secondary antibody (such as mouse anti-actin, 1:250; bovine anti-mouse IgG-HRP, 1:2000) according to the procedure described above. For the quantification of the Western blot data, the

developed films were scanned, the immunoreactive bands were digitized, and the densitometry was performed using Scion Image for Windows (Scion, Frederick, MD).

2.8 Flow Cytometry

Cells were plated into 60 mm dishes and transfected as described previously. 1 day after transfection, the cells were detached using 0.025% trypsin (Invitrogen) and were harvested into centrifuge tubes. After being centrifuged at 200 rpm for 5 min, the cells were washed and then dispersed with cold PBS. The cells were then subjected to separation according to GFP fluorescence using Flow Cytometry (Cell Core facility, University of Missouri-Columbia). GFP was excited with a laser at the wavelength of 488 nm. Both the GFP-negative and GFP-positive cells were collected. The cells were put into culture media to recover for about 4 hr, and then subjected to centrifugation again and treated with or without PMA for 30 min. After this treatment, the cells were lysed with RIPA buffer and subjected to immonoblot assay.

2.9 Cell Imaging

Confocal image of INS-1 cells: INS-1 cells were plated onto the glass coverslips

(25 mm OD) in 35mm dishes and transfected with SNAP-25 as described above. Before image capture, coverslips with the cells were mounted in a custom chamber. Bath solution was added into the chamber to cover the cells. The cells were then imaged using a Leica Confocal Microscope **(**Exton, PA**)**.

Image of hippocampal neurons: The samples were imaged using an IX-50 microscope (Olympus) with a 40 X objective lens.

2.10 Data Analysis

Data analysis and curve fitting were performed by using Igor software (Wavemetrics). In patch-clamp experiments, only the cells with desired value of pre-flash $[Ca^{2+}]_i$ (~ 500 nM) and post-flash $[Ca^{2+}]_i$ (< 10 μM with "hybrid" protocol, 10 – 50 μM with intensive flash) were chosen for data analysis. The data out of the range in which most other data sit were also excluded. The capacitance trace and Ca^{2+} current trace were decimated in a group of 12. Results and histograms were expressed as mean $\pm$ SEM except otherwise stated.

CHAPTER 3

INVESTIGATING THE IMPORTANCE OF SNAP-25 PHOSPHORYLATION AT SER187 IN PHORBOL ESTER-MEDIATED ENHANCEMENT OF EXOCYTOSIS: STUDIES AT LOW $[Ca^{2+}]_i$ IN INS-1 CELLS

To further address the importance of SNAP-25 phosphorylation at Ser187, I performed experiments to express SNAP-25 mutants in a background where the endogenous protein is disabled. There are several methods to knock out a specific protein from the cell. The most common one is using knockout mice to produce cells with a null background of the protein of interest. However, there are several drawbacks to using SNAP-25 knockout mice for this study. (1). Compared with the availability of large quantities of bovine adrenal chromaffin cells, the adrenal glands from mice can only provide very limited amount of cells. (2). Compensatatory mechanisms may appear during development to alter the balance of proteins in cells of knock-out mice (Pich and Epping-Jordan 1998;

Branchi and Ricceri 2002). (3). Mouse colonies are expensive and labor-intensive to maintain. Another possible approach is the use of SiRNA (small interfering RNA), but this also can invoke compensatory mechanisms (Jensen, Joseph et al. 2006) and non-specific off target effect (Jackson and Linsley 2004). SiRNA approach is also complicated to carry out. On the basis of these concerns, an alternative method was chosen to acutely inactivate the endogenous SNAP-25 by expressing Botulinum neurotoxin E (BoNT/E) in target cells (Graham, Fisher et al. 2000; Graham, Washbourne et al. 2001; Bajohrs, Rickman et al. 2004).

This chapter describes electrophysiological experiments to explore the importance of SNAP-25 phosphorylation at Ser187 in PMA-enhanced exocytosis at low $[Ca^{2+}]_i$. The biochemical experiments that confirm cleavage of SNAP-25 (endogenous SNAP-25 or mutants) proteins by BoNT/E are presented in Chapter 4.

3.1 Phosphomimetic mutation strategy of SNAP-25

Using phosphomimetic mutations to specifically study the role of protein phosphorylation has been successfully applied in many studies(Gonelle-Gispert, Costa et al. 2002; Nagy, Matti et al. 2002; Finley, Scheller et al. 2003; Xu, Yu et al. 2004). A negatively charged residue [glutamic acid (E) or aspartic acid (D)] is used to substitute the targeted amino acid. As control, a non-phosphorylatable

residue such as cysteine (C) or alanine (A) is used. As shown in figure 3.1, I chose Glu (E) and Cys (C) as the phosphomimetic mutation and nonphosphomimetic mutation, respectively. Glu (E) is both negatively charged and structurally resembles phosphoserine. Cys (C) is a neutral amino acid which can not be phosphorylated, and structurally resembles Serine. A potential problem with Cys (C) is the SH group, which may form disulfide bridges with other SH groups. This may cause dysfunction of the proteins. However, previous studies with this mutation showed that it did not affect exocytosis (Nagy, Matti et al. 2002). As described in Material and Methods, green fluorescent protein (GFP) was fused to the N-terminal of the SNAP-25 to indicate the expression of the mutants in cells (figure 3.1B)

A.

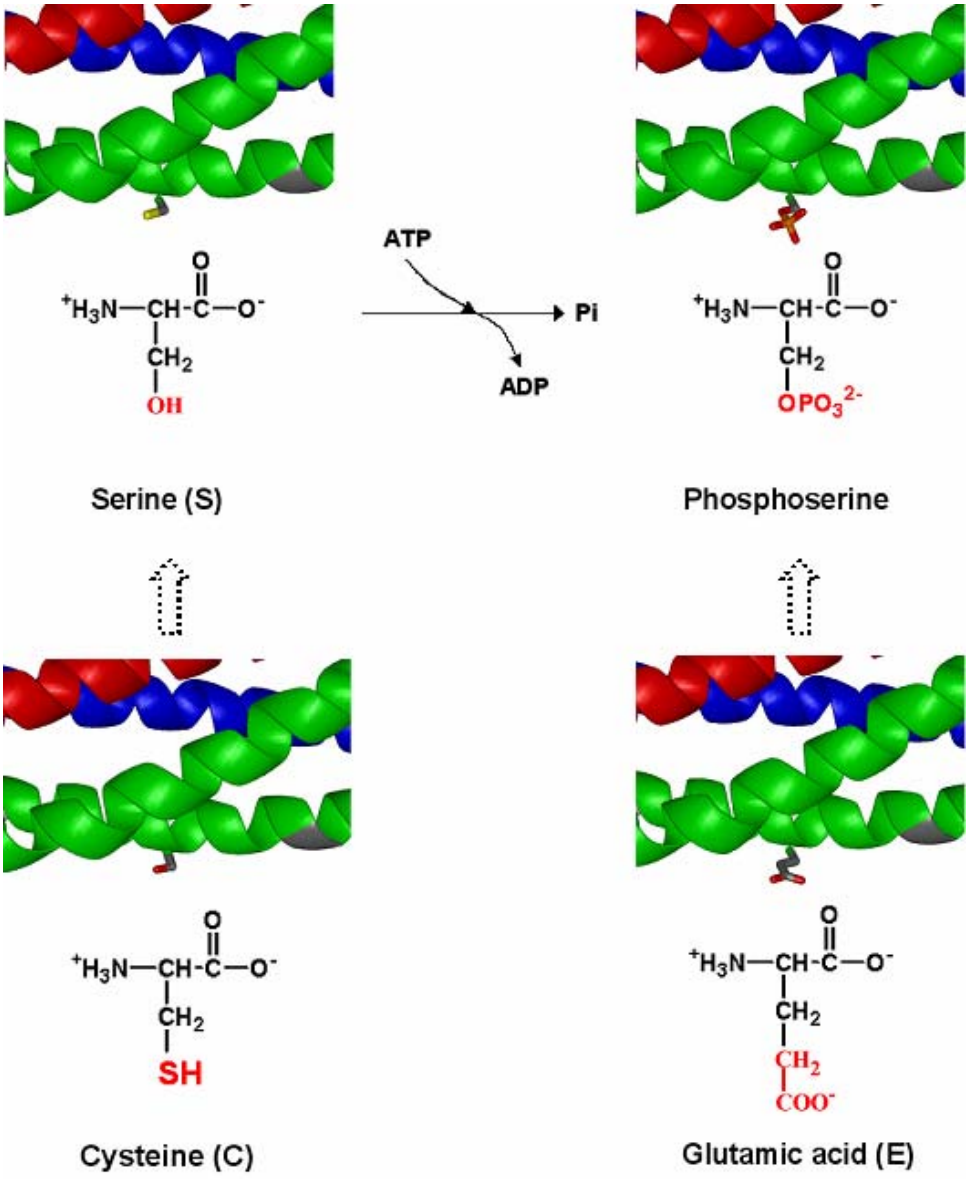
ATP
Pi
ADP
Serine (S)
Phosphoserine
Cysteine (C)
Glutamic acid (E)

B.

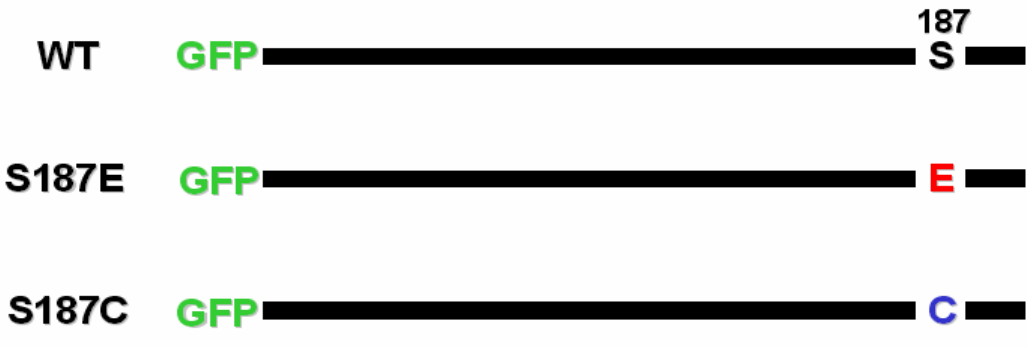
187
WT
GFP
S
S187E
GFP
E
S187C
GFP
C

Figure 3.1: Schematic demonstration of the phosphomimetic mutation Strategy. (A), Phosphorylation of Serine (Ser). The structures of Cystenine (Cys) and Glutamic acid (Glu) are also present for the comparison. (B), Schematic demonstration of GFP-SNAP-25 (WT), phosphomimetic mutant SNAP-25 (S187E) and the non-phosphorylatable control (S187C). GFP is fused to the N-terminal of SNAP-25.

3.2 Mutation of SNAP-25 to confer resistance to BoNT/E cleavage

As discussed above, my goal is to use BoNT/E to cleave the endogenous SNAP-25. BoNT/E is a member of a botulinum neurotoxin family, which is produced by Clostridial botulinum bacteria. BoNTs have been very helpful in identifying the importance of SNARE proteins in exocytosis. There are seven members identified, BoNT/A, /B, /C, /D, /E, /F and /G. These BoNTs hydrolyze various SNARE proteins specifically (figure 3.2). BoNT/B, BoNT/D, BoNT/F and BoNT/G cleave synaptobrevin at specific sites(Link, Edelmann et al. 1992; Schiavo, Benfenati et al. 1992; Schiavo, Rossetto et al. 1993; Schiavo, Shone et al. 1993; Schiavo, Malizio et al. 1994; Yamasaki, Binz et al. 1994). BoNT/C cleaves syntaxin and SNAP-25(Blasi, Chapman et al. 1993; Schiavo, Shone et al. 1995; Foran, Lawrence et al. 1996). BoNT/A and BoNT/E act on SNAP-25 at different sites(Blasi, Chapman et al. 1993; Binz, Blasi et al. 1994). BoNTs consist of two subunits, the heavy chain (~ 100 KDa) and the light chain (~50 KDa). The heavy chain is mainly responsible for transporting the toxin into the cell. The light

chain contains the endoprotease component. More details about the structure and functions of BoNTs can be found in the review by (Pellizzari, Rossetto et al. 1999)

Figure 3.2: BoNTs cleave SNARE proteins specifically. Seven BoNTs cleave SNARE proteins at different sites. The site for Tetanus neurotoxin (TeNT) is also shown (from figure 5, Sutton RB, Fasshauer D et al., Nature, 1998).

BoNT/E specifically cleaves SNAP-25 between Arg^{180} and Ile^{181} and profoundly inhibits exocytosis(Binz, Blasi et al. 1994; Lawrence, Foran et al. 1997) (figure 3.3). The residual C- terminal fragment containing Ser187 is released from SNAP-25 after cleavage by BoNT/E. In principle, introducing recombinant BoNT/E toxin into cells could be used to disable endogenous SNAP-25. However, the use of the recombinant toxin has several limitations. For example, cells vary in how efficiently they take up the toxin. In addition, handling the potentially dangerous toxin requires stringent safeguards. Therefore, I took the approach of

transfecting cells with DNA encoding the light chain of BoNT/E (Aguado, Gombau et al. 1997; Ahmed and Smith 2000).

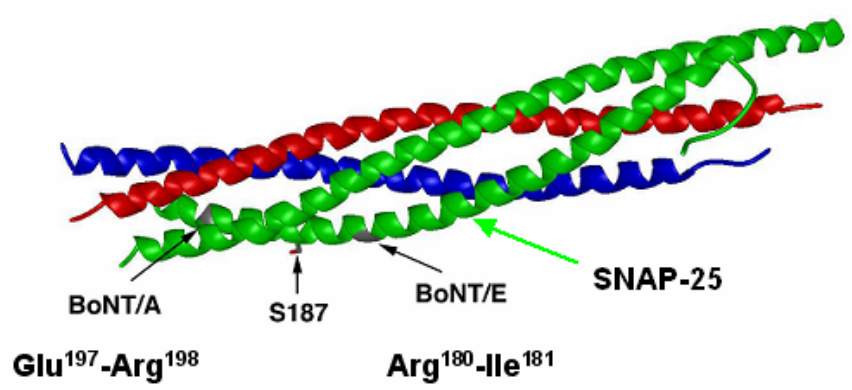

Figure 3.3: BoNT/E cleaves SNAP-25 to exclude Ser187.

Bovine adrenal chromaffin cells were not suitable for this approach because these primary cells are refractory to common transfection approaches such as the use of cationic lipids reagents. A viral transfection approach is the most efficient method to express extrinsic proteins in chromaffin cells. However, we could not virally express BoNT/E because of potential security problems. Therefore, I chose rat insulin-secreting INS-1 cells as the cell model. The INS-1 cell is a pancreatic beta cell line which has been widely used to study Ca^{2+}-regulated secretion of insulin and exocytotic mechanisms(Kennedy, Rizzuto et al. 1996; Scheenen, Wollheim et al. 1998; Maechler, Kennedy et al. 1999; Tsuboi, Zhao et al. 2000; Yang and Gillis 2004). It exhibits many of the characteristics of primary beta cells, including high insulin content and

glucose-stimulated release (Asfari, Janjic et al. 1992). INS-1 cells also exhibit a similar Ca^{2+}-sensitivity to exocytosis and modulation by PMA/PKC modification that is similar to primary cells (Yang and Gillis 2004). This cell line can also be transfected easily. therefore, I used cationic lipid-based transfecion agents such as Lipofectamine for expressing proteins.

My goal is to completely cleave endogenous SNAP-25 with BoNT/E, yet still leave exogenously expressed SNAP-25 mutants intact. To avoid proteolysis of the transfected SNAP-25 by BoNT/E, I introduced mutations that render SNAP-25 resistant to BoNT/E. As indicated in figure 3.4, for the mutant SNAP-25 (TR), the amino acids Arg (R)^{176}, Asp (D)^{179} and Met (M)^{182} are mutated to Pro (P)^{176}, Lys (K)^{179} and Thr (T)^{182} to make the protein resistant to proteolysis (Sadoul, Berger et al. 1997; Gonelle-Gispert, Halban et al. 1999). The sequence of the amino acids is then changed from R^{176}QIDRIM^{182} to P^{176}QIKRIT^{182} which is the homologous sequence found in (human) SNAP-23, a SNAP-25 analogue (Sadoul, Berger et al. 1997). Toxin-resistant S187E-SNAP-25 (TR S187E) and Toxin-resistant S187C-SNAP-25 (TR S187C) are the phosphomimetic mutant and the non-phosphorylatable mutant of SNAP-25 respectively. DNA encoding the green fluorescence protein (GFP) was also fused to the N-terminus of SNAP-25 to allow fluorescent identification of cell expressing the protein.

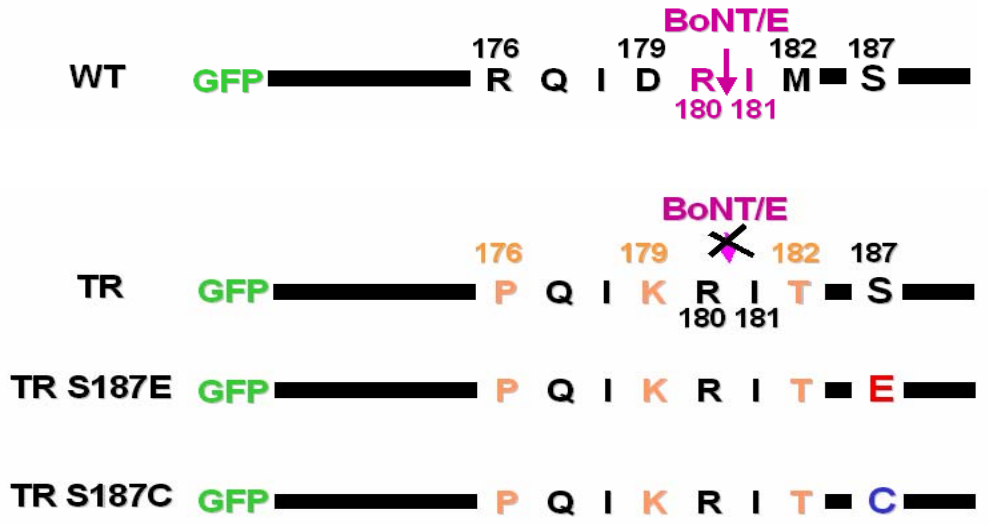

Figure 3.4: Schematic depiction of BoNT/E resistant mutants of SNAP-25.

3.3 The localization of SNAP-25 is not affected by the phosphomimetic and toxin-resistant mutations

SNAP-25 is primarily associated with the plasma membrane. Since the SNAP-25 mutants used in this study bear several mutations, I first confirmed whether the localization of the SNAP-25 is normal or not. I first transfected INS-1 cells with GFP-SNAP-25 (WT) and acquired images using a Confocal microscope. Figure. 3.5A clearly shows that the expressed SNAP-25 is primarily localized in the plasma membrane, which is consistent with a previous study(Gonelle-Gispert, Costa et al. 2002). There is also some fluorescence inside the cell, which may indicate areas of protein synthesis. I also acquired images of cells transfected

with TR S187C and BoNT/E. The distribution of SNAP-25 was similar in all cases (figure 3.5B).

A. **B.**

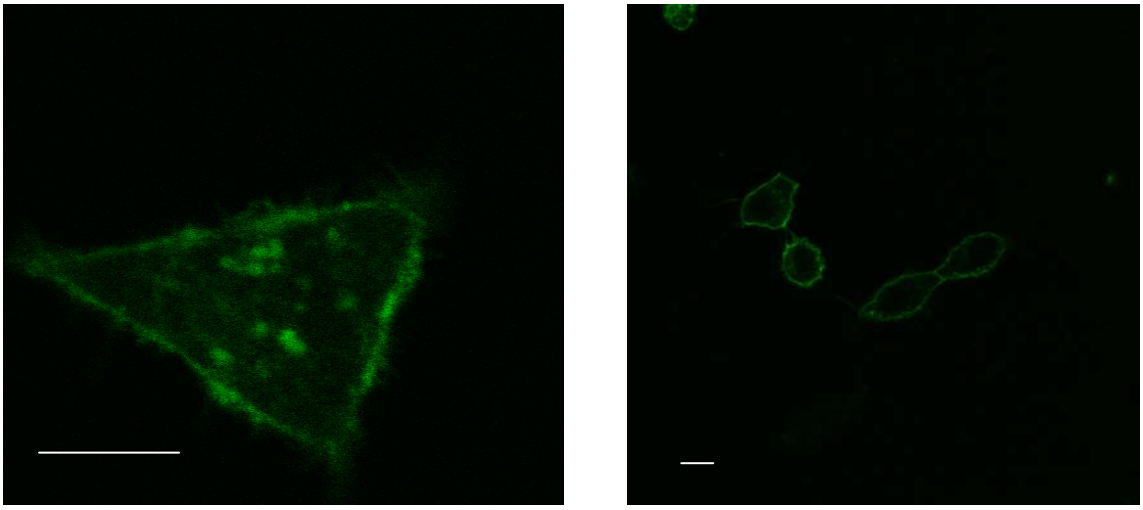

Figure 3.5: SNAP-25 was primarily localized in the plasma membrane. (A), Confocal image from cell transfected with GFP-SNAP-25 (WT). (B), Cofocal image from cells transfected with TR S187C and BoNT/E. The bar is 5 µm in (A) and (B).

3. 4. The phosphomimetic mutant TR S187E was detected by the specific anti-Pi-SNAP-25 antibody.

The anti-Pi-SNAP-25 antibody specifically recognizes the SNAP-25 phosphorylated at Ser187(Shimazaki, Nishiki et al. 1996; Kataoka, Kuwahara et al. 2000). PMA (1µM) has been shown to induce phosphorylation of SNAP-25 at Ser187 in INS-1 cells (Gonelle-Gispert, Costa et al. 2002). The efficiency of this

antibody was first tested with the time course of SNAP-25 phosphorylation by PMA. In my study, even 5 min exposure to 100 nM PMA results in robust phosphorylation of SNAP-25 at Ser^{187} (figure 3.6A). There was no obvious further increase in the phosphorylation of SNAP-25 upon incubation with PMA for up to 60 min. I also used an antibody that recognizes the N-terminus of SNAP-25 (anti-SNAP-25) to probe the total SNAP-25. PMA application within 1 hr did not change the total SNAP-25 in this assay.

In the phosphomimetic mutant S187E, I predict that the Glu substitution will mimic the phosphorylation of SNAP-25 at Ser187 by PMA/PKC. I therefore expect S187E will be recognized by the anti-Pi-SNAP-25 antibody (Yang, Craig et al. 2007). To confirm this, I probed cells expressing SNAP-25 mutants with the anti-Pi-SNAP-25 antibody (figure 3.6B). The control cells (without any transfection) treated with PMA (100 nM) for 30 min were used as the positive control. The samples in all other groups were incubated with bath solution for 30 min before immunoblot assay. The data shows that anti-Pi-SNAP-25 only recognizes the TR S187E mutant (~52 kDa band, GFP-SNAP-25-Pi) but does not recognize GFP-SNAP-25 (WT), TR SNAP-25 or TR S187C. The anti-SNAP-25 antibody recognized both the endogenous SNAP-25 (~25 kDa) and the expressed GFP-SNAP-25 (~52 kDa) following stimulation with PMA. The expression of the SNAP-25 mutants did not change the level of the endogenous SNAP-25. This result indicates that the TR S187E protein is able to mimic PKC-phosphorylated

SNAP-25.

A.

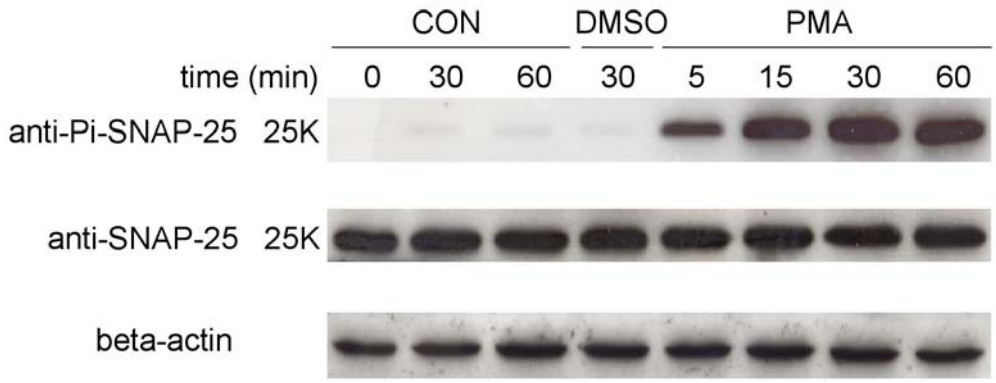

B.

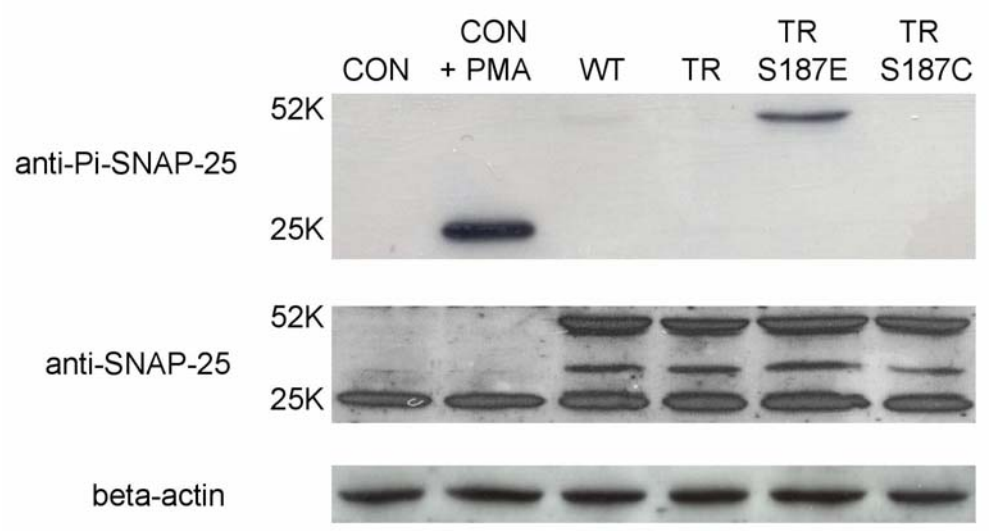

Figure 3.6: Anti-Pi-SNAP-25 antibody recognizes TR S187E. (A), Time course of SNAP-25 phosphorylation at Ser187 by PMA (100nM) probed with the specific anti-Pi-SNAP-25 antibody (Upper panel). The SNAP-25 was probed with anti-SNAP-25 (Middle panel). (B), Probing SNAP-25 mutants with the anti-Pi-SNAP-25 antibody.

Nevertheless, the TR S187E band probed by the anti-Pi-SNAP-25 is not as

prominent as SNAP-25 (CON) following PMA treatment (figure 3.6B). This may indicate that this SNAP-25 Ser^{187} phosphorylation-specific antibody did not bind to TR S187E with the same affinity as the PMA-phosphorylated SNAP-25 Ser^{187}. Thus, this phosphomimetic mutation may only partially mimic the phosphorylation of SNAP-25 at Ser187 with respect to protein binding reactions.

3.5. A phosphomimetic mutant of SNAP-25 at Ser^{187} preferentially enhances exocytosis of the HCSP in INS-1 cells.

In bovine adrenal chromaffin cells, the phosphomimetic mutant S187E enhanced the HCSP to a greater extent than the RRP (Yang, Craig et al. 2007). The phosphomimetic mutant TR S187E is able to mimic PMA-induced SNAP-25 phosphorylation at Ser187 with regard to anti-Pi-SNAP-25 antibody binding. Does it also have the same physiological effect on exocytosis as S187E did in bovine adrenal chromaffin cells? To test whether the phosphomimetic mutation of SNAP-25 at Ser187 can enhance exocytosis in INS-1 cells, I used the “hybrid” stimulus protocol (see figure 1.10) to elicit exocytosis in TR S187E transfected cells. As discussed in Materials and Methods (Chapter 2), only the cells with right value of pre-flash $[Ca^{2+}]_i$ (~ 500 nM) and post-flash $[Ca^{2+}]_i$ (< 10 μM with “hybrid” protocol) were chosen for data analysis. The pre-flash $[Ca^{2+}]_i$ and post-flash $[Ca^{2+}]_I$ for each group of cells in this chapter are summarized in the end of this

chapter in table 1 (Page 68).

Figure 3.7A shows sample traces from an untransfected cell (CON), a TR S187E transfected cell (TR S187E) and a TR S187C transfected cell (TR S187C). Expression of TR S187E preferentially enhances the response to photorelease of caged-Ca^{2+}, i.e., the HCSP. In average, the size of the HCSP in TR S187E transfected cells (56.8 $\pm$ 6.3 fF, N=26) was about 2.5 fold of that in the control cells (23.2 $\pm$ 1.6 fF, N=49) (figure 3.7B). However, the size of the ΔC_{10} in TR S187E transfected cells (164.7 $\pm$ 10.7 fF, N=26) was only about 1.2 fold of that in the control cells (135.6 $\pm$ 6.9 fF, N=49). Figure 3.7B also shows the responses from cells expressing other SNAP-25 constructs including GFP-SNAP-25 (WT), TR SNAP-25 and TR S187C. Overexpression of GFP-SNAP-25 (WT) had no effect on exocytosis, which was consistent with the results in bovine adrenal chromaffin cells (Nagy, Matti et al. 2002). In addition, expression of the toxin resistant mutations of SNAP-25 did not alter exocytosis, which was consistent with the results obtained from cells population secretion assays in INS-1 cells (Gonelle-Gispert, Costa et al. 2002). ΔC_{10} was induced by depolarizing pulses which caused Ca^{2+} influx. The I_{Ca} values in SNAP-25 mutant transfected cells were not changed compared with that in control cells. This indicates that transfection of SNAP-25 did not affect the Ca^{2+} current. Therefore, any change in the ΔC_{10} response was not due to the change in Ca^{2+} influx. PMA enhanced the HCSP and the RRP around 5 fold and 2 fold respectively (Yang and Gillis 2004).

Expression of TR S187E thus had a much weaker effect on exocytosis than treatment with a phorbol ester, yet partially mimics effects of the drug.

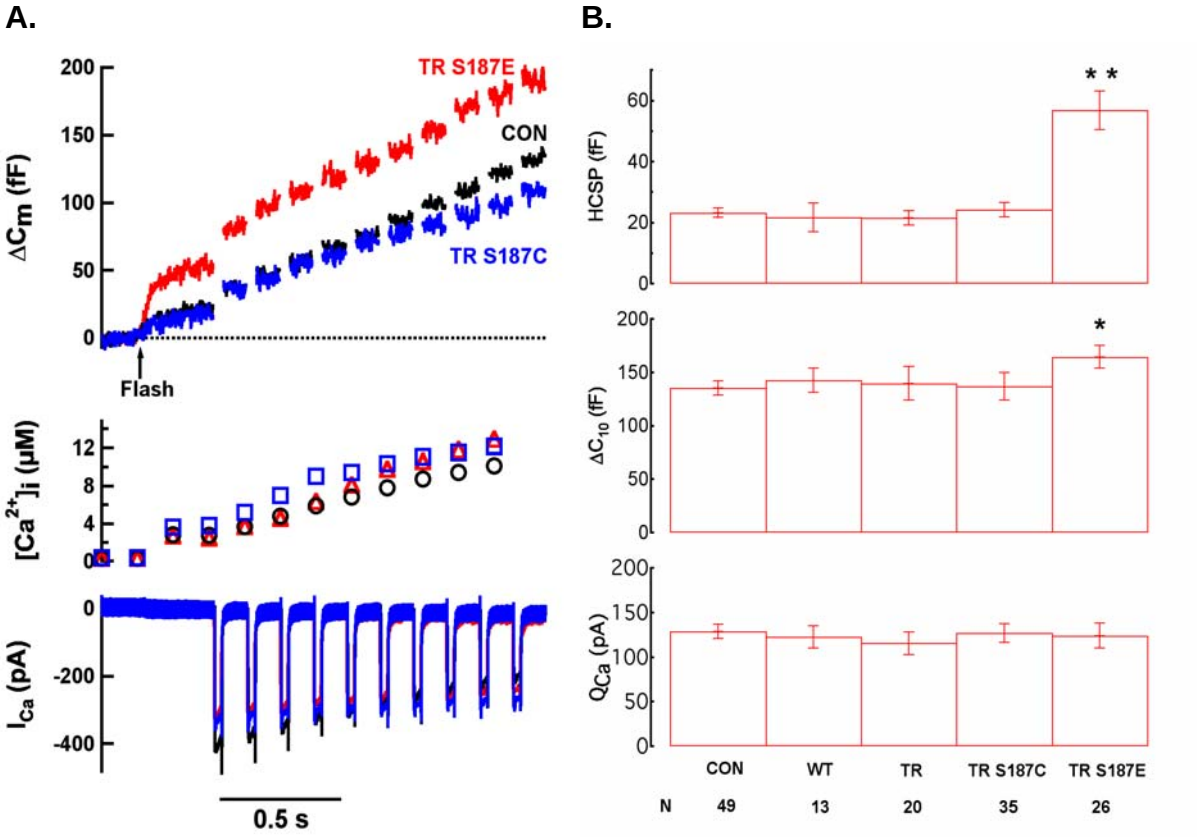

Figure 3.7: The phosphomimetic mutant TR S187E enhances the HCSP and the RRP. A. Sample traces from untransfected control (CON), TR S187E and TR S187C. B. Summary of the effect of expression of SNAP-25 mutants in INS-1 cells. The significance analysis was conducted with the Anova test. "" and "**" correspond to P<0.05 and P<0.001, respectively.*

3.6 Expressing non-phosphorylatable Ser187 mutants of SNAP-25 at Ser187 did not block the enhancement of exocytosis by PMA in INS-1 cells

PMA still enhances exocytosis of both the HCSP and the RRP in bovine adrenal chromaffin cells expressing the non-phosphorylatable Ser187 mutants of SNAP-25 (figure 1.10). A similar result was found in INS-1 cells expressing TR S187C or TR S187E. Figure 3.8A shows sample traces from cells expressing TR S187C with or without PMA treatment. PMA still causes a robust enhancement of exocytosis that is indistinguishable from the effect on untransfected cells. In the summarized data (figure 3.8B), PMA enhanced exocytosis of the HCSP and the RRP in GFP-SNAP-25 (WT) transfected cells also (figure 3.8B). The size of the HCSP (97.05 $\pm$ 19.23 fF, N=22) was increased about 4 fold and the size of ΔC_{10} was increased about 1.5 fold (211.45 $\pm$ 21.57 fF, N=22) compared with the control cells without PMA treatment. A similar enhancement of exocytosis by PMA was found in other test groups (control, WT, TR S187E and TR S187C).

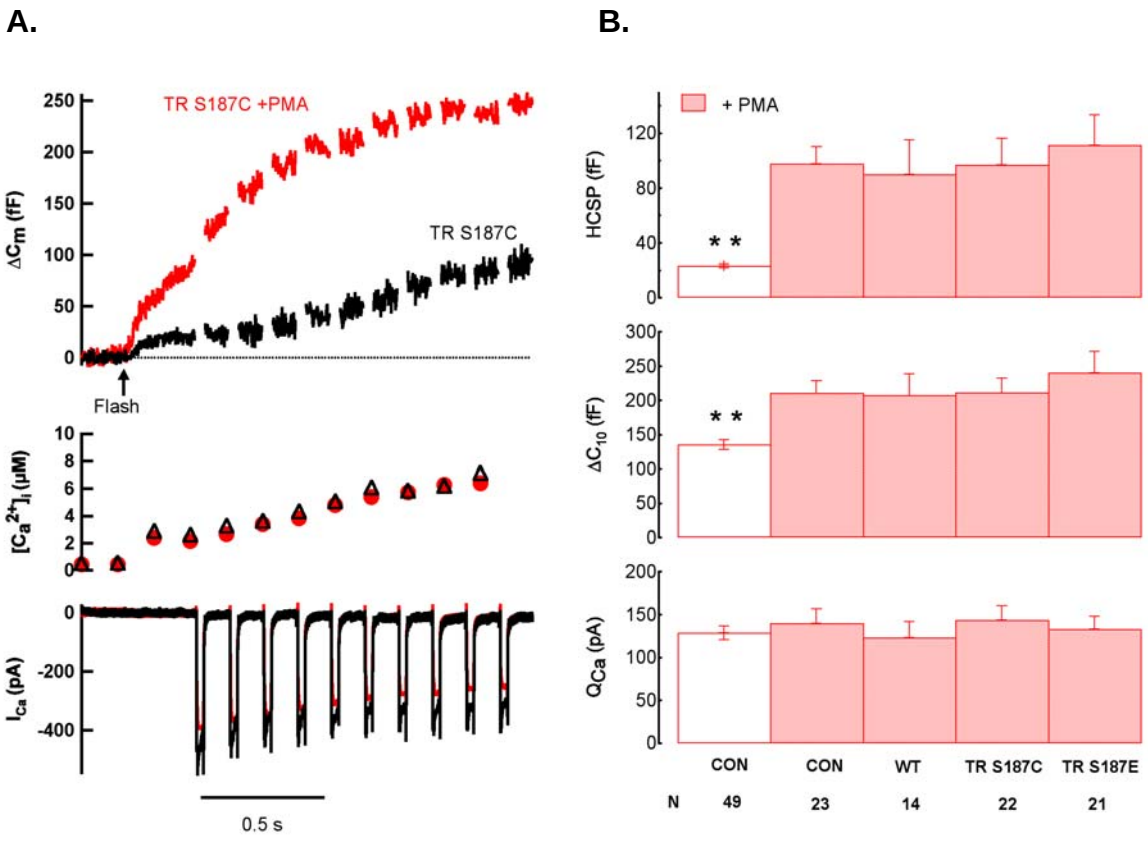

*Figure 3.8: PMA still enhanced exocytosis in cells expressing non-phosphorylatable Ser187 mutants of SNAP-25. (A), Sample traces from TR S187C with or without PMA treatment. (B). Summary of the effect of PMA on exocytosis in cells expressing SNAP-25 mutants. The significance analysis was conducted with the Anova test. "**" means P<0.001.*

I also collected the rate constants of the HCSP from exponential fits of the C_m response to photorelease of caged-Ca^{2+}. The data for the various experimental conditions are compared in Figure 3.9. The rate constants are plotted against the $[Ca^{2+}]_i$ after flash. Note that, although the data show significant scatter, there is a roughly linear relation between the rate of release and the $[Ca^{2+}]_i$ on average. The data show that the phosphomimetic mutation and the

toxin-resistant mutations of SNAP-25 do not change the release kinetics of the HCSP. PMA application also does not affect the rate of release from the HCSP. The enhancement of the size of the HCSP and the RRP by the phosphomimetic mutation or PMA application thus can reasonably be interpreted as affecting the number of vesicles in theses putative pools.

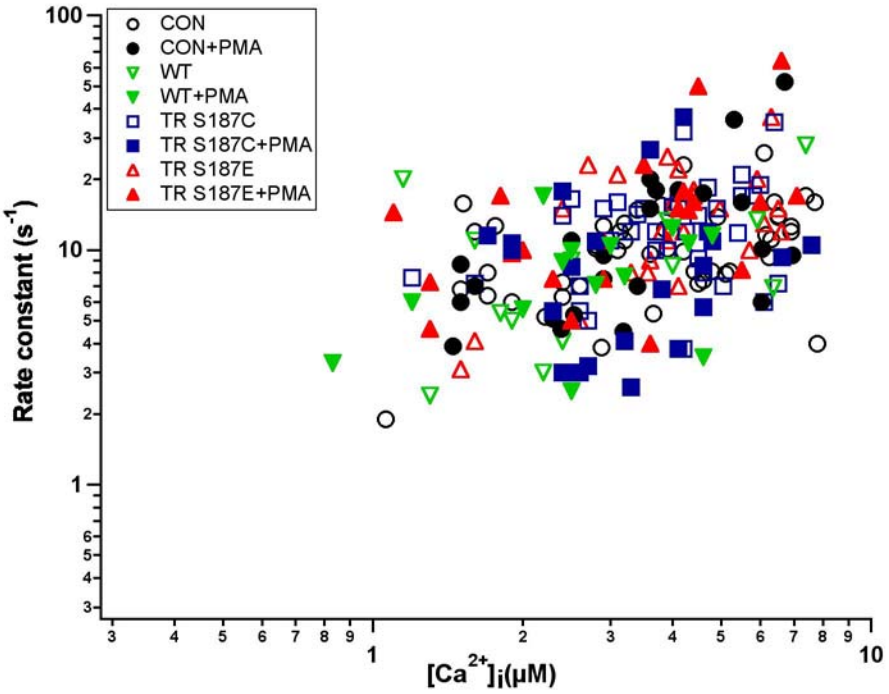

Figure 3.9: The rate constant of the exocytosis of the HCSP was not changed by the phosphomimetic mutation or PMA application. The value of the rate constant was obtained from the exponential fit of the HCSP and plotted against the $[Ca^{2+}]_i$ measured after photorelease of caged-Ca^{2+}.

Based on these results, I conclude that expression of the toxin-resistant mutant has no obvious detrimental effect on exocytosis measured with the high-resolution assays.

3.7 Expression of BoNT/E effectively inhibits exocytosis in INS-1 cells

As discussed above, I planed to test the hypothesis that endogenous SNAP-25 might be responsible for the enhancement effect of PMA on exocytosis in cells expressing Ser187 mutants. My approach is to transfect BoNT/E to cleave the endogenous SNAP-25 and then study whether the SNAP-25 phosphorylation at Ser187 is important for PMA to enhance exocytosis in INS-1 cells.

The first step in this approach is to demonstrate that expression of BoNT/E indeed inhibits exocytosis as expected. Even though I used a 3-fold higher concentration of BoNT/E DNA than the GFP-SNAP-25 DNA, no obvious change in the cell morphology was observed compared with cells transfected with SNAP-25 only (data not shown). However, I did find a decrease in the number of fluorescent cells, which might be due to the toxicity resulting from the increasing total amount of DNA and transfection reagent. Figure 3.10 presents data demonstrating that co-transfection with GFP-SNAP-25 (WT) and BoNT/E dramatically inhibits exocytosis of both the HCSP and the ΔC_{10} (HCSP, 5.21 $\pm$ 0.74 fF; ΔC_{10}, 41.43 $\pm$ 5.36 fF; N=37). 31 out of 37 cells showed almost complete inhibition of exocytosis (HCSP, 4.64 $\pm$ 0.71 fF; ΔC_{10}, 29.82 $\pm$ 3.52 fF; N=31). The remaining cells (6 out of 37) showed an almost normal ΔC_{10} response even though the HCSP was inhibited (HCSP, 8.13 $\pm$ 2.54 fF; ΔC_{10}, 101.42 $\pm$ 5.46 fF; N=6). These results suggest that the great majority of fluorescent cells expressing

GFP-SNAP-25 also expressing BoNT/E. The data also demonstrate that overexpressing “wilde type” SNAP-25 cannot rescue cells from BoNT/E expression. I next tested whether the toxin-resistant mutation of SNAP-25 (TR SNAP-25) could “rescue” exocytosis in cells transfected with BoNT/E. Figure 3.10 demonstrates that co-transfection of BoNT/E had no effect on exocytosis in TR SNAP-25 transfected cells (HCSP, 24.9 $\pm$ 1.95 fF; ΔC_{10}, 137.5 $\pm$ 12.6 fF; N=24).

Note that the Ca^{2+} current in the WT-SNAP-25 plus BoNT/E co-transfected cells was inhibited dramatically (figure 3.10A, B), suggesting that intact SNAP-25 is necessary to support normal Ca^{2+} currents, which was also suggested in previous studies (Wiser, Bennett et al. 1996; Rettig, Heinemann et al. 1997; Andres-Mateos, Renart et al. 2005).

These results confirm that the C-terminus of SNAP-25 is important for exocytosis. They also show that BoNT/E transfection was highly efficient in inhibiting exocytosis in INS-1 cells and the toxin-resistant mutant of SNAP-25 was capable of functionally substituting the BoNT/E-cleaved SNAP-25 to restore normal exocytosis. Further immunoblot data supporting this hypothesis are presented in Chapter 4.

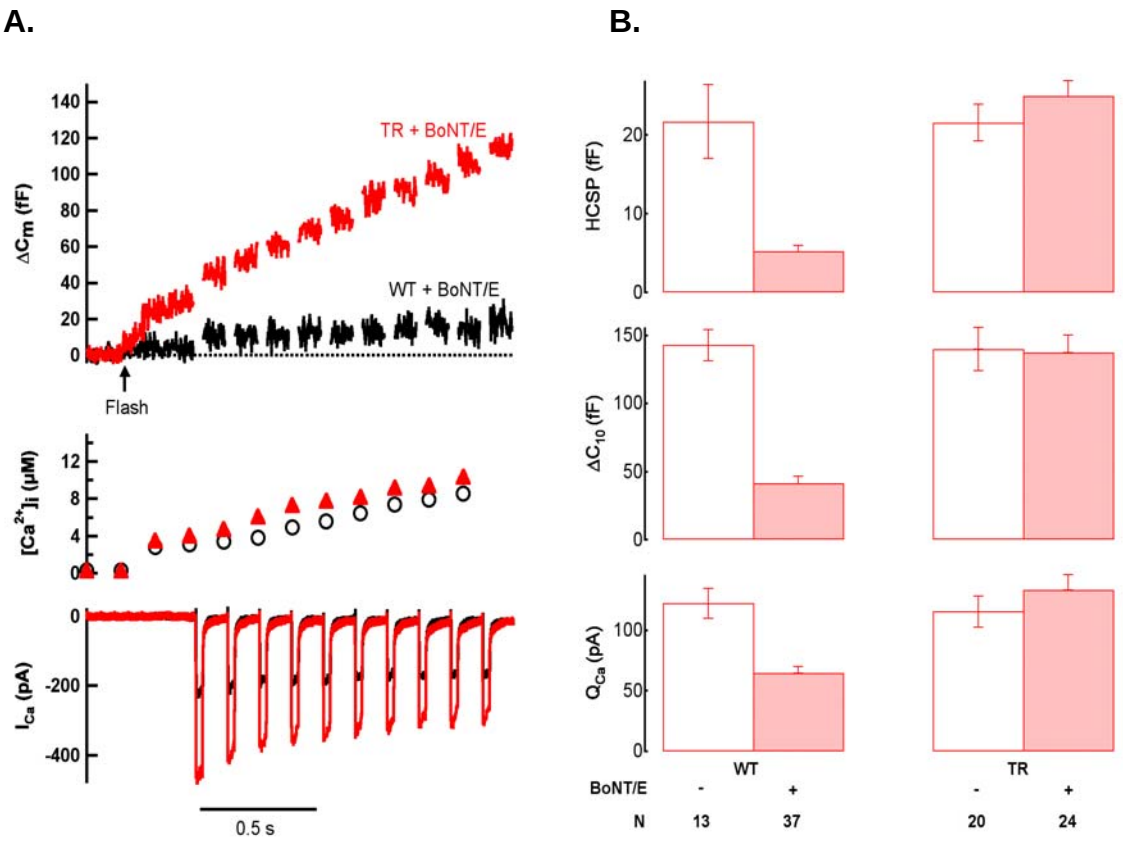

Figure 3.10: Transfection of BoNT/E inhibited exocytosis of the HCSP and the RRP (ΔC_{10}) in INS-1 cells. (A), Sample traces from cells transfected with GFP-SNAP-25 (WT) plus BoNT/E or TR SNAP-25 (TR) plus BoNT/E. (B), Summary of result about the inhibitory effect of BoNT/E on exocytosis of the HCSP and the RRP in INS-1 cells.

3.8 The enhancement of exocytosis by PMA is blocked in cells co-transfected with BoNT/E and the non-phosphorylatable Ser187 mutants of SNAP-25

Using BoNT/E allows us to evaluate the effect of Ser187 mutants of

SNAP-25 in clean background without the interference of the endogenous SNAP-25. I then tested the importance of SNAP-25 phosphorylation at Ser187 in PMA-enhanced exocytosis from cells transfected with BoNT/E. In cells co-transfected with TR SNAP-25 and BoNT/E, PMA enhanced exocytosis of both the HCSP (90.93 $\pm$ 12.63 fF, N=14) and the ΔC_{10} (203.21 $\pm$ 21.8 fF, N=14) in a manner similar to untransfected cells (figure 3.11A, C, compared with figure 3.8B). This indicates that TR SNAP-25 does not interfere with the ability of PMA to enhance exocytosis. In cells co-transfected with GFP-SNAP-25 (WT) and BoNT/E, exocytosis of the HCSP (2.94 $\pm$ 1.34 fF, N=18) and the ΔC_{10} (37.9 $\pm$ 7.97 fF, N=18) was greatly inhibited even with PMA treatment (figure 3.11C). This indicates that the C-terminus of SNAP-25 is important for PMA to enhance exocytosis of the HCSP and the RRP in INS-1 cells.

Perhaps the most significant finding of this dissertation is that I observed no effect of PMA on exocytosis in cells co-expressing BoNT/E and non-phosphorylatable TR S187C (HCSP, 26.26 $\pm$ 2.66 fF; ΔC_{10}, 132.39 $\pm$ 9.4 fF, N=23) (figure 3.11B, C). Furthermore, PMA was ineffective in cells co-transfected with TR S187E and BoNT/E (figure 3.11C). The results also show that BoNT/E did not alter exocytosis in cells expressing the toxin-resistant SNAP-25 (TR, TR S187E and TR S187C). TR S187E still kept its ability to enhance exocytosis of the HCSP and the RRP upon co-transfection with BoNT/E (figure 3.11C). Thus, these results suggest that Ser187 of SNAP-25 is essential for PMA to enhance

exocytosis of the HCSP and the RRP in INS-1 cells. I also measured the rate constant of release from the HCSP in the experiments with BoNT/E. There is no change in the rate constants in these toxin rescue experiments (figure 3.11D, compared with figure 3.9),

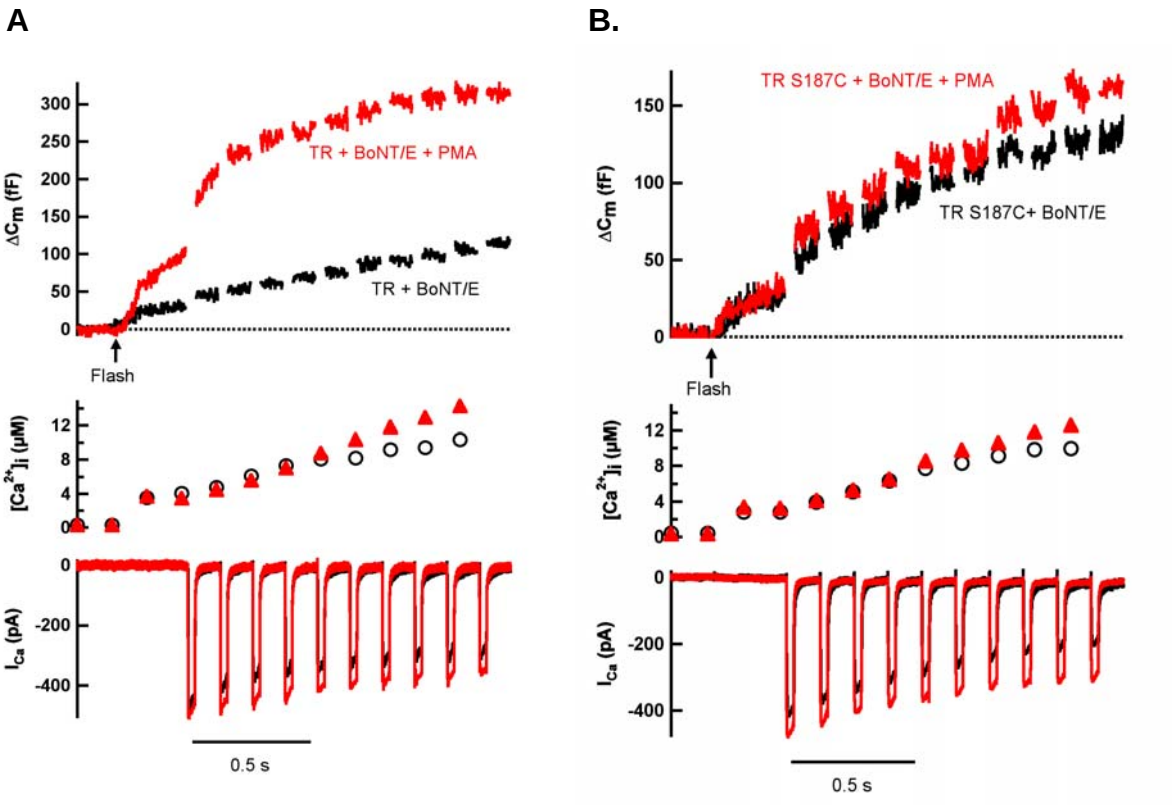

C.

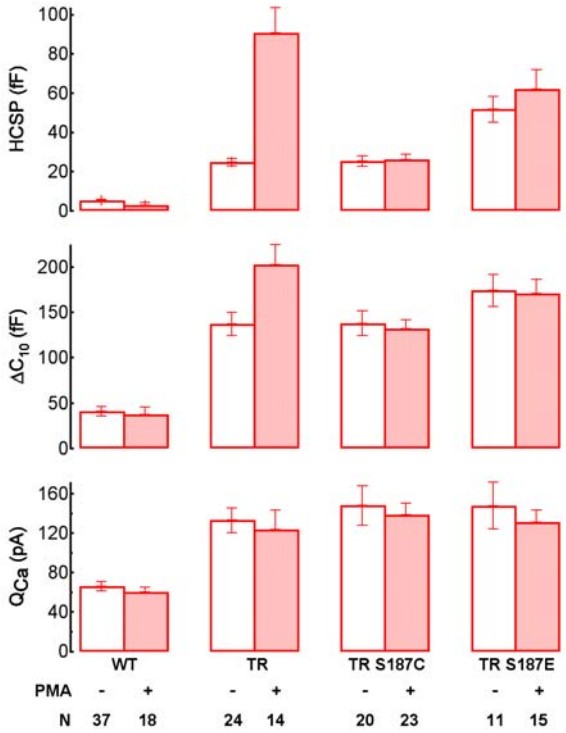

D.

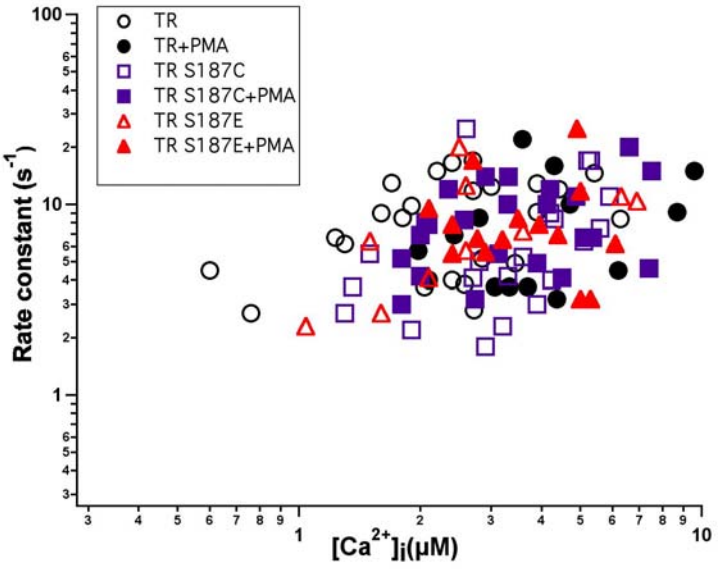

Figure 3.11: PMA is ineffective at enhancing exocytosis in cells expressing the non-phosphorylatable Ser187 mutants of SNAP-25 after the endogenous SNAP-25 was

inactivated by BoNT/E. (A), Sample traces to show that PMA enhances exocytosis in cells transfected with TR SNAP-25 (TR) and BoNT/E. (B), Sample traces to show that co-transfection of TR S187C and BoNT/E blocked PMA-enhancement of exocytosis. C. Data summary. The bars are expressed as Mean ± SEM. D. Rate constants of release from the experiments with BoNT/E as indicated.

3.9 The effect of Ser187 mutations of SNAP-25 on exocytosis of the immediately releasable pool (IRP)

A brief depolarization elicited a very fast component of exocytosis in both neuronal preparations and neuroendocrine cells (Horrigan and Bookman 1994; Hsu and Jackson 1996; Mennerick and Matthews 1996; Giovannucci and Stuenkel 1997; Moser and Neher 1997; Voets, Neher et al. 1999). This ultrafast component is believed to result from fusion of vesicles located near Ca2+ channel, the so-called "immediately releasable pool" (IRP). Studies with photorelease of caged-Ca^{2+} which uniformly elevates $[Ca^{2+}]_i$ in the cell did not find a kinetic component corresponding to the IRP, supporting the hypothesis that the IRP consists of vesicles near Ca^{2+} channel. In a previous study from the Gillis lab, the IRP was probed using a pair of brief depolarizing pulses (Yang, Udayasankar et al. 2002; Yang and Gillis 2004). The IRP was found to remain even after the HCSP was exhausted with the photorelease of caged-Ca^{2+}. This suggested that the IRP

and the HCSP are different vesicle pools. Here, I used the same method to define the IRP as the increase in C_m in response to the first 30 ms depolarizing pulse given following release of the HCSP with photorelease of caged-Ca^{2+}(ΔC_1) (figure 3.12A). ΔC_1 can serve as a rough indicator of the size of the IRP (Yang, Udayasankar et al. 2002). The data in figure 3.12 show that mutations of Ser187 of SNAP-25 also block enhancement of the IRP by PMA. The cells in these groups were all transfected with BoNT/E. BoNT/E transfection inhibited ΔC_1 in GFP-SNAP-25 (WT) transfected cells with or without PMA treatment. The phosphomimetic mutation S187E did not show an obvious enhancement of on ΔC_1 compared with TR or TR S187C. This follows the results withΔC_{10} that show the depolarization-induced exocytosis in INS-1 cells is not very sensitive to the phosphomimetic mutation of SNAP-25. As shown in figure 3.7, TR S187E only enhanced ΔC_{10} by ~15%. However, PMA augmented ΔC_1 dramatically in TR SNAP-25 expressing cells.

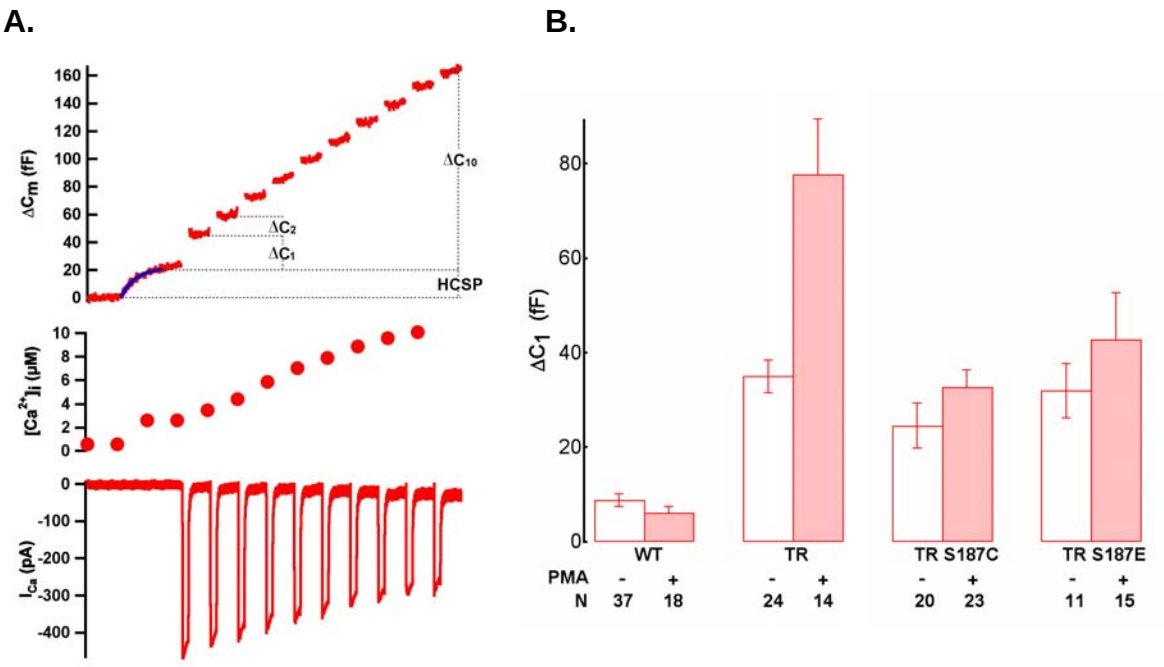

Figure 3.12: Ser187 of SNAP-25 is important for PMA to enhance the IRP. (A), Definition of the IRP by ΔC_1 and ΔC_2. (B), Summary of the effects of PMA on ΔC_1 for SNAP-25 mutations at Ser187. All the cells were transfected with BoNT/E.

Group	Cell #	Pre-flash $[Ca^{2+}]_i$ (μM)	Post-flash $[Ca^{2+}]_i$ (μM)
Control (CON)	49	0.42 $\pm$ 0.2	4.07 $\pm$ 1.85
GFP-SNAP-25 (WT)	13	0.49 $\pm$ 0.13	3.26 $\pm$ 2.08
TR SNAP-25 (TR)	20	0.44 $\pm$ 0.19	2.66 $\pm$ 1.56
TR S187E	26	0.49 $\pm$ 0.22	4.16 $\pm$ 1.42
TR S187C	35	0.49 $\pm$ 0.18	4.07 $\pm$ 1.35
CON + PMA	23	0.44 $\pm$ 0.25	3.66 $\pm$ 1.71
WT + PMA	14	0.52 $\pm$ 0.31	2.88 $\pm$ 1.2
TR S187E + PMA	21	0.48 $\pm$ 0.28	3.51 $\pm$ 1.77
TR S187C + PMA	22	0.45$\pm$ 0.21	3.56 $\pm$ 1.52
WT + BoNT/E	37	0.54 $\pm$ 0.25	2.65 $\pm$ 1.02
TR + BoNT/E	24	0.48 $\pm$ 0.22	2.66 $\pm$ 1.37
TR S187E + BoNT/E	11	0.51 $\pm$ 0.15	3.01 $\pm$ 1.9
TR S187C + BoNT/E	20	0.53 $\pm$ 0.21	3.55 $\pm$ 1.43
WT + BoNT/E + PMA	18	0.45 $\pm$ 0.16	3.31 $\pm$ 2.12
TR + BoNT/E + PMA	14	0.44 $\pm$ 0.27	4.35 $\pm$ 2.33
TR S187E + BoNT/E +PMA	15	0.53 $\pm$ 0.21	3.77 $\pm$ 1.26
TR S187C + BoNT/E + PMA	23	0.45 $\pm$ 0.29	3.72 $\pm$ 1.75

Table 1: Summary of the averaged pre-flash $[Ca^{2+}]_i$ and post-flash $[Ca^{2+}]_i$ from the experiments using "hybrid" protocol. The data is expressed as Mean $\pm$ SD.

CHAPTER 4

DEMONSTRATION OF THE CLEAVAGE OF SNAP-25 BY BONT/E USING IMMUNOBLOTS

Electrophysiological data presented in Chapter 3 show that BoNT/E transfection successfully inhibits exocytosis in INS-1 cells. However, whether the SNAP-25 protein was cleaved by BoNT/E needs to be confirmed. I took advantage of the anti-Pi-SNAP-25 antibody again for this purpose. If SNAP-25 is cleaved by BoNT/E, then the loss of the C terminal fragment will prevent this antibody from recognizing SNAP-25.

4.1 Expression of BoNT/E in INS-1 cells cleaves GFP-SNAP-25 (WT)

Since transfection of BoNT/E inhibited exocytosis in cells expressing GFP-SNAP-25 (WT) (figure 3.10), I first tested whether the GFP-SNAP-25 (WT) was cleaved (figure 4.1). The cells were treated with or without 100 nM PMA and

then subjected to immunobot analysis. Without PMA treatment, no phosphorylation bands were detected even though the GFP-SNAP-25 (52 kDa) was detected by the anti-SNAP-25 antibody. PMA phosphorylated both the endogenous 25 kDa SNAP-25 and the expressed 52 kDa GFP-SNAP-25. The co-expression of BoNT/E with GFP-SNAP-25 (WT) almost completely abolished the phosphorylated GFP-SNAP-25 band (52 kDa). However, the 25 kDa phosphorylated endogenous SNAP-25 band was not greatly changed by expression of BoNT/E. This is because the transfection efficiency is only about 10%. So, ~90% of cells do not express the toxin. Presumbly, on the other hand, the complete loss of the phosphorylated GFP-SNAP-25 band upon toxin expression indicates that the great majority of cells that express GFP-SNAP-25 also express the toxin. This is consistent with the electrophysiological experiments (figure 3.10).

I observed that co-transfection of BoNT/E and SNAP-25 caused a decrease in the number of fluorescent cells compared with the transfection of SNAP-25 alone. This decrease in transfection efficiency is also confirmed here by a slight decrease in the level of expressed GFP-SNAP-25 (figure 4.1A). Therefore, in my analysis of the bands I normalized the phosphorylated 52 kDa GFP-SNAP-25 with the 52 kDa GFP-SNAP-25 in the same group. The transfection of BoNT/E caused a more than 90% decrease in the phosphorylated 52 kDa GFP-SNAP-25 (figure 4.1B). If we consider that the amount of expressed

52 kDa GFP-SNAP-25 is much more than the endogenous 25 kDa SNAP-25 in the transfected cells, we can indirectly infer that the endogenous 25 kDa SNAP-25 is also cleaved by the transfected BoNT/E. More direct demonstration of the cleavage of endogenous SNAP-25 requires sorting transfected cells and then performing immunoblots (section 4.3).

Note that there are two slightly separated endogenous SNAP-25 bands evident in all samples with BoNT/E transfection (figure 4.1A). However, there are no such double bands in the groups without BoNT/E transfection. One of the "double bands" was selected and enlarged in figure 4.1C. I think the lower band is likely to be the truncated endogenous SNAP-25 and the upper one is the intact endogenous SNAP-25. I typically observed that only ~10% of the cells are GFP-positive. The ratio between these two bands is roughly around 10%. This indicates that BoNT/E did cleave part of the endogenous SNAP-25.

Overall, these results strongly support that the transfection of BoNT/E is very effective in cleaving SNAP-25 (exogenous GFP-SNAP-25 or endogenous SNAP-25).

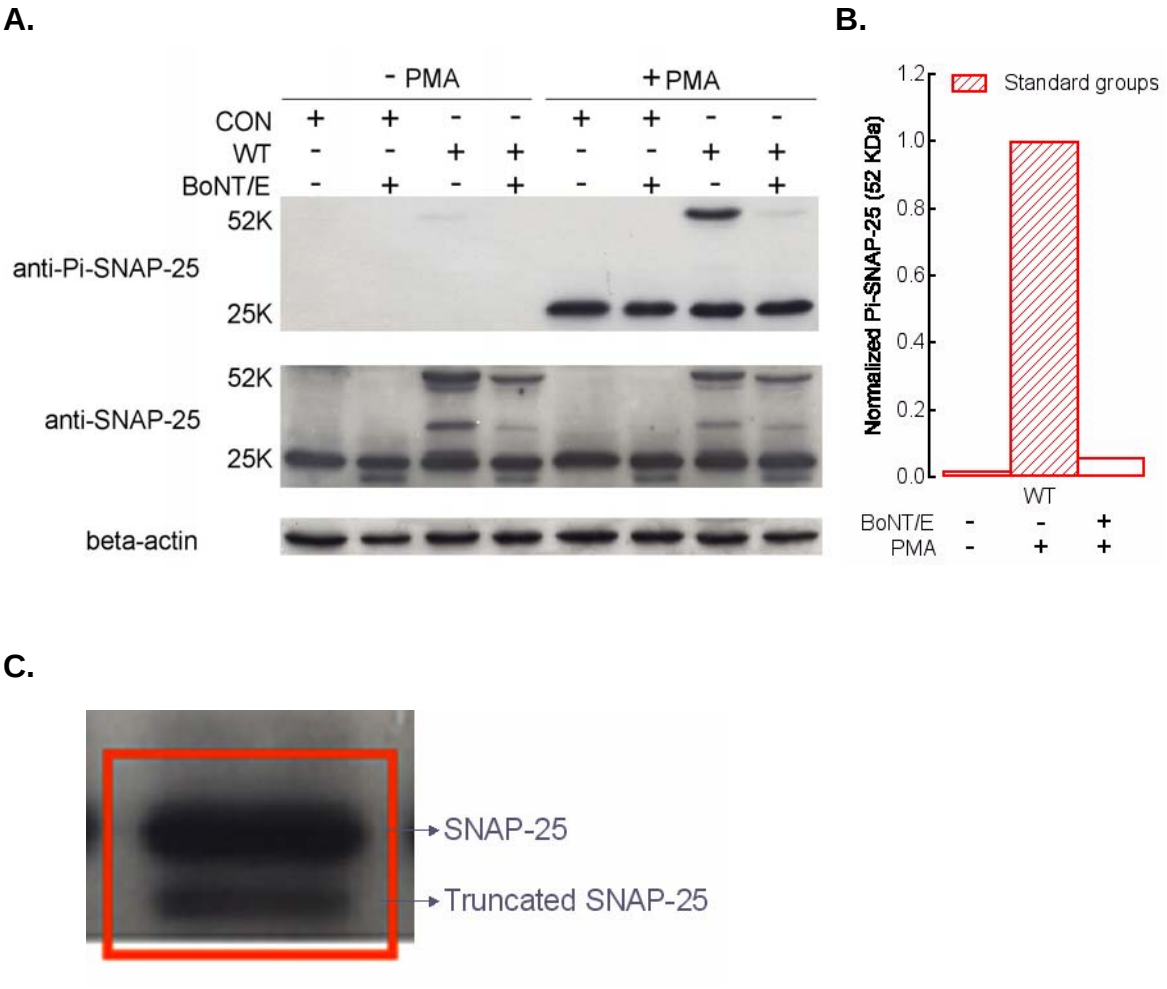

Figure 4.1: BoNT/E cleaves exogenously expressed GFP-SNAP-25 (WT) and endogenous SNAP-25. (A), Immunoblot to show effect of BoNT/E on SNAP-25 in cells transfected with GFP-SNAP-25 (WT). (B), Normalized 52 kDa Pi-SNAP-25 in cells expressing GFP-SNAP-25 (WT). (C), An endogenous SNAP-25 band from cells transfected with BoNT/E.

4.2 Expression of BoNT/E cleaves the great majority of endogenous SNAP-25 demonstrated by cell sorting

The results discussed above indicated that part of the endogenous SNAP-25 was cleaved by BoNT/E. In the electrophysiological experiments, I patch clamped only fluorescence-positive cells, whereas immnoblot experiments probe the entire cell population. In order to quantify the extent of cleavage of endogenous SNAP-25 by BoNT/E expression in fluorescence-positive cells, I sorted cells using Flow cytometry and then performed immunoblots. Both non-fluorescent cells and fluorescent cells were collected and treated with PMA (figure 4.2). To get highly purified fluorescent cells, I set up the threshold value for fluorescent cell separation such that cells with a slight amount of fluorescence were rejected. That is why I still observed some phosphorylated 52 kDa GFP-SNAP-25 in the “non-fluorescent” group. However, the immunoreactivity is much lower than that observed in fluorescent cells. In the fluorescent group, the expressed 52 kDa GFP-SNAP-25 in both the TR SNAP-25 group and the TR SNAP-25 plus BoNT/E group are phosphorylated upon PMA treatment. The relative phosphorylation levels of these two groups are not changed after normalization with the expressed 52 kDa GFP-SNAP-25 (figure 4.2B), consistent with the results of figure 4.1. However, the band from the anti-Pi-SNAP-25 antibody binding to 25 kDa SNAP-25 was completely abolished for toxin co-transfected cells compared with cells not expressing BoNT/E. This result demonstrates that BoNT/E transfection cleaved essentially all the endogenous 25 KDa SNAP-25 in the BoNT/E and SNAP-25 co-transfected cells.

One possible concern is that, even if BoNT/E does not cleave TR SNAP-25, it may bind with a high affinity and thus become inactive for cutting the endogenous SNAP-25. There is no change in the relative amount of 52 kDa phosphorylated GFP-SNAP-25 with or without BoNT/E. This indicates that BoNT/E did not cleave the TR SNAP-25. Nevertheless, expression of TR SNAP-25 did not prevent the BoNT/E from cleaving the endogenous SNAP-25.

A.

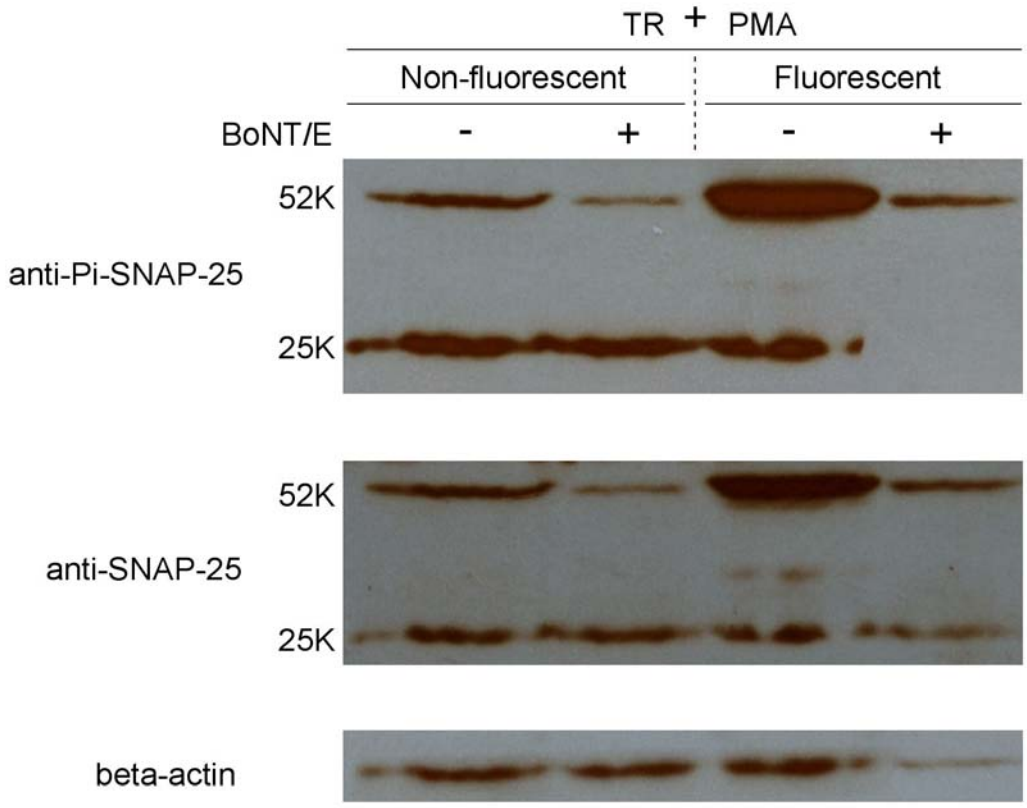

B.

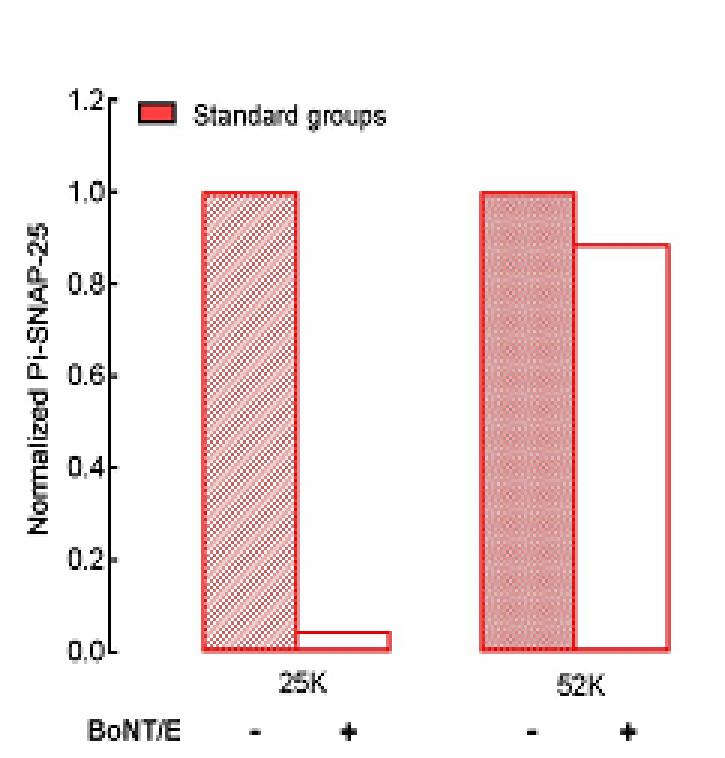

Figure 4.2: BoNT/E cleaves the endogenous SNAP-25 in purified fluorescent cells. (A), Immunoblot assay of the purified cells to show the effect of BoNT/E on SNAP-25. (B), Pi-SNAP-25 (25 kDa and 52 kDa) was normalized to the corresponding SNAP-25.

4.3 Expression of BoNT/E does not cleave toxin-resistant SNAP-25

I also tested whether BoNT/E cleaved other toxin-resistance mutants including TR S187E and TR S187C (figure 4.3). The cells were not sorted by Flow cytometry in this experiment. The TR SNAP-25 was used as the control. Both the endogenous 25 kDa SNAP-25 and the expressed 52 kDa GFP-SNAP-25 are phosphorylated upon treatment with PMA. In TR S187E transfected cells, a

52 kDa Pi-SNAP-25 band was observed without PMA treatment, which is consistent with the result in figure 3.5. PMA induced the phosphorylation of the endogenous 25 kDa SNAP-25 but had no effect on the immunoreactivity of the 52 kDa GFP-SNAP-25 (TR S187E). In both TR SNAP-25 and TR S187E groups, BoNT/E expression did not change the level of the phosphorylated 52 kDa GFP-SNAP-25 after normalized to the 52 kDa GFP-SNAP-25 detected with the N-terminal SNAP-25 antibody (figure 4.3B). In TR S187C transfected cells, the endogenous 25 kDa SNAP-25 was phosphorylated but there was no phosphorylated 52 kDa GFP-SNAP-25. I also observed the “double bands” of endogenous SNAP-25 in the groups with BoNT/E. This indicated the BoNT/E was functional.

A.

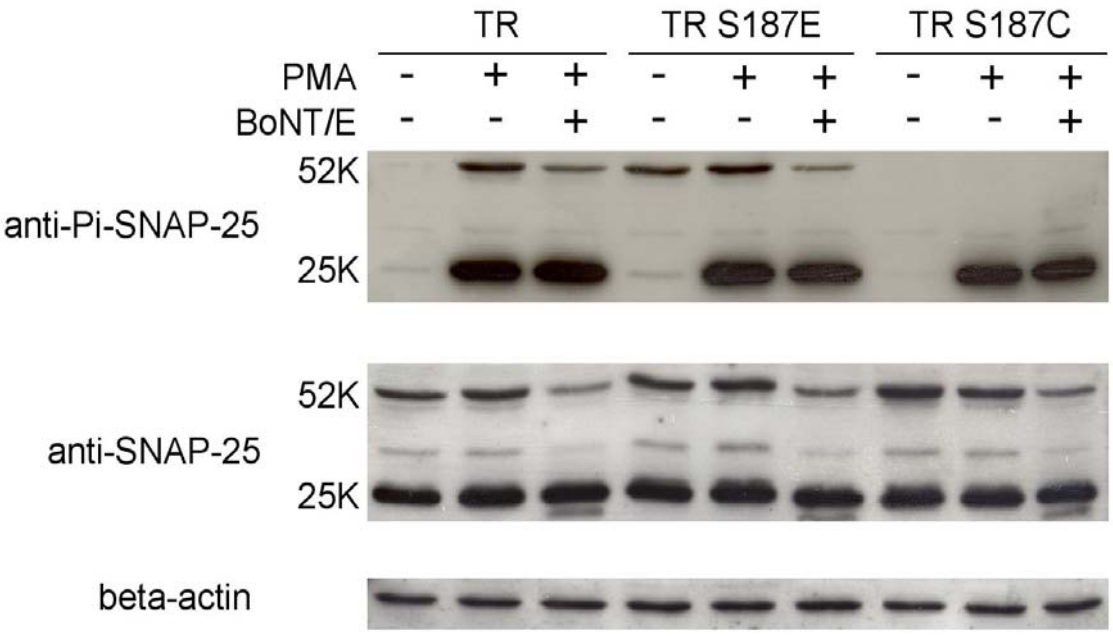

B.

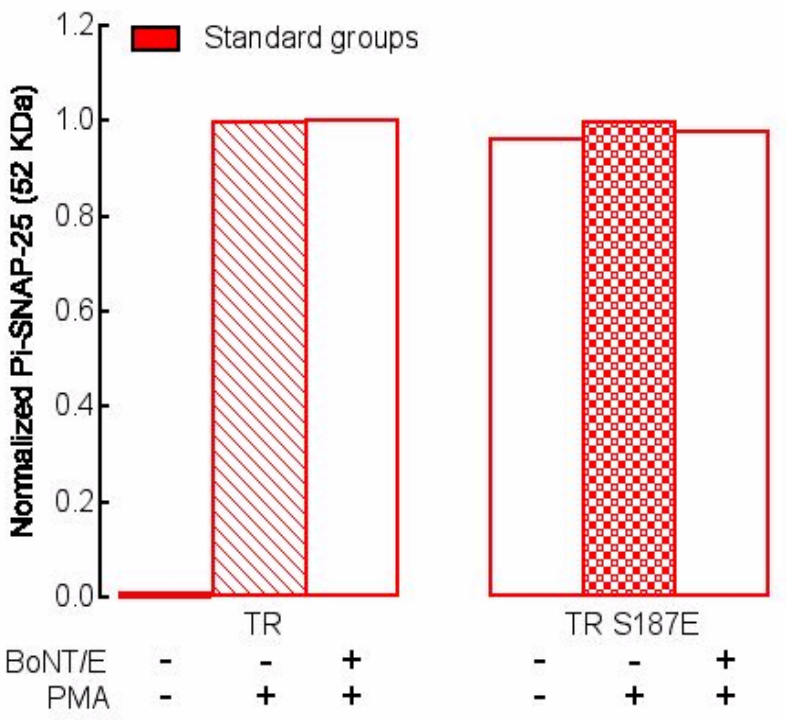

Figure 4.3: BoNT/E had no effect on toxin-resistant Ser187 mutants of SNAP-25. (A), Immunoblot assay to show the effect of BoNT/E on SNAP-25. (B), Pi-SNAP-25 (52 kDa) was normalized to SNAP-25 (52 kDa) in TR and TR S187E groups.

CHAPTER 5

EXPLORING THE IMPORTANCE OF SNAP-25 PHOSPHORYLATION AT SER187 IN EXOCYTOSIS AT HIGH $[Ca^{2+}]_i$ IN INS-1 CELLS

In the study described in chapter 3, I had been using a “hybrid” protocol to assay exocytosis induced by low $[Ca^{2+}]_i$ (the HCSP evoked by photorelease of caged-Ca^{2+}) and membrane depolarization (the RRP or ΔC_{10}). Whereas this protocol provides detailed information about the kinetics of exocytosis at the low $[Ca^{2+}]_i$, limited information is obtained about exocytosis evoked by higher $[Ca^{2+}]_i$. ΔC10 elicited by depolarization-evoked Ca^{2+} influx gives a crude idea of the size of the less Ca^{2+}-senstive RRP. I found the BoNT/E had a large effect on the Ca^{2+} current in GFP-SNAP-25 (WT) transfected cells (figure3.10). Therefore, it is difficult to conclude much about the size of the RRP under this condition. The best way to characterize the size and release kinetics of the RRP is through photorelease of caged-Ca^{2+} to high $[Ca^{2+}]_i$ (usually > 20 μM) because the $[Ca^{2+}]_i$ stimulus is spatially uniform and is approximately constant in time. Most of the previous studies about exocytosis using photorelease of caged-Ca^{2+} have been

carried out at levels of $[Ca^{2+}]_i$ around 20 – 50 μM. I thus carried out a set of experiments to ask if phosphorylation of SNAP-25 at Ser^{187} has different effects on exocytosis at high $[Ca^{2+}]_i$.

5.1 The Kinetics of exocytosis in INS-1 cells induced by high $[Ca^{2+}]_i$

INS-1 cells were studied in the whole-cell patch-clamp configuration and caged-Ca^{2+} and Ca^{2+} fluorescent dyes (Bisfura-2 and Fura2-ff) were delivered into cells through the patch clamp pipette. An intensive UV flash was applied to elevate the $[Ca^{2+}]_i$ up to about 20 μM. A second flash was applied about 90 seconds later to probe recovery of exocytosis (Nagy, Matti et al. 2002). Here, I directly tested the importance of SNAP-25 phosphorylation at Ser187 in exocytosis in cells of which the endogenous SNAP-25 was inactivated by BoNT/E. Cells transfected with TR SNAP-25 were compared with cells expressing Ser187 mutants of TR SNAP-25.

Photorelease of caged-Ca^{2+} usually induces at least two kinetic components of exocytosis, i.e., the resulting increase in capacitance is fitted by at least 2 exponentials (Neher and Zucker 1993; Kasai, Takagi et al. 1996; Takahashi, Kadowaki et al. 1997). In INS-1 cells, I observed high $[Ca^{2+}]_i$ from photorelease of caged-Ca^{2+} induced a fast but small amplitude component

(C_m-fast) followed by a slower but larger amplitude component (C_m-slow) in most of the cells examined (Figure 5.1). A sharp but small decrease in capacitance after the fast component was reported in pancreatic beta cells and presumably reflects a fast phase of endocytosis (Takahashi, Kadowaki et al. 1997). However, INS-1 cells did not show a similar phenomena in my study. Both the 1st flash and the second flash elicited the same biphasic pattern of exocytosis except there was a decrease in the total size of the response to the 2nd flash (e.g., figure 5.3). This is presumably because releasable vesicles cannot be completely replenished within 90 s of their exhaustion by the 1st flash.

If the $[Ca^{2+}]_i$ after the flash was too high (> 50 μM), many cells showed a rapid decrease in capacitance which may be due to endocytosis after strong stimulation(data not shown). In addition, the rate of capacitance increase was saturated at $[Ca^{2+}]_i$ > 50 μM (Takahashi, Kadowaki et al. 1997). Therefore, I limited my study to $[Ca^{2+}]_i$ < 50 μM. The pre-flash $[Ca^{2+}]_i$ and post-flash $[Ca^{2+}]_l$ for each group of cells in this chapter are summarized in the end of this chapter in table 2 (Page 89).

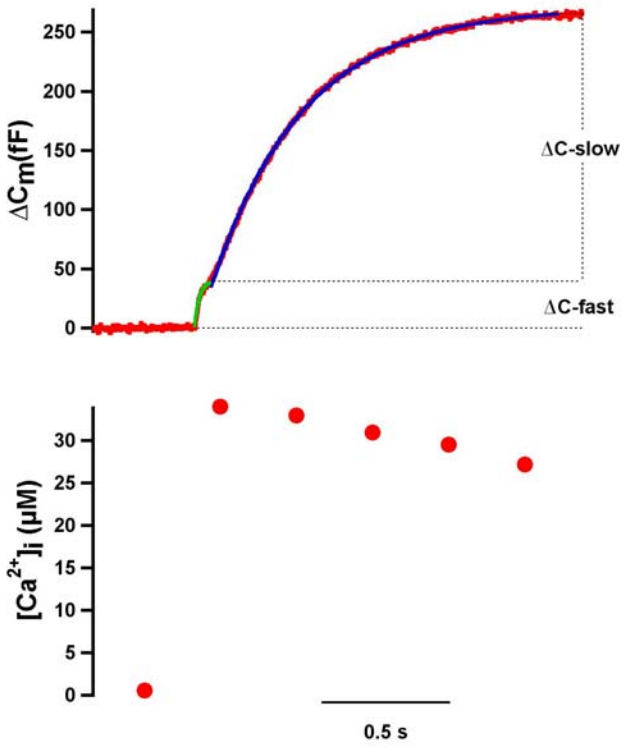

Figure 5.1: A sample trace to show the biphasic kinetics of exocytosis in response to photorelease of caged-Ca^{2+} to above 20 μM in INS-1 cells. The fast (green) and slow (blue) phases are fitted with double exponentials.

5.2 Expression of BoNT/E inhibits exocytosis induced by high $[Ca^{2+}]_i$ in INS-1 cells

I first tested the inhibitory effect of expression of BoNT/E on exocytosis at high $[Ca^{2+}]_i$. The capacitance response was measured from cells co-transfected with BoNT/E and GFP-SNAP-25 (WT) or TR SNAP-25 (TR) (figure 5.2A). The

trace was fitted with two exponentials to obtain the amplitudes of ΔC_m-fast and ΔC_m-slow as well as the rate constants of release (K-fast and K-slow). Here I only show the response from the 1st flash experiment. In some of the cells transfected with GFP-SNAP-25 (WT) and BoNT/E, exocytosis in response to the 2nd flash was completely blocked. Compared with the cells expressing TR SNAP-25, the overall exocytosis in the cells expressing GFP-SNAP-25 (WT) was greatly, but not totally inhibited (figure 5.2A). Surprisingly, upon analysis, I found that the ΔC_m-fast was not affected (WT, 19.61 ± 2.45 fF, N=28; TR, 25.57 ± 3.8 fF, N=21) but ΔCm-slow was inhibited (WT, 81.96 ± 8.66 fF, N=28; TR, 264.43 ± 17.94 fF, N=21) (figure 5.2B).

A.

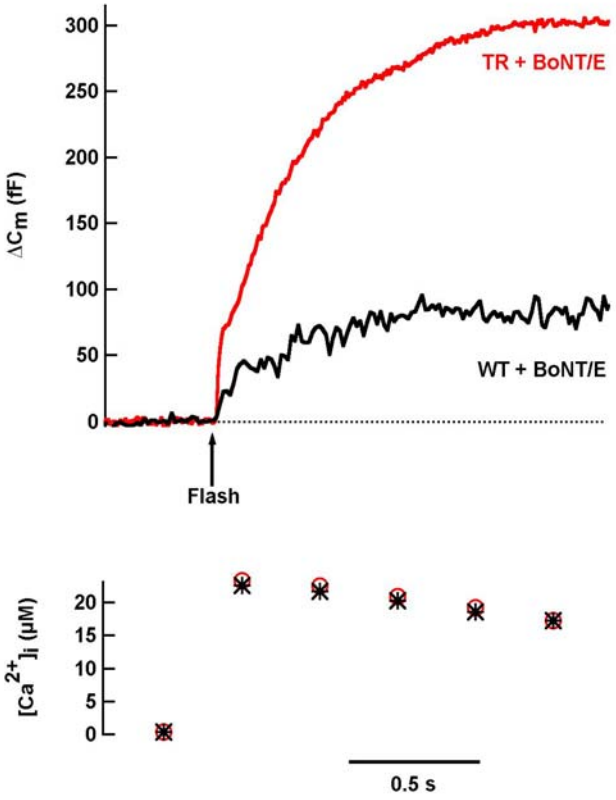

B.

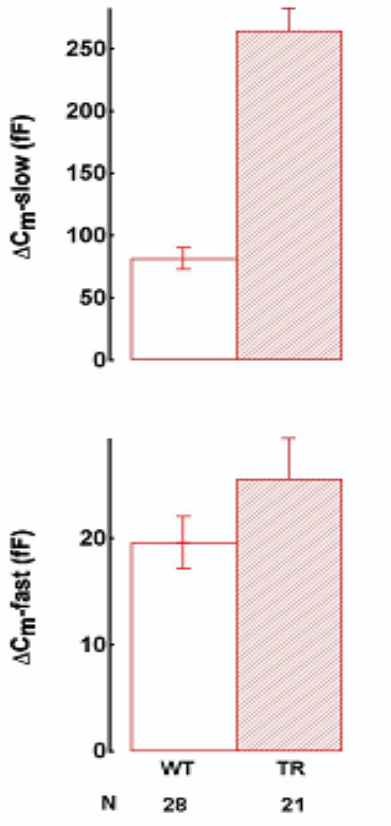

Figure 5.2: BoNT/E inhibited exocytosis in INS-1 cells at high $[Ca^{2+}]_i$. (A), Sample traces from cells transfected with BoNT/E plus GFP-SNAP-25 (WT) or TR SNAP-25 (TR). (B), Summary of result. ΔCm-fast and ΔCm-slow1 were obtained with the exponential fits of t*he capacitance traces. Data are expressed as mean ± SEM.*

Note that this result is different from what I got with the "hybrid" protocol, in which the response to elevation of Ca^{2+} (the HCSP) and the response to depolarization (ΔC_{10}) were almost completely inhibited (figure 3.10). This suggests that higher $[Ca^{2+}]_i$ can partially overcome the defect in exocytosis caused by the truncation of the 26 amino acid residue from the C-terminus of SNAP-25 by BoNT/E. Previous reports demonstrate that high $[Ca^{2+}]_i$ partially rescues exocytosis from cells intoxicated with BoNT/A which cleaves 9 amino acid residues from the C-terminal of SNAP-25 (Lawrence, Foran et al. 1996; Capogna, McKinney et al. 1997) (figure 3.2). The BoNT/E-truncated SNAP-25 may still be able to bind with other SNARE proteins and form a "truncated" core complex. This "truncated" core complex may be partially effective at participating in exocytosis at high, but not low, $[Ca^{2+}]_i$.

5.3 Enhancement of exocytosis by the phosphomimetic mutant TR S187E TR at high $[Ca^{2+}]_i$

In bovine adrenal chromaffin cells, the phosphomimetic mutants of SNAP-25 (S187E or S187D) enhance the sustained component of exocytosis following photorelease of caged-Ca^{2+} to high levels (Nagy, Matti et al. 2002). Other mutants of SNAP-25 (S187A and S187C) cause an obvious inhibition of exocytosis in response to the 2nd flash in that study. The authors conclude that SNAP-25 phosphorylation at Ser187 is important for vesicle recruitment because the late sustained component is thought to correspond to this process. The findings in INS-1 cells are similar, but not identical (figure 5.3). The phosphomimetic mutant TR S187E enhanced exocytosis in response to both the 1st flash and the 2nd flash, with the greatest effect being enhancement of the amplitude of the fast components (figure 5.3A, B). However, the non-phosphomimetic mutant TR S187C has no effect on the response to the 1st flash and reduces the slow component of exocytosis in response to the 2nd flash (figure 5.3A, B).

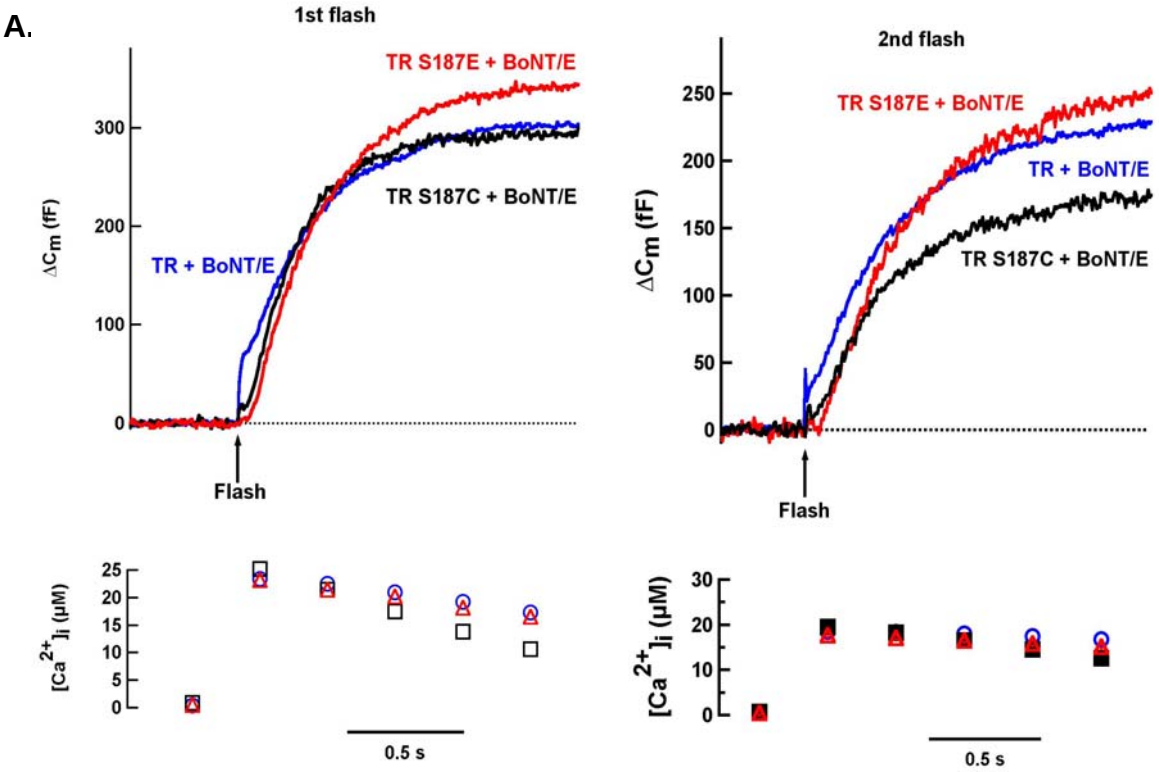
A.
1st flash
2nd flash
TR S187E + BoNT/E
TR + BoNT/E
TR S187C + BoNT/E
ΔCm (fF)
Flash
[Ca2+]i (μM)
0.5 s

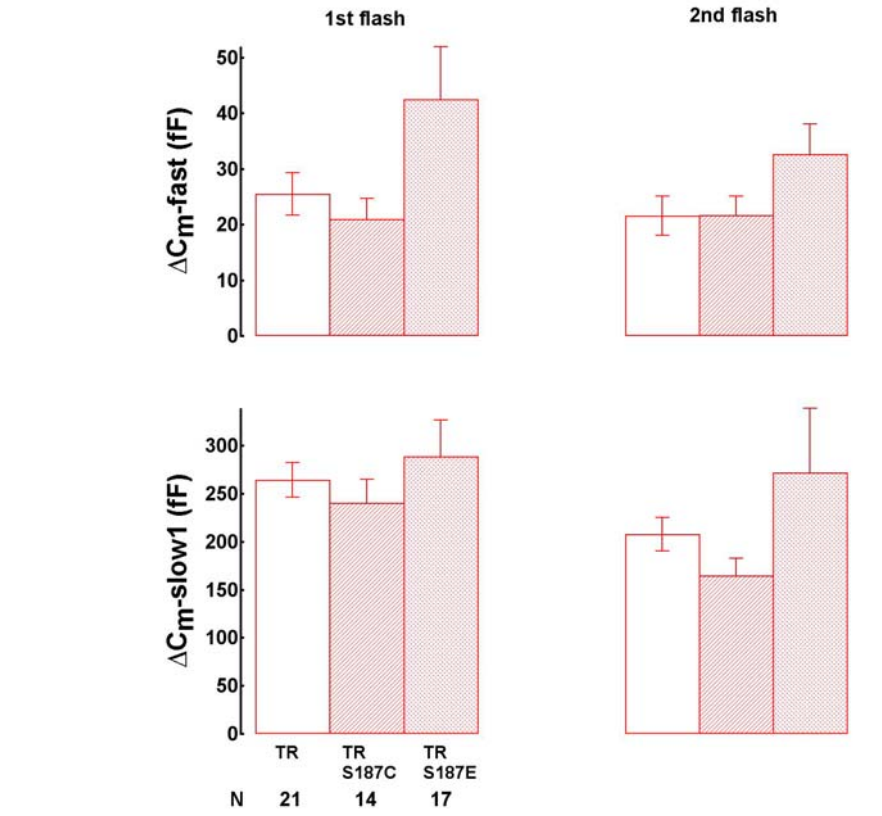
B.
1st flash
2nd flash
ΔCm-fast (fF)
ΔCm-slow1 (fF)
TR
TR S187C
TR S187E
N 21 14 17

Figure 5.3 A phosphomimetic mutation of SNAP-25 at Ser187 enhances exocytosis but a non-phosphorylatable Ser187 mutation reduced exocytosis in response to the 2nd flash. (A), Sample traces in response to the 1st and 2nd flash from cells transfected with BoNT/E plus TR SNAP-25 (TR), TR S187E or TR S187C. (B), Summary of results.

5.4 Most of the PMA-enhanced exocytosis was blocked in cells transfected with BoNT/E and the non-phosphorylatable Ser187 mutants of SNAP-25

I next applied PMA to cells co-transfected with BoNT/E and TR SNAP-25 mutants. In cells co-transfected with GFP-SNAP-25 (WT) and BoNT/E, PMA still had some effect on exocytosis (sample trace not shown). ΔCm-fast is enhanced, but ΔCm-slow is not (figure 5.4B). This could also be explained by the residual function of the "truncated" SNAP-25 at high $[Ca^{2+}]_i$ but not at low $[Ca^{2+}]_i$. On the other hand, this effect of PMA is unlikely to be mediated by phosphorylation of Ser187 of SNAP-25.

PMA enhanced exocytosis in BoNT/E and TR SNAP-25 co-transfected cells (figure 5.4A). ΔCm-fast was much more sensitive to PMA application than ΔCm-slow (figure 5.4B), which is reminiscent of the effect of PMA on the HCSP versus ΔC_{10}. It is not clear whether there are some correlations between the HCSP and the ΔCm-fast, which may need further study. The effects of PMA were

partially blocked in BoNT/E and TR S187C co-transfected cells (figure 5.4A). In particular, the S187C mutation entirely blocked the effect of PMA on enhancement of ΔCm-slow and partially blocked the enhancement of ΔCm-fast (~ 65%) (figure 5.4B).

I also obtained rate constants of release from the double exponential fits. The Ser187 mutations and PMA application do not affect the rate constants of release (figure 5.4C).

In summary, all the data suggest that phosphorylation of SNAP-25 at Ser187 is important for PMA to enhance exocytosis. However, whereas the enhancement of exocytosis by PMA evoked by low $[Ca^{2+}]_i$ is absolutely dependent on Ser187 phosphorylation, the enhancement of exocytosis by PMA driven by higher $[Ca^{2+}]_i$ may involve other mechanisms.

A.

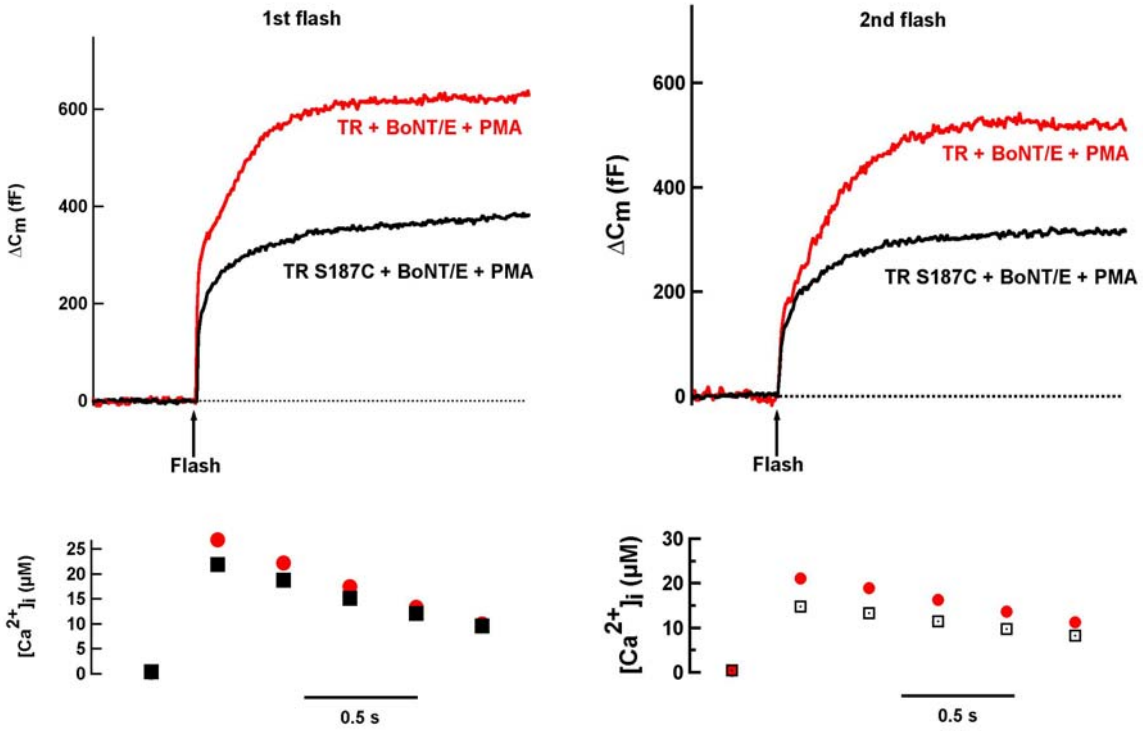

B.

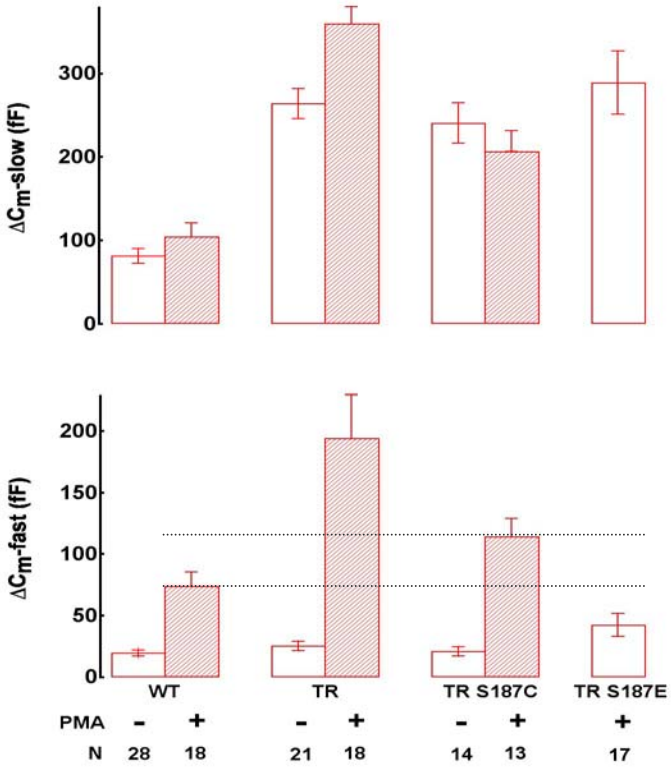
ΔCm-slow (fF)
300
200
100
0
ΔCm-fast (fF)
200
150
100
50
0
WT
TR
TR S187C
TR S187E
PMA - + - + - + +
N 28 18 21 18 14 13 17

C.

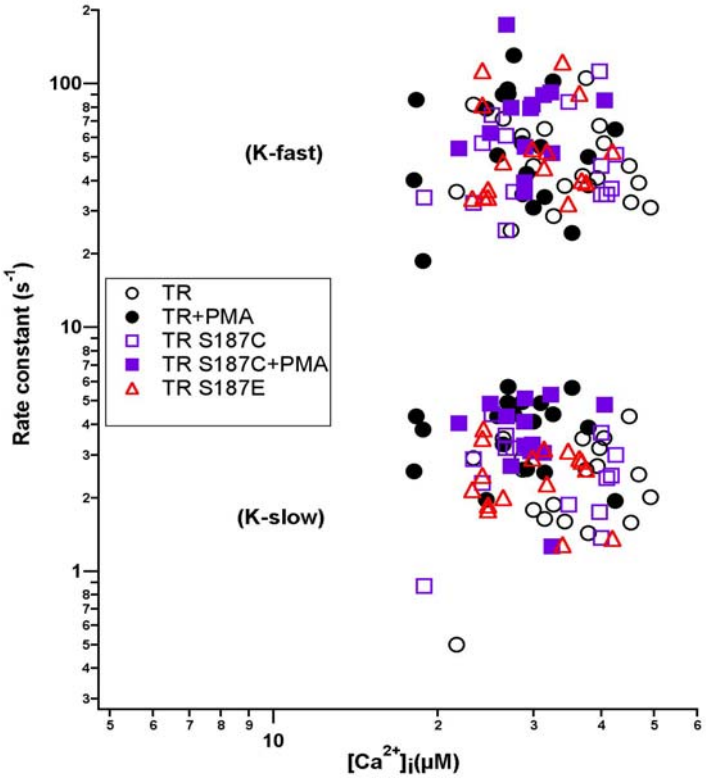
Rate constant (s-1)
100
10
1
(K-fast)
(K-slow)
TR
TR+PMA
TR S187C
TR S187C+PMA
TR S187E
5 6 7 8 9 10 2 3 4 5 6
[Ca2+]i(μM)

Figure 5.4: A non-phosphorylatable mutation of SNAP-25 at Ser187 blocked most of the enhancement of exocytosis by PMA at high $[Ca^{2+}]_i$ if the endogenous SNAP-25 was inactivated. (A), Sample traces from cells transfected with BoNT/E plus TR SNAP-25 (TR) or TR S187C with or without PMA treatment. (B), Summarized data. (C), Rate constants of the fast component and the slow component were plotted against the post-flash $[Ca^{2+}]_i$ right after the flash.

Group (+ BoNT/E)	Cell #	1st flash		2nd flash	
		Pre-flash $[Ca^{2+}]_i$ (μM)	Post-flash $[Ca^{2+}]_i$ (μM)	Pre-flash $[Ca^{2+}]_i$ (μM)	Post-flash $[Ca^{2+}]_i$ (μM)
GFP-SNAP-25 (WT)	28	0.47 ± 0.16	26.66 ± 7.33	0.46 ± 0.17	27.81 ± 5.9
TR SNAP-25 (TR)	21	0.47 ± 0.15	36.19 ± 9.13	0.50 ± 0.17	31.04 ± 8.65
TR S187C	14	0.49 ± 0.17	32.31 ± 8.36	0.51 ± 0.18	25.4 ± 8.98
TR S187E	17	0.51 ± 0.1	29.43 ± 7.07	0.49 ± 0.07	22.63 ± 7.76
WT + PMA	18	0.46± 0.14	32.14 ± 12.18	0.45± 0.15	27.14 ± 12.34
TR + PMA	18	0.41 ± 0.11	28.45 ± 6.43	0.55 ± 0.28	22.37 ± 7.8
TR S187C + PMA	13	0.43 ± 0.06	29.55 ± 4.42	0.43± 0.1	24.92 ± 3.31

Table 2: Summary of the averaged pre-flash $[Ca^{2+}]_i$ and post-flash $[Ca^{2+}]_i$ from the experiments using photoelevation of $[Ca^{2+}]_i$ to high levels (~ 20 – 50 μM). The data is expressed as Mean ± SD.

CHAPTER 6

PRELIMINARY STUDY OF THE IMPORTANCE OF SNAP-25 PHOSPHORYLATION AT SER187 IN SYNAPTIC TRANSMISSION IN RAT HIPPOCAMPAL NEURONS

It would be interesting to extend the study of the role of Ser187 of SNAP-25 in exocytosis from endocrine cells to neurons. Here I described some preliminary experiments to study synaptic transmission in rat hippocampal neurons.

PKC-activating agents such as PMA increase the rate of both spontaneous transmitter release (Parfitt and Madison 1993; Capogna, Gahwiler et al. 1995; Waters and Smith 2000) and stimulus-evoked responses in neuronal preparations (Malenka, Madison et al. 1986; Malinow, Madison et al. 1988; Muller, Turnbull et al. 1988) (Parfitt and Madison 1993; Capogna, Gahwiler et al. 1995; Waters and Smith 2000). SNAP-25 phosphorylation at Ser187 can be induced by PMA or depolarization in hippocampal neurons (Genoud, Pralong et al. 1999; Finley, Scheller et al. 2003). A previous study using phosphomimetic mutants of SNAP-25 at Ser187 reports that the phosphorylation of SNAP-25 at Ser187 does

not mediate the enhancement of hippocampal synaptic transmission by PMA in CA3 pyramidal cells in organotypic hippocampal slices (Finley, Scheller et al. 2003). However, this brief report represents only a modest effort at understanding the roles of SNAP-25 phosphorylation at Ser187 in synaptic transmission.

The postsynaptic response measured at a synapse in response to an action potential consists of at least 2 kinetic components (Stevens 2003). At hippocampal synapses, the largest component (>90%) of the postsynaptic response occurs within several milliseconds of the action potential and has been referred to as “phasic” release of transmitter. This is followed by a much smaller phase that lasts for tens of milliseconds and is termed “asynchronous” release. In addition, there is spontaneous release of individual quanta of neurotransmitter. It has been suggested that these three release processes may be mediated by different mechanisms, differentially regulated, and have different roles in neurodevelopment or neurophysiology (Stevens 2003). Here I proposed to begin the process of relating these release processes to vesicle pools defined from photorelease of caged-Ca^{2+} in order to gain a greater mechanistic understanding of synaptic transmission. This part described my initial efforts on this project.

6.1 Autapses from patterned microisland culture of hippocampal neurons

Autapses from microisland cultures of hippocampal neurons have been widely used in studying the molecular mechanisms of synaptic transmission (Bekkers and Stevens 1991; Tong and Jahr 1994; Feng, Chi et al. 2002; Nishiki and Augustine 2004; Nishiki and Augustine 2004). An autapse is formed if a neuron synapses onto itself (Mennerick, Que et al. 1995). The main advantage of this configuration is that a single patch-clamp pipette can be used to excite the presynaptic cell and record the post-synaptic response. In addition, autaptic responses are more homogeneous than normal synaptic responses (Mennerick, Que et al. 1995). In general, in traditional *in vitro* neuronal cell cultures on homogeneous substrates, it is nearly impossible to find autaptic synapses because of complicated connections within neuronal networks. In many cases, it is also found that autapses are intermixed with synapses from neighboring neurons. To increase the odds of inducing the formation of autapses in cell culture, I planed to utilize micropatterning techniques.

In the late 1990's, methods for micropatterning neuronal cell cultures using "soft" lithography with PDMS (polydimethylsiloxane) stamps were introduced (Branch, Corey et al. 1998; Folch and Toner 1998). Later, many cell types were patterned by this method such as human umbilical vein endothelial cells (HUVEC)

(De Silva, Desai et al. 2004), cortical neurons (Vogt, Lauer et al. 2003) and hippocampal neurons (Liu, Coulombe et al. 2000; Kam, Shain et al. 2001).

In this study, the dissociated hippocampal neurons were plated on the microislands formed by stamping collagen spots (100 – 150 μm in diameter) on agarose. The collagen supports neuron attachment and neurite outgrowth, whereas neuritis will seldom enter the “non-permissive” agarose regions. Thus, neurites grow within the collagen islands and form synapses onto the same or other neurons in the island. If, by chance, only one neuron falls on the island, then autapses may form (figure 6A).

A. **B.**

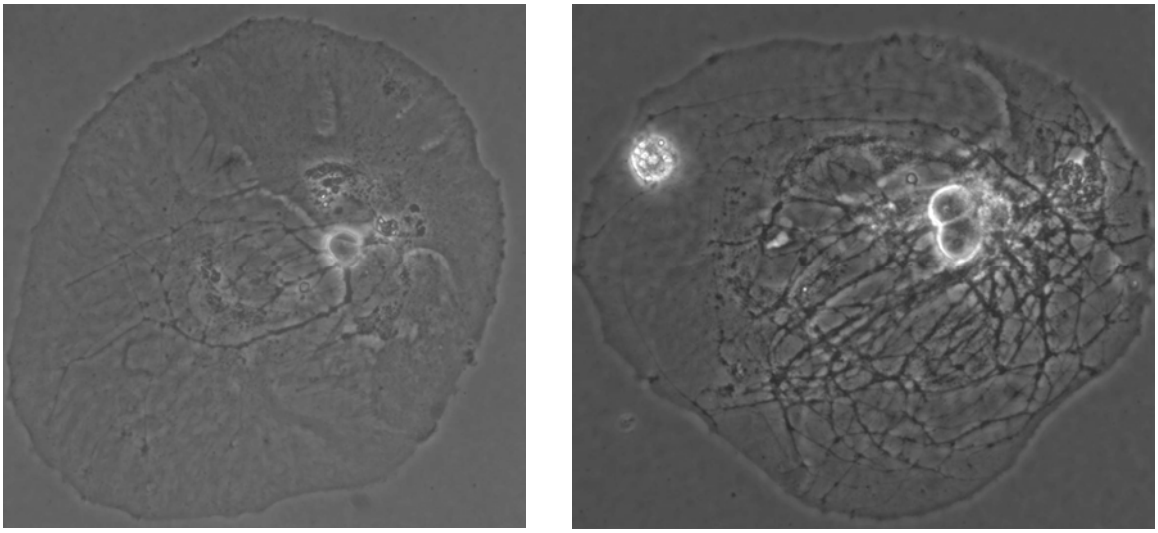

Figure 6: Rat hippocampal neuronal culture on microislands. (A), Example of autapses obtained from the prepatterned microisland culture of hippocampal neurons. (B), Example of two hippocampal neurons in one microisland. The diameter of the microisland is around 100μm.

6.2. Expression of SNAP-25 and BoNT/E in cultured hippocampal neurons

I made some preliminary attempts at transfecting cultured hippocampal neurons using the lipofectamine 2000 reagent. Initial results (not shown) were not favorable in that the transfection efficiency was much lower in neurons compared with that in INS-1 cells. In addition, transfection of the combination of SNAP-25 (1 μg/dish) and BoNT/E (3 μg/dish) was toxic to neurons. Therefore, other transfection methods need to be tested while varying the concentration of DNA.

CHAPTER 7

SUMMARY AND FUTURE DIRECTIONS

Exocytosis is a complicated process regulated by a host of molecular signals. Understanding the regulation of exocytosis is important to understand cell-cell communication. For example, exocytosis of neurotransmitters is a fundamental component of neurotransmission and thus information processing in the brain. Information transmission between organs in the body is mediated by exocytosis of hormones and the release of digestive enzymes also occurs via this process. In this thesis, I specially addressed regulation of exocytosis by a protein kinase.

Protein Kinases C (PKC) is a potent regulator of exocytosis. Several molecular mechanisms have been suggested to explain the effects of PKC on exocytosis (Silinsky and Searl 2003). Among them, phosphorylation of SNAP-25 at Ser187 by PKC is of high interest because SNAP-25 is a key protein of the putative vesicle fusion machinery, the SNARE complex. Thus, SNAP-25 is well poised to modulate exocytosis.

One of the problems to study the importance of SNAP-25 phosphorylation at Ser187 in PKC-mediated exocytosis is that PKC or PKC-activating agents

potentially have multiple substrates that are involved in exocytosis such as Munc-18, Munc-13, and GAP-43 (DeGraan, Hens et al. 1994; Fujita, Sasaki et al. 1996; Rhee, Betz et al. 2002). Therefore, I tested the role of SNAP-25 phosphorylation at Ser187 by specifically mutating the Serine residue believed to by phosphorylated by PKC (Shimazaki, Nishiki et al. 1996). In particular, my strategy was to substitute Serine187 (S) with either the phosphomimetic Glutamic acid (E) or non-phosphorylatable Cystine (C). A previous study using photorelease of caged-Ca^{2+} to elevate $[Ca^{2+}]_i$ to above 20 μm in bovine adrenal chromaffin cells showed that the phosphomimetic mutation of SNAP-25 (S187E) enhanced exocytosis, especially the sustained component which occurs seconds after $[Ca^{2+}]_i$ elevation (Nagy, Matti et al. 2002). Recent results from Gillis lab show that the Ser187 mutation is particularly effective in enhancing exocytosis triggered by photorelease of caged-Ca^{2+} to low micromolar range (the HCSP) in bovine adrenal chromaffin cells (Yang, Craig et al. 2007). My results in the present study extended this finding to the insulin-secreting INS-1 cells. Moving to INS-1 cells allowed me to perform a whole new line of experiments not practical in primary chromaffin cells, namely the inactivation of endogenous SNAP-25 with the expression of BoNT/E. This allowed me to perform experiments to determine if endogenous SNAP-25 accounts for the ineffectiveness of expressing Ser187 mutants in blocking effects of the PKC stimulation agent PMA (figure 1.11).

In rat insulin-secreting cells, expression of BoNT/E inhibited exocytosis in cells expressing GFP-SNAP-25 (WT) (figure 3.10 and figure 5.2). However, toxin-resistant SNAP-25 mutants including TR SNAP-25, TR S187E and TR S187C could “rescue” exocytosis in the presence of BoNT/E. Immunoblots demonstrate that BoNT/E efficiently cleaves GFP-SNAP-25 (WT) and endogenous SNAP-25, but has no effect on the TR SNAP-25 mutants. The most significant finding of this work is that if endogenous SNAP-25 is disabled, PMA is virtually completely ineffective in enhancing exocytosis elicited by photorelease of caged-Ca^{2+} to several μM or a brief depolarization (figure 7.1A). This result suggests a critical role of SNAP-25 phosphorylation at Ser187 in PKC activating-agent enhanced exocytosis. Exocytosis evoked by brief depolarization (the IRP) is also shown to be regulated by SNAP-25 phosphorylation at Ser187 (figure 7.1A).

Photorelease of caged-Ca^{2+} to bring the $[Ca^{2+}]_i$ to a high level (>20 μM) was also used to stimulate exocytosis in INS-1 cells. This high $[Ca^{2+}]_i$ partially overcame the inhibition of exocytosis by BoNT/E in INS-1 cells. PMA had a slightly different effect on exocytosis when $[Ca^{2+}]_i$ was high (figure 7.1B, also figure 5.4C). Most of the enhancement of exocytosis by PMA is blocked in cells co-transfected with BoNT/E and non-phosphorylatable SNAP-25 (TR S187E or TR S187C). However, there is still a residual part (~35%) of the fast kinetic

component of release which was not inhibited. This may indicate other mechanisms are involved for PMA to enhance exocytosis at high $[Ca^{2+}]_i$.

The amplitudes of the fastest exponential component are similar for low $[Ca^{2+}]_i$ (which we call the HCSP) and high $[Ca^{2+}]_i$ (which we call ΔC_m-fast). We have been cautious about assuming these two represent the same vesicle pool. Both putative "fast" pools show a high sensitivity to PMA and are selectively enhanced by the phosphomimetic mutation of Ser187 of SNAP-25. If these two components are grouped together, the rate constant of release is approximately linear with post-flash $[Ca^{2+}]_i$ (figure 7.1C).

A surprising finding is that the fast kinetic component is almost completely ablated with BoNT/E expression when $[Ca^{2+}]_i$ is several μM, but partially "re-appears" (especially following PMA treatment) when $[Ca^{2+}]_i$ is elevated to high level (> 20μM). This suggests that high $[Ca^{2+}]_i$ may be able to partially compensate for the inhibition of exocytosis by cleaved SNAP-25.

The relationship between ΔC_{10} and ΔC_m-slow, defined by membrane depolarization and photorelease of caged-Ca2+, respectively, is even less clear. ΔC_{10} is roughly half of the size of ΔC_m-slow which may simply reflect that this depolarization protocol doesn't entirely deplete the ΔC_m-slow vesicle pool, which is termed as the "Readily Releasable Pool" (RRP) in chromaffin cells. However, it is also possible that the "fast" pool (the HCSP) is simultaneously refilled and released during the depolarization trains.

How do the amplitude and kinetics of exocytosis compare between the INS-1 cells and the more thoroughly studied chromaffin cells? The amplitude and kinetics of the fast kinetic component of exocytosis (the HCSP) evoked by photorelease of caged-Ca^{2+} to low $[Ca^{2+}]_i$ are quite similar between the two cell types (Yang, Udayasankar et al. 2002; Yang and Gillis 2004). However, the rate constant of release in the INS-1 cells may be 2-fold slower than that in chromaffin cells for the same $[Ca^{2+}]_i$. The next-fastest kinetic component, however, is an order of magnitude slower in the INS-1 cells (ΔC_m-slow) (this work; Yang and Gillis 2004) compared to the chromaffin cells (the RRP) (Voets 2000). In fact, the kinetics of ΔC_m-slow in the INS-1 cells are comparable to the "slowly Releasable Pool" (SRP) kinetics in the chromaffin cells (Voets 2000). Therefore, it is possible that the INS-1 cell simply lacks the RRP found in chromaffin cells.

A.

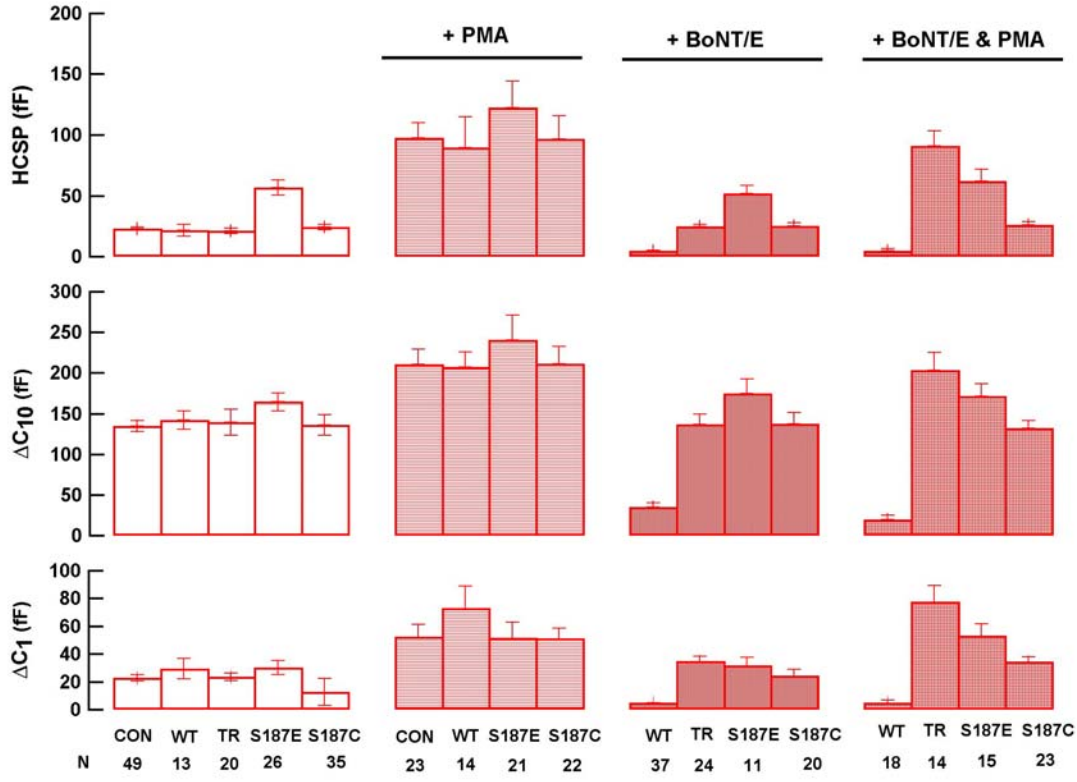

B.

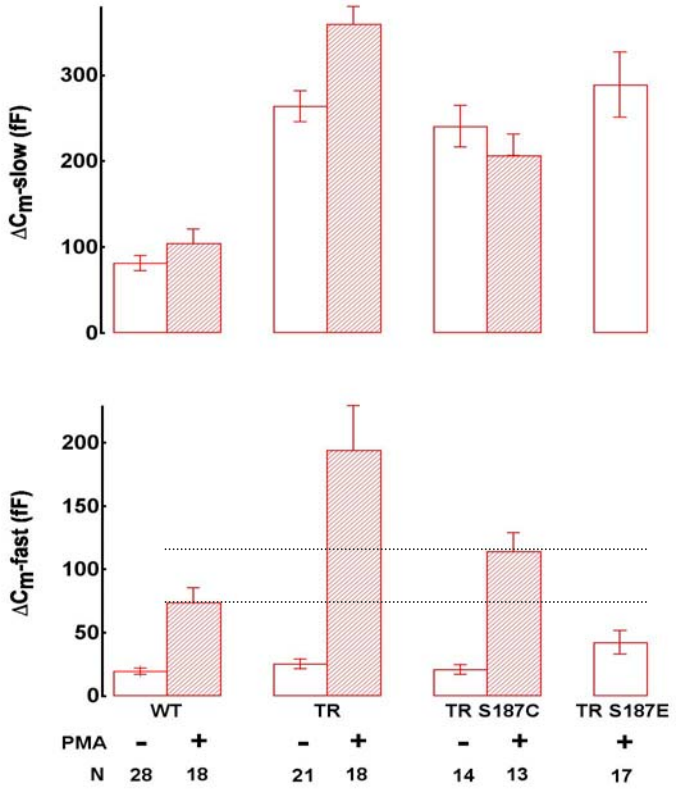
ΔCm-slow (fF)
300
200
100
0
ΔCm-fast (fF)
200
150
100
50
0
WT
TR
TR S187C
TR S187E
PMA - + - + - + +
N 28 18 21 18 14 13 17

C.

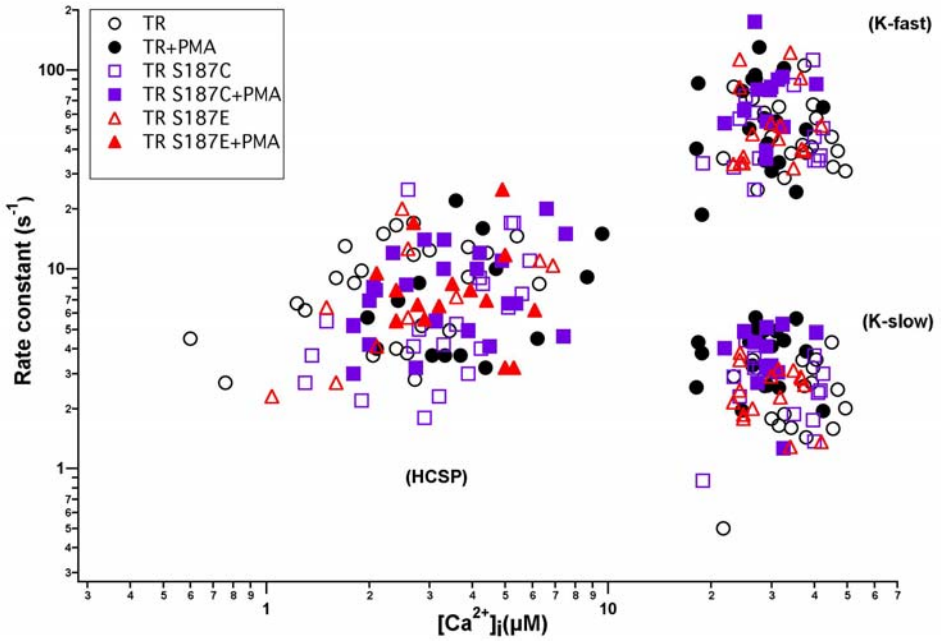
TR
TR+PMA
TR S187C
TR S187C+PMA
TR S187E
TR S187E+PMA
(K-fast)
(K-slow)
(HCSP)
Rate constant (s-1)
[Ca2+]i(μM)

Figure 7.1: Summary of results about the importance of SNAP-25 phosphorylation at Ser187 on PMA-enhanced exocytosis in INS-1 cells. (A), Amplitude of exocytosis components found by using "hybrid" protocol. (B), Amplitude of the fast and slow kinetic components found by photoelevation of $[Ca^{2+}]_i$ to ~ 20 to 50 μM. (C), Rat constants of exocytosis of the HCSP, ΔC_m-fast andΔC_m-slow are plotted versus post-flash $[Ca^{2+}]_i$. All the cells are transfected with BoNT/E besides SNAP-25 mutants. The dash line is showing the linear relation between the K(HCSP) at low $[Ca^{2+}]_I$ and K-fast at higher $[Ca^{2+}]_i$.

Using carbon fiber amperometry, the Gillis lab has previously confirmed that the capacitance change during exocytosis of the HCSP and the RRP is correlated with the release of vesicle contents in INS-1 cells (Yang and Gillis 2004). In this study, I also tried to confirm the results using membrane capacitance change with the release of vesicle content using carbon fiber amperometry. However, I was not successful in the endeavor because of technical problems with the carbon fiber electrodes (CFE). My attempts to identify the problems associated with the CFEs are documented in the Appendix (Chapter 8).

A future direction of this study is to extend my findings in neuroendocrine cells to a neuronal preparation. In neuroendocrine cells, the low $[Ca^{2+}]_i$-stimulated exocytosis is very sensitive to PMA or SNAP-25 phosphorylation at Ser187. A similar differential sensitivity to PMA was observed in neurons (Waters and Smith 2000) (figure 7.2). This study found that spontaneous neurotransmission was

much more enhanced than evoked release by phorbol ester PDBu. In presynaptic neurons, a high-affinity Ca^{2+} sensor to mediate basal or spontaneous release of transmitter as well as mediate the asynchronous release of transmitter that occurs milliseconds after the action potential. The mechanisms of these highly Ca^{2+} sensitive releases to phorbol ester may be similar to that of the HCSP in endocrine cells. Therefore, I hypothesize that hippocampal neurons, like chromaffin cells and insulin-secreting cells, contain both a Highly Ca^{2+} Sensitive Pool and a less-Ca^{2+}-sensitive Readily Releasable Pool of vesicles. I further hypothesize that the HCSP, as the fastest-releasing vesicle population at low $[Ca^{2+}]_i$, is the predominant population that is released under basal conditions (as spontaneous “minis”). I also hypothesize that the HCSP contributes prominently to the “asynchronous” phase of the postsynaptic response because the results from INS-1 cells and chromaffin cells showed that the HCSP is not located close to Ca^{2+} channels and is therefore likely to be released with a delay upon membrane depolarization. Finally, I hypothesize that SNAP-25 phosphorylation at Ser187 plays important roles in regulating the low $[Ca^{2+}]_i$-mediated neurotransmission in hippocampal neurons.

Figure 7.2: Phorbol ester PDBu enhanced neuronal transmission in neurons. The spontaneous component was much more enhanced by PDBu compared with the evoked component (from figure 5, Waters J and Smith SJ, J Neurosci, 2000).

CHPTER 8 (APPENDIX)

IDENTIFYING THE TECHNICAL PROBLEMS WITH THE CARBON FIBER ELECTRODES USED FOR CARBON FIBER AMPEROMETRY IN INS-1 CELLS

The whole-cell capacitance measurement is a very powerful technique to assay exocytosis in high time resolution. It also has high sensitivity even for a single vesicle fusion in certain cells(Alvarez de Toledo, Fernandez-Chacon et al. 1993; Albillos, Dernick et al. 1997; Klyachko and Jackson 2002). However, the capacitance measurement has several disadvantages as well. First, it is not able to distinguish exocytosis and endocytosis. The measured capacitance change is the net outcome from those two processes. Second, it has no specificity in detecting the release of the vesicle contents. Sometimes the capacitance change may not correlate with the real release of the vesicle contents (von Ruden and Neher 1993; Coorssen, Schmitt et al. 1996; Henkel and Almers 1996; Oberhauser, Robinson et al. 1996; Ninomiya, Kishimoto et al. 1997). An alternative method to surpass these problems of capacitance measurement is amperometric detection with carbon fiber.

Some secretory cells release easily oxidizable vesicle contents, such as dopamine (DA), serotonin (5-HT), norepinephrine (NE) and epinephrine (E) (figure 8.1A). A sufficiently high potential (e.g., ~700 mV) is usually applied to the carbon fiber to oxidize the transmitters. The oxidation of these transmitters will release electrons, which can be captured and recorded as current spikes with the carbon fiber (figure 8.1B, C). The amplitude of the current spikes is proportional to the amount of oxidizable transmitters reaching the carbon fiber surface. By calculating the integrals of the current spikes, I can roughly determine the number of vesicles released and the amount of transmitter secreted per vesicle (Chow and Ruden 1995). In the typical configuration of carbon fiber amperometry experiment (figure 8.1D), the carbon fiber electrode (CFE) is placed against the cell surface within 1 μm or even in touch with the cell. The carbon fiber amperometry can be used separately as well as combined with other methods such as cell capacitance measurement. Usually, another pipette is used for stimulation and recording as well as delivery of drug, Ca^{2+} dyes, caged-Ca^{2+}, etc). The carbon fiber amperometry was first applied to single cell to monitor exocytosis around 1990s(Duchen, Millar et al. 1990; Leszczyszyn, Jankowski et al. 1991; Chow, von Ruden et al. 1992). The vesicles in bovine adrenal chromaffin cells are enriched of catecholamine which includes NE, E and DA, etc. Therefore, bovine adrenal chromaffin cell has been the most widely used cell model to study exocytosis with carbon fiber amperometry.

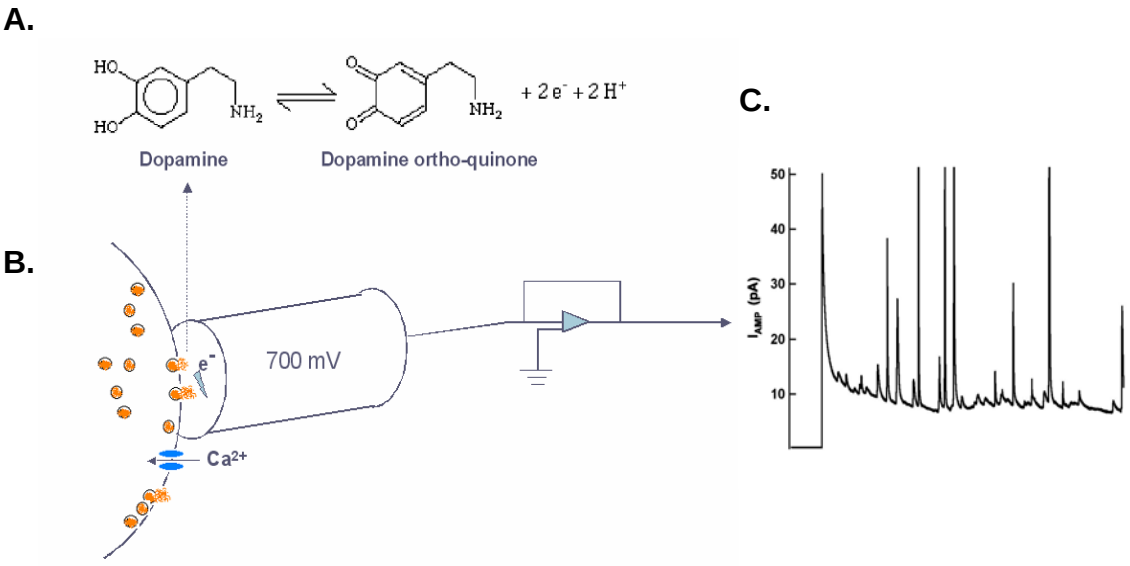

Figure 8.1: Schematic demonstration of carbon fiber amperometry. (A), Oxidation of dopamine releases two protons and two electrons. (B), Experiment set-up of carbon fiber amperometry (Modified after figure 1, Westerink RH, NeuroToxicology, 2004: 461-470). (C), Current spikes from the Amperometric recording with carbon fiber. (D), The typical configuration of carbon fiber amperometry experiment (from figure 8, Chow and Ruden, Single Channel Recording, 1995).

The insulin peptide secreted from pancreatic beta cells and INS-1 cells can be oxidized, but usually in a small amount and with a slow diffusion speed(Kennedy, Huang et al. 1993). Therefore, it is difficult to directly detect the insulin secretion with CFE. Insulin is stored in the large-dense core vesicles (LVs) in pancreatic beat-cells(Thomas-Reetz and De Camilli 1994). A more oxidizable transmitter Serotonin (5-HT) has been shown to be selectively uptaken into LVs and secreted along with insulin(Jaim-Etcheverry and Zieher 1968; Gylfe 1978; Smith, Duchen et al. 1995; Zhou and Misler 1996). The release of 5-HT was considered as marker for insulin secretion (Aspinwall, Huang et al. 1999). Thus, detection of serotonin secretion with carbon fiber amperometry can be employed to reflect insulin release from pancreatic beta cells (primary or cell line).

Since the CFE can only cover a limited fraction of the cell surface, the detectable exocytotic events by the CFE ranges from 2% (Chan and Smith 2001) to15%(Chow and Ruden 1995) of the total events. To capture more events, the carbon fiber with larger surface area is required. The 5 μm-diameter CFE is enough for bovine adrenal chromaffin cell because of its abundance in the oxidizable transmitters. However, for INS-1 cells, CFE with a larger diameter such as 8-10 μm is preferred (Kang and Holz 2003; Yang and Gillis 2004). Because the 10 μm-diameter CFEs are not commercially available, I made the 10 μm-diameter CFEs customerized as previously described(Chow and Ruden 1995; Schulte and Chow 1996). For detailed procedure, please refer to these two references.

Several points need to be pointed out about the CFEs here (figure 8.2). (1). The carbon fiber is covered with a very thin layer of insulation paint. (2). The carbon fiber is directly attached to the conducting copper bar, mounted with glue.

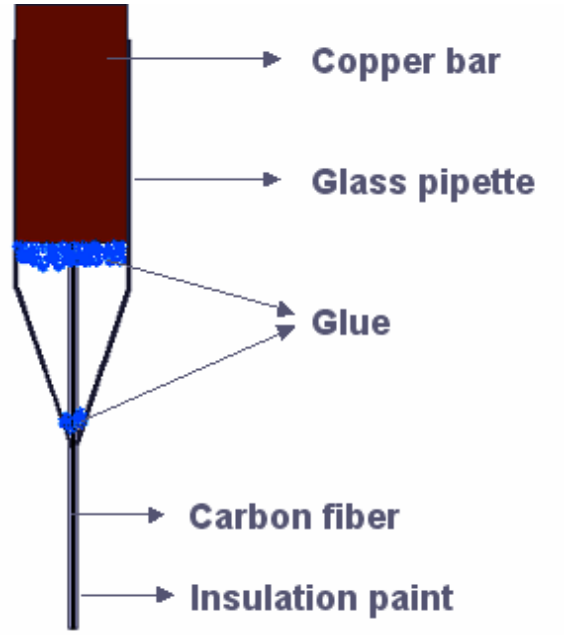

Figure 8.2: Schematic demonstration of CFE structure.

In this study, I tried to use both capacitance measurement and carbon fiber amperometry to confirm that the correlate the results obtained with capacitance measurement are correlated with insulin secretion. However, I did not succeed at the end due to some technical problems of the 10 μm-diameter CFE. This part mainly described my endeavors to dissect the problems with the CFE.

8.1 Materials and methods

Materials: All cell culture reagents were from Gilbco (Invitrogen) unless stated otherwise. All other materials were from Sigma (St. Louis, MO) except special indication.

Bovine adrenal chromaffin cell culture: Cells were prepared according to the published protocol (Yang, Craig et al. 2007). Bovine adrenal glands from a local slaughterhouse were kept in a Ca^2- and Mg^2-free isolation buffer and transported to the laboratory at room temperature. Fat was trimmed from the glands using scissors under a sterile hood. Blood was washed out of the glands by gently injecting isolation buffer into the portal vein and then allowing the solution to run out while gently massaging the glands. This was repeated several times until the liquid running out was clear. Collagenase type P (Roche Diagnostics) was dissolved in isolation buffer at a concentration of 1 mg/ml, injected into the portal vein, and then the glands were placed in a beaker in a 37°C shaking water bath for 20–25 min. The glands were opened by cutting around the circumference of the cortex with scissors, and the medulla was peeled away from the cortex and placed into a culture dish containing isolation buffer. The medullae were then minced to small pieces with a scalpel. The medullae-containing suspension was

filtered through a nylon mesh (70 μm; Fisher Scientific). The filtered liquid was collected in a 50-ml tube and centrifuged at 1,000 rpm for 10 min at room temperature. The supernatant was aspirated and discarded, and then the pellet was resuspended in isolation buffer. In another tube, a 10-fold concentrated isolation buffer solution was mixed with percoll at a ratio of 1:9 to make a solution with physiological tonicity and a pH of 7.2. The percoll solution was combined with the cell solution at a 1:1 ratio and this mixture was centrifuged at 15,000 rpm for 30 min at 15°C. This resulting solution contains several distinct layers: cell debris in the top layer, chromaffin cells in the middle layer, and red blood cells in the bottom layer. The middle layer was gently transferred to a centrifuge tube using a pipette. Isolation buffer was added again to fill the tube and the suspension was centrifuged at 1,000 rpm for 5 min. The supernatant was aspirated and discarded and the pellet resuspended in isolation buffer. Chromaffin cell culture media was added at a 1:3 ratio to the cell suspension to begin the adaptation of cells to the Ca^2-containing media. The suspension was centrifuged again at 1,000 rpm for 5 min and the supernatant was discarded. After resuspending the pellet in chromaffin cell media, the cells were counted using a hemacytometer. The solution was then diluted with media to give a density of 6×10^5 cells/ml. The cell suspension was then plated into six-well culture plates, containing 25-mm diameter round glass coverslips that had been previously coated with 0.0025% poly-L-lysine. Cells were plated at a density of 6×10^3 cells per coverslip for

experiments using virus infection and at a density of 10^3 cells per coverslip for patch-clamp experiments. The cells were housed in a humidified incubator at 37°C with 5% CO_2 and used 1–3 d after preparation.

INS-1 cells culture: Rat insulinoma INS-1 cells (provided by C. Wollheim, University of Geneva, Geneva, Switzerland) were prepared as described (Asfari, Janjic et al. 1992; Yang and Gillis 2004). Briefly, the cells were maintained in culture media consisting of RPMI 1640 medium supplemented with 50 μM 2-mercaptoethanol, 2 mM L-glutamine, 10 mM HEPES, 100 U/ml penicillin, 100 μg/ml streptomycin, 1 mM sodium pyruvate, and 10% FBS. Cells were kept in a humidified 37^{o}C incubator with 5% CO_2 and were subcultured once per week. In experiments for patch clamp, INS-1 cells were plated onto glass coverslips (25mm OD) in 35mm dishes at the density of 5 X10^5 cells per dish.

Carbon fiber amperometry in bovine adrenal chromaffin cells: Carbon fiber amperometry was performed as described (Yang, Craig et al. 2007). Carbon fiber electrodes (CFE, 5μm diameter) were directly purchased from ALA Scientific Inc.. The 10μm diameter Carbon fibers were a kind gift from Dr. George G. Holz (Department of Physiology and Neuroscience, New York University School of Medicine, New York, NY 10016, USA). The 10μm diameter carbon fibers were sent to ALA Scientific Inc. and customerized into CFE. CFE was positioned to just

touch the surface of the cell using a micromanipulator (PCS-5000, Burleigh). The amperometric current was measured using a patch-clamp amplifier (EPC-9, HEKA) at a holding potential of +700 mV. The amperometric signal was filtered at 200 Hz and sampled at 1 kHz. After acquisition, samples were averaged ("decimated") in groups of 12 to give a final temporal resolution of ~0.7 ms per point.

Carbon fiber amperometry in INS-1 cells: INS-1 cells were incubated in media containing 0.6 mM 5-HT and 0.6 mM 5-hydroxytryptophan for 5–10 h before initiating amperometric measurements (Smith et al., 1995; Zhou and Misler, 1996). The amperometric signal was filtered at 200 Hz and sampled at 1 kHz. After acquisition, samples were averaged ("decimated") in groups of 12 to give a final temporal resolution of ~0.7 ms per point.

Cyclic Voltammetry: CFE was mounted to the headstage of patch clamp system. The amperometric current was measured using a patch-clamp amplifier (EPC-9, HEKA). CFE was immersed in the solutions containing 1 mM ferricyanide in 0.5 M KCl (pH=3.0). The reference electrode was a Ag/AgCl reference electrode. A triangular wave of voltage (-0.6 to 0.6 V or -0.5 to 0.5 V) was generated with the computer-controlled program and applied to CFE at different scanning rates.

Data analysis: Data analysis was performed by using Igor software (Wavemetrics).

8.2. Carbon fiber amperometry in bovine adrenal chromaffin cells and INS-1 cells

In this study, I used bovine adrenal chromaffin cells as the control to test whether the CFEs worked properly or not. The cells were held in whole-cell patch-clamp configuration. The caged-Ca^{2+} and Ca^{2+} fluorescent dyes (Bisfura-2 and Fura2-ff) were delivered into cells through the patch pipette. Photorelease of caged-Ca^{2+} to high $[Ca^{2+}]_i$ was applied to stimulate exocytosis. The amperometric current and the capacitance were recorded simultaneously. With the 5μm-diameter CFE, we successfully detected the spikes from bovine adrenal chromaffin cells (figure 8.3A, B). However, with the customized 10μm-diameter CFE, I seldom detected spikes from both chromaffin cells and INS-1 cells (figure 8.3C, D)

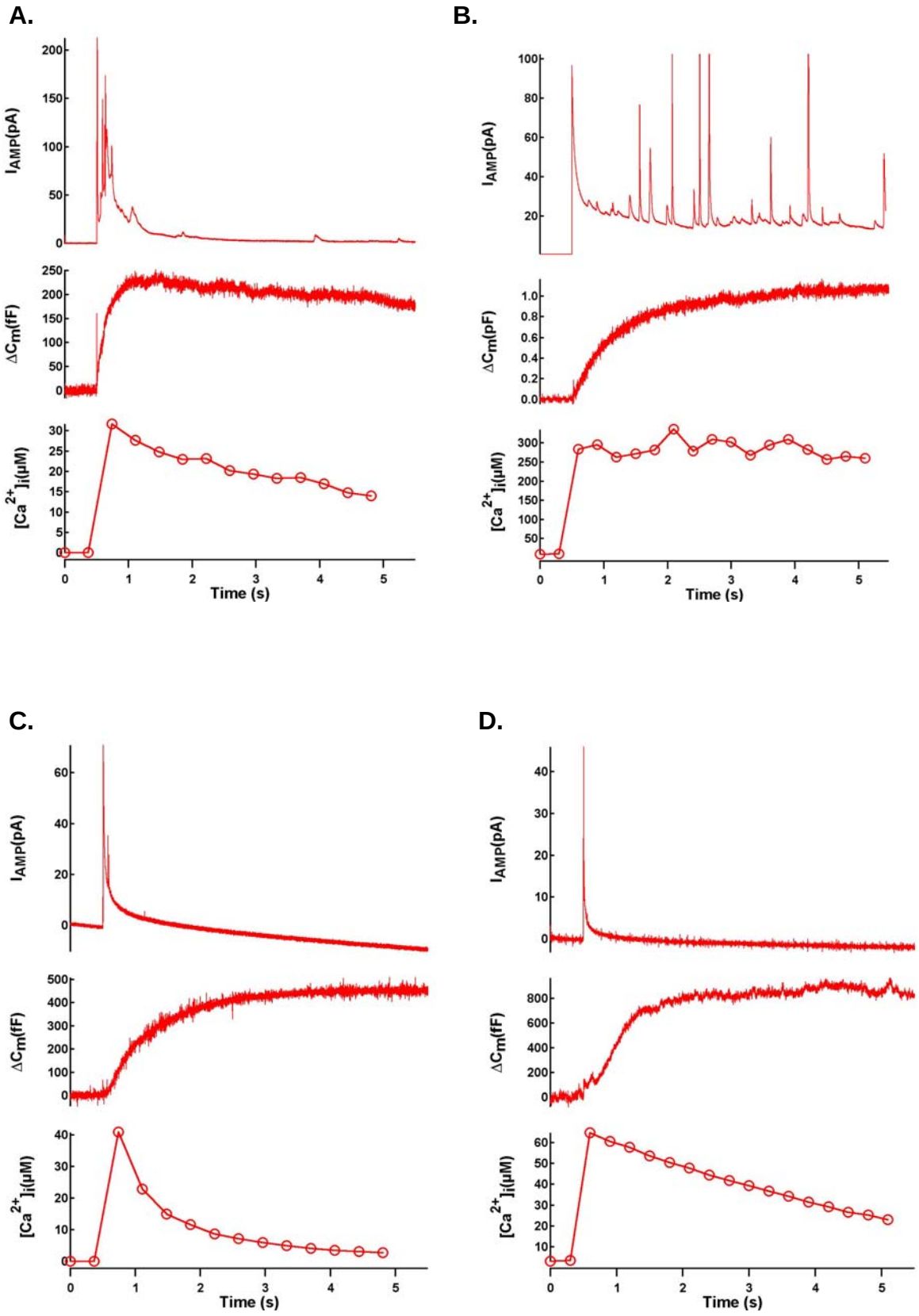
A.
B.
C.
D.
I_{AMP}(pA)
ΔC_m(fF)
ΔC_m(pF)
$[Ca^{2+}]_i$(μM)
Time (s)

Figure 8.3: Detection of amperometric currents with the 5 μm-diameter CFE and 10 μm-diameter CFE in bovine adrenal chromaffin cells and INS-1 cells. Amperometric spikes (upper traces), capacitance change (middle traces) and $[Ca^{2+}]_I$ (bottom traces) were recorded simontaneously. (A) and (B), Two sample traces from bovine adrenal chromaffin cells with the 5 μm-diameter CFE. (C), Sample traces from INS-1 cells with the 10 μm-diameter CFE. (D), Sample traces from bovine adrenal chromaffin cells with the 10 μm-diameter CFE.

These results above indicated there might be some problems with the customerized 10 μm-diameter CFEs. I then compared several electrochemical properties between the 5 μm-diameter CFEs and the customerized 10 μm-diameter CFEs.

8.3. Cyclic Voltammetry

The measurement of the current response to an applied voltage is called “voltammetry”(Schulte and Chow 1996). Cyclic voltammetry measures the current response from the periodic voltage waveform (figure 8.4). The applied periodic voltage rises from V_1 to V_2 then comes back to V_1. The ramp rate of the voltage change can vary from several hundred V/sec (fast) to several mV/sec (slow).

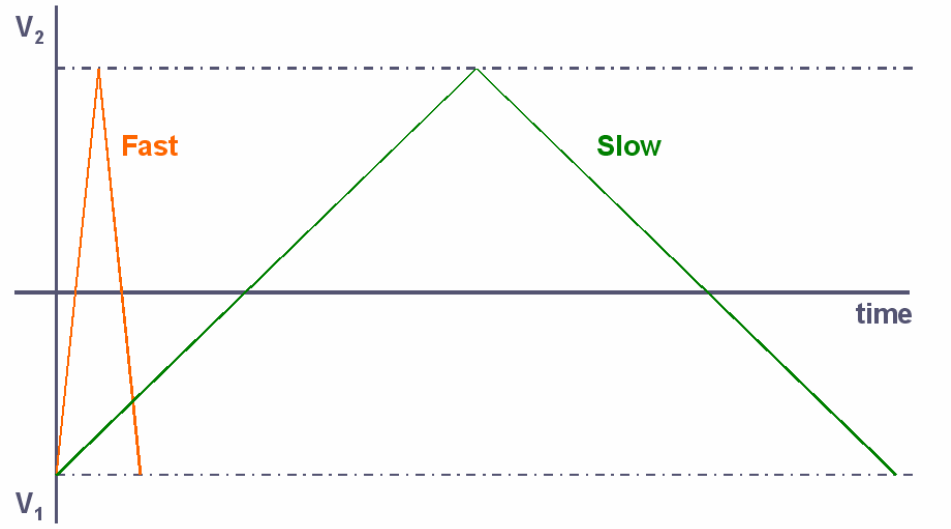

Figure 8.4: Periodic voltages in cyclic voltammetry.

The applied voltage starts from a negative point and heads to the positive direction. When the potential at the CFEs reaches a sufficiently positive level beyond the redox potential, the oxidation of the substrate at the CFE surface is triggered. The oxidation current increases as the applied voltage increases. During this process, the substrate around the CFE surface is continuously depleted and then replenished by the diffusion of the fresh substrate from the bulk solution. As this process goes on, more and more oxidized substrates build up around the CFE surface, which prevents the access of the fresh substrate. Thus, the oxidation current starts to drop from the “peak” when the depletion rate exceeds the replenishing rate. After the positive voltage, the oxidized substrate is exposed to the negative potential from the CFE. This negative potential enables

the reduction of the oxidized substrate. A reduction current is observed during this process. When all oxidized substrates are reduced, the current falls back to the resting stage.

The cyclic voltammogram can tell us the electrochemical behavior of the CFE tested, including the electron delivery capacity, the reduction/oxidation ability (by current peaks), and unexpected current peaks indicating metal/insulator leakage, etc. (Hu, Troyk et al. 2005). In this study, I simply compared the cyclic voltammograms from the 5 μm and 10 μm-diameter CFEs for some possible differences that may implicate the dysfunction of the 10 μm-diameter CFEs.

The CFEs were randomly picked and freshly cut with a scalpel. I performed both fast cyclic voltammetry (FCV) and slow cyclic voltammetry (SCV). In FCV, the voltage was from –0.5 V to 0.5 V and the ramp of voltage change was 100V/s. In SCV, the voltage was from –0.6 V to 0.6 V and the ramp of voltage change was 10 mV/s. I also repeated the scan after the first round was completed. Figure 8.5 shows cyclic voltammograms from each two of the 5 μm and 10 μm-diameter CFEs. I did not observe evident differences in the morphology of the cyclic voltammograms. However, the results from the 5 μm-diameter CFEs (technically tested by the company) were more stable than those from the 5 μm-diameter CFEs. In the fast cyclic voltammograms (figure 8.5A), All the CFEs had the same the oxidation voltage for the oxidation peak current (the dash line). Compared with

the 5 μm-diameter CFE, the 10 μm-diameter CFE may have a larger reduction voltage for the reduction peak current. In the slow cyclic voltammograms (figure 8.5B), the half-wave reduction potentials for the 5 μm-diameter CFEs are quit similar, around 160 mV vs Ag/Ag/Cl. However, the half-wave reduction potentials for of the 10 μm-diameter CFEs vary in a big range. All of these may indicate the 10 μm-diameter CFEs have different electrochemical properties from the 5 μm-diameter CFEs.

A.

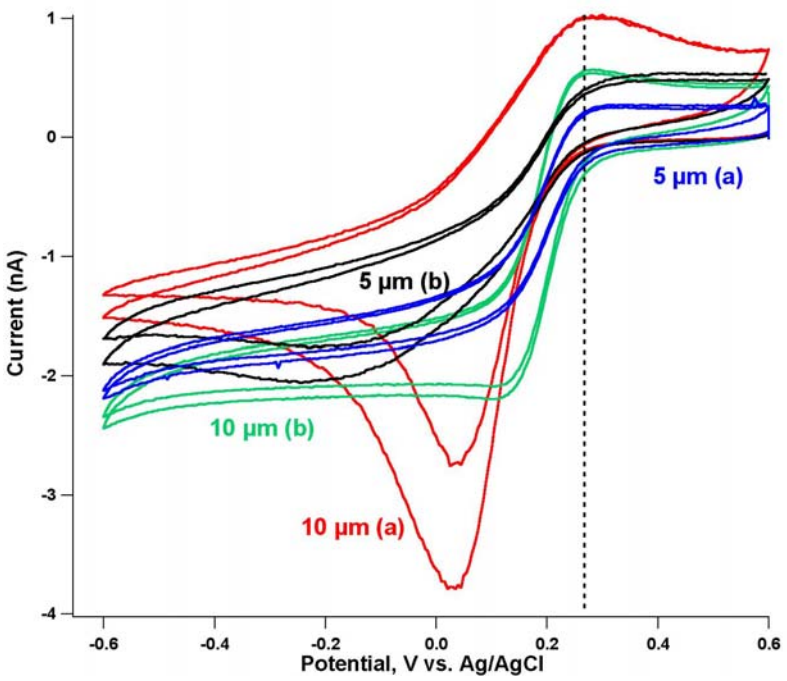

B.

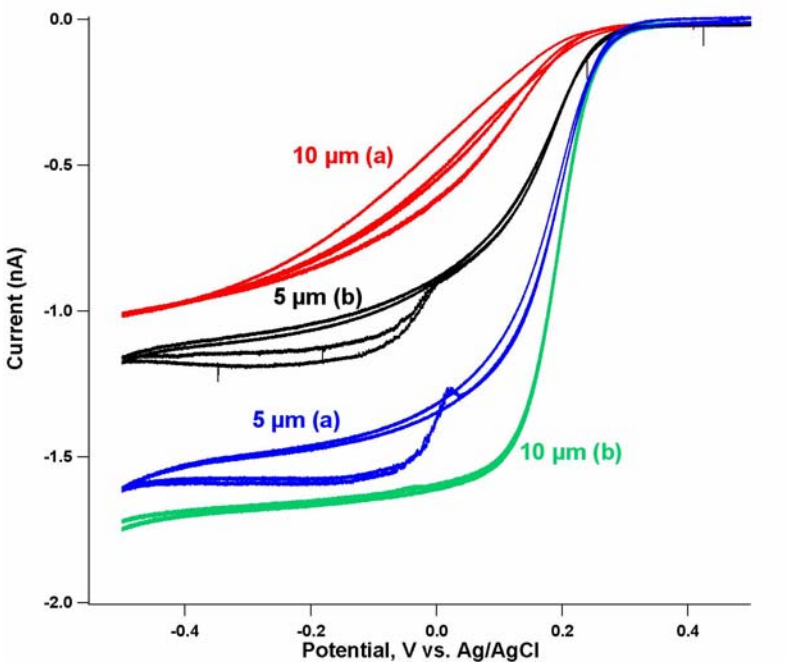

Figure 8.5: Cyclic voltammograms from the 5 µm and 10 µm-diameter CFEs. (A), Fast cyclic voltammograms. The voltage for oxidation peak current is also shown (the dash line). (B), Slow cyclic voltammograms from the same CFEs in (A).

8.4 The capacitance measurement.

CFE is coated with the insulation paint. This makes CFE a capacitor. I also measured the capacitance of the CFEs with the patch-clamp system (HEKA). The CFEs from each group were randomly selected and freshly cut with a scalpel before the measurement. The measured capacitances are listed in Table 3.

CFE #	1	2	3	4	5	6	7	8	AVE	SEM
Cm-5 μm(pF)	3.8879	6.0665	3.0406	2.8193	3.8229				3.9274	0.57
Cm-10 μm(pF)	2.5326	5.7824	6.7072	4.8427	7.4049	13.833	3.4217	2.43	5.8693	1.31

Table 3: Measured capacitances from the 5 μm and 10μm-diameter CFEs.

The surface area of the 10 μm-diameter CFE is 4 fold of the surface area of the 5 μm-diameter CFE. Since the capacitance is proportional to the surface area, the measured capacitance of the 10 μm-diameter CFE should be about 4 times larger than that of the 5 μm-diameter CFE. However, the result did not agree with this prediction. Thus, there might be some problems with the paint insulation on the 10 μm-diameter CFE.

8.5 Checking the access resistance

The carbon fiber is glued to the connecting copper bar (figure 8.2). Therefore, the attachment of the carbon fiber with the copper bar is very important for the electrical signal transduction. To test whether the connection between the carbon fiber and the copper bar is good or not, I measured the access resistance of the CFE. My results showed that the access resistances between the 5 and 10 μm-diameter CFE were not different from each other (Detailed data not shown here).

Based on all the data in this part, we had an impression that the dysfunction of the 10 μm-diameter CFE was due to the material of the carbon fiber and the paint insulation.

Reference

Aguado, F., L. Gombau, et al. (1997). "Regulated secretion is impaired in AtT-20 endocrine cells stably transfected with botulinum neurotoxin type A light chain." J Biol Chem **272**(41): 26005-8.

Ahmed, S. A. and L. A. Smith (2000). "Light chain of botulinum A neurotoxin expressed as an inclusion body from a synthetic gene is catalytically and functionally active." J Protein Chem **19**(6): 475-87.

Albillos, A., G. Dernick, et al. (1997). "The exocytotic event in chromaffin cells revealed by patch amperometry." Nature **389**(6650): 509-12.

Alvarez de Toledo, G., R. Fernandez-Chacon, et al. (1993). "Release of secretory products during transient vesicle fusion." Nature **363**(6429): 554-8.

Andres-Mateos, E., J. Renart, et al. (2005). "Dynamic association of the Ca2+ channel alpha1A subunit and SNAP-25 in round or neurite-emitting chromaffin cells." Eur J Neurosci **22**(9): 2187-98.

Asaoka, Y., S. Nakamura, et al. (1992). "Protein kinase C, calcium and phospholipid degradation." Trends Biochem Sci **17**(10): 414-7.

Asfari, M., D. Janjic, et al. (1992). "Establishment of 2-mercaptoethanol-dependent differentiated insulin-secreting cell lines." Endocrinology **130**(1): 167-78.

Aspinwall, C. A., L. Huang, et al. (1999). "Comparison of amperometric methods for detection of exocytosis from single pancreatic beta-cells of different species." Anal Chem **71**(24): 5551-6.

Atluri, P. P. and W. G. Regehr (1998). "Delayed release of neurotransmitter from cerebellar granule cells." J Neurosci **18**(20): 8214-27.

Augustine, G. J., M. P. Charlton, et al. (1987). "Calcium action in synaptic transmitter release." Annu Rev Neurosci **10**: 633-93.

Bajohrs, M., C. Rickman, et al. (2004). "A molecular basis underlying differences in the toxicity of botulinum serotypes A and E." EMBO Rep **5**(11): 1090-5.

Bekkers, J. M. and C. F. Stevens (1991). "Excitatory and inhibitory autaptic currents in isolated hippocampal neurons maintained in cell culture." Proc Natl Acad Sci U S A **88**(17): 7834-8.

Bennett, M. K., N. Calakos, et al. (1992). "Syntaxin: a synaptic protein implicated in docking of synaptic vesicles at presynaptic active zones." Science **257**(5067): 255-9.

Berridge, M. J. (1998). "Neuronal calcium signaling." Neuron **21**(1): 13-26.

Binz, T., J. Blasi, et al. (1994). "Proteolysis of SNAP-25 by types E and A botulinal neurotoxins." J Biol Chem **269**(3): 1617-20.

Bittner, M. A. and R. W. Holz (1992). "Kinetic analysis of secretion from permeabilized adrenal chromaffin cells reveals distinct components." J Biol Chem **267**(23): 16219-25.

Blasi, J., E. R. Chapman, et al. (1993). "Botulinum neurotoxin A selectively cleaves the synaptic protein SNAP-25." Nature **365**(6442): 160-3.

Blasi, J., E. R. Chapman, et al. (1993). "Botulinum neurotoxin C1 blocks neurotransmitter release by means of cleaving HPC-1/syntaxin." Embo J **12**(12): 4821-8.

Bonner, P. H., A. F. Friedli, et al. (1994). "Botulinum A toxin stimulates neurite branching in nerve-muscle cocultures." Brain Res Dev Brain Res **79**(1): 39-46.

Brager, D. H., X. Cai, et al. (2003). "Activity-dependent activation of presynaptic protein kinase C mediates post-tetanic potentiation." Nat Neurosci **6**(6): 551-2.

Brager, D. H., M. Capogna, et al. (2002). "Short-term synaptic plasticity, simulation of nerve terminal dynamics, and the effects of protein kinase C activation in rat hippocampus." J Physiol **541**(Pt 2): 545-59.

Branch, D. W., J. M. Corey, et al. (1998). "Microstamp patterns of biomolecules for high-resolution neuronal networks." Med Biol Eng Comput **36**(1): 135-41.

Branchi, I. and L. Ricceri (2002). "Transgenic and knock-out mouse pups: the growing need for behavioral analysis." Genes Brain Behav **1**(3): 135-41.

Burgess, T. L. and R. B. Kelly (1987). "Constitutive and regulated secretion of proteins." Annu Rev Cell Biol **3**: 243-93.

Burns, M. E. and G. J. Augustine (1995). "Synaptic structure and function: dynamic organization yields architectural precision." Cell **83**(2): 187-94.

Capogna, M., B. H. Gahwiler, et al. (1995). "Presynaptic enhancement of inhibitory synaptic transmission by protein kinases A and C in the rat hippocampus in vitro." J Neurosci **15**(2): 1249-60.

Capogna, M., R. A. McKinney, et al. (1997). "Ca2+ or Sr2+ partially rescues synaptic transmission in hippocampal cultures treated with botulinum toxin A and C, but not tetanus toxin." J Neurosci **17**(19): 7190-202.

Chan, S. A. and C. Smith (2001). "Physiological stimuli evoke two forms of endocytosis in bovine chromaffin cells." J Physiol **537**(Pt 3): 871-85.

Chen, Y. A. and R. H. Scheller (2001). "SNARE-mediated membrane fusion." Nat Rev Mol Cell Biol **2**(2): 98-106.

Chow, R. H. and L. V. Ruden (1995). "Electrochemical detection of secretion from single cells. ." In: Sakman B, Neher E. Single Channel Recording. New York, Plenum Press: 245-275.

Chow, R. H., L. von Ruden, et al. (1992). "Delay in vesicle fusion revealed by electrochemical monitoring of single secretory events in adrenal chromaffin cells." Nature **356**(6364): 60-3.

Cole, K. S. (1968). "Membranes, Ions and Impulses." Berkeley, University of California Press.

Coorssen, J. R., H. Schmitt, et al. (1996). "Ca2+ triggers massive exocytosis in Chinese hamster ovary cells." Embo J **15**(15): 3787-91.

De Silva, M. N., R. Desai, et al. (2004). "Micro-patterning of animal cells on PDMS substrates in the presence of serum without use of adhesion inhibitors." Biomed Microdevices **6**(3): 219-22.

DeGraan, P. N., J. J. Hens, et al. (1994). "Presynaptic PKC substrate B-50 (GAP-43) and neurotransmitter release: studies with permeated synaptosomes." Neurotoxicology **15**(1): 41-7.

Del Castillo, J. and B. Katz (1954). "Quantal components of the end-plate potential." J Physiol **124**(3): 560-73.

Dinkelacker, V., T. Voets, et al. (2000). "The readily releasable pool of vesicles in chromaffin cells is replenished in a temperature-dependent manner and transiently overfills at 37 degrees C." J Neurosci **20**(22): 8377-83.

Dobrunz, L. E. and C. F. Stevens (1997). "Heterogeneity of release probability, facilitation, and depletion at central synapses." Neuron **18**(6): 995-1008.

Dodge, F. A., Jr. and R. Rahamimoff (1967). "Co-operative action a calcium ions in transmitter release at the neuromuscular junction." J Physiol **193**(2): 419-32.

Douglas, W. W. (1968). "Stimulus-secretion coupling: the concept and clues from chromaffin and other cells." Br J Pharmacol **34**(3): 453-74.

Duchen, M. R., J. Millar, et al. (1990). "Voltammetric measurement of catecholamine release from isolated rat chromaffin cells. ." J. Physiol. **426**: 5P.

Eliasson, L., E. Renstrom, et al. (1997). "Rapid ATP-dependent priming of secretory granules precedes Ca(2+)-induced exocytosis in mouse pancreatic B-cells." J Physiol **503 (Pt 2)**: 399-412.

Ellis-Davies, G. C. and J. H. Kaplan (1994). "Nitrophenyl-EGTA, a photolabile chelator that selectively binds Ca2+ with high affinity and releases it rapidly upon photolysis." Proc Natl Acad Sci U S A **91**(1): 187-91.

Ellis-Davies, G. C., J. H. Kaplan, et al. (1996). "Laser photolysis of caged calcium: rates of calcium release by nitrophenyl-EGTA and DM-nitrophen." Biophys J **70**(2): 1006-16.

Fatt, P. and B. Katz (1952). "Spontaneous subthreshold activity at motor nerve endings." J Physiol **117**(1): 109-28.

Feng, J., P. Chi, et al. (2002). "Regulation of neurotransmitter release by synapsin III." J Neurosci **22**(11): 4372-80.

Finley, M. F., R. H. Scheller, et al. (2003). "SNAP-25 Ser187 does not mediate phorbol ester enhancement of hippocampal synaptic transmission." Neuropharmacology **45**(6): 857-62.

Folch, A. and M. Toner (1998). "Cellular micropatterns on biocompatible materials." Biotechnol Prog **14**(3): 388-92.

Foran, P., G. W. Lawrence, et al. (1996). "Botulinum neurotoxin C1 cleaves both syntaxin and SNAP-25 in intact and permeabilized chromaffin cells: correlation with its blockade of catecholamine release." Biochemistry **35**(8): 2630-6.

Fujita, Y., T. Sasaki, et al. (1996). "Phosphorylation of Munc-18/n-Sec1/rbSec1 by protein kinase C: its implication in regulating the interaction of Munc-18/n-Sec1/rbSec1 with syntaxin." J Biol Chem **271**(13): 7265-8.

Genoud, S., W. Pralong, et al. (1999). "Activity-dependent phosphorylation of SNAP-25 in hippocampal organotypic cultures." J Neurochem **72**(4): 1699-706.

Geppert, M., Y. Goda, et al. (1994). "Synaptotagmin I: a major Ca2+ sensor for transmitter release at a central synapse." Cell **79**(4): 717-27.

Gerona, R. R., E. C. Larsen, et al. (2000). "The C terminus of SNAP25 is essential for Ca(2+)-dependent binding of synaptotagmin to SNARE complexes." J Biol Chem **275**(9): 6328-36.

Gillis, K. D. (1995). "Techniques for membrane capacitance measurements." In: Sakamann B, Neher E, editors. Single channel recording. New York, NY: Plenum Press: P.155-98.

Gillis, K. D. (2000). "Admittance-based measurement of membrane capacitance using the EPC-9 patch-clamp amplifier." Pflugers Arch **439**(5): 655-64.

Gillis, K. D., R. Mossner, et al. (1996). "Protein kinase C enhances exocytosis from chromaffin cells by increasing the size of the readily releasable pool of secretory granules." Neuron **16**(6): 1209-20.

Giovannucci, D. R. and E. L. Stuenkel (1997). "Regulation of secretory granule recruitment and exocytosis at rat neurohypophysial nerve endings." J Physiol **498 (Pt 3)**: 735-51.

Goda, Y. and C. F. Stevens (1994). "Two components of transmitter release at a central synapse." Proc Natl Acad Sci U S A **91**(26): 12942-6.

Gonelle-Gispert, C., M. Costa, et al. (2002). "Phosphorylation of SNAP-25 on serine-187 is induced by secretagogues in insulin-secreting cells, but is not correlated with insulin secretion." Biochem J **368**(Pt 1): 223-32.

Gonelle-Gispert, C., P. A. Halban, et al. (1999). "SNAP-25a and -25b isoforms are both expressed in insulin-secreting cells and can function in insulin secretion." Biochem J **339 (Pt 1)**: 159-65.

Graham, M. E., R. J. Fisher, et al. (2000). "Measurement of exocytosis by amperometry in adrenal chromaffin cells: effects of clostridial neurotoxins and activation of protein kinase C on fusion pore kinetics." Biochimie **82**(5): 469-79.

Graham, M. E., P. Washbourne, et al. (2001). "SNAP-25 with mutations in the zero layer supports normal membrane fusion kinetics." J Cell Sci **114**(Pt 24): 4397-405.

Gray, R., A. S. Rajan, et al. (1996). "Hippocampal synaptic transmission enhanced by low concentrations of nicotine." Nature **383**(6602): 713-6.

Gutierrez, L. M., J. M. Canaves, et al. (1995). "A peptide that mimics the carboxy-terminal domain of SNAP-25 blocks Ca(2+)-dependent exocytosis in chromaffin cells." FEBS Lett **372**(1): 39-43.

Gylfe, E. (1978). "Association between 5-hydroxytryptamine release and insulin secretion." J Endocrinol **78**(2): 239-48.

Harata, N. C., A. M. Aravanis, et al. (2006). "Kiss-and-run and full-collapse fusion as modes of exo-endocytosis in neurosecretion." J Neurochem **97**(6): 1546-70.

Heidelberger, R., C. Heinemann, et al. (1994). "Calcium dependence of the rate of exocytosis in a synaptic terminal." Nature **371**(6497): 513-5.

Heinemann, C., R. H. Chow, et al. (1994). "Kinetics of the secretory response in bovine chromaffin cells following flash photolysis of caged Ca2+." Biophys J **67**(6): 2546-57.

Henkel, A. W. and W. Almers (1996). "Fast steps in exocytosis and endocytosis studied by capacitance measurements in endocrine cells." Curr Opin Neurobiol **6**(3): 350-7.

Hessler, N. A., A. M. Shirke, et al. (1993). "The probability of transmitter release at a mammalian central synapse." Nature **366**(6455): 569-72.

Horrigan, F. T. and R. J. Bookman (1994). "Releasable pools and the kinetics of exocytosis in adrenal chromaffin cells." Neuron **13**(5): 1119-29.

Hsu, S. F. and M. B. Jackson (1996). "Rapid exocytosis and endocytosis in nerve terminals of the rat posterior pituitary." J Physiol **494 (Pt 2)**: 539-53.

Hu, Z., P. Troyk, et al. (2005). "Comprehensive Cyclic Voltammetry Characterization of AIROF Microelectrodes." Conf Proc IEEE Eng Med Biol Soc **5**: 5246-9.

Iwasaki, S., M. Kataoka, et al. (2000). "Two distinct mechanisms underlie the stimulation of neurotransmitter release by phorbol esters in clonal rat pheochromocytoma PC12 cells." J Biochem (Tokyo) **128**(3): 407-14.

Jackson, A. L. and P. S. Linsley (2004). "Noise amidst the silence: off-target effects of siRNAs?" Trends Genet **20**(11): 521-4.

Jahn, R., P. I. Hanson, et al. (1995). "Botulinum and tetanus neurotoxins: emerging tools for the study of membrane fusion." Cold Spring Harb Symp Quant Biol **60**: 329-35.

Jahn, R., T. Lang, et al. (2003). "Membrane fusion." Cell **112**(4): 519-33.

Jaim-Etcheverry, G. and L. M. Zieher (1968). "Electron microscopic cytochemistry of 5-hydroxytryptamine (5-HT) in the beta cells of guinea pig endocrine pancreas." Endocrinology **83**(5): 917-23.

Jensen, M. V., J. W. Joseph, et al. (2006). "Compensatory responses to pyruvate carboxylase suppression in islet beta-cells. Preservation of glucose-stimulated insulin secretion." J Biol Chem **281**(31): 22342-51.

Ji, J., S. Tsuk, et al. (2002). "The 25-kDa synaptosome-associated protein (SNAP-25) binds and inhibits delayed rectifier potassium channels in secretory cells." J Biol Chem **277**(23): 20195-204.

Ji, J., S. N. Yang, et al. (2002). "Modulation of L-type Ca(2+) channels by distinct domains within SNAP-25." Diabetes **51**(5): 1425-36.

Kam, L., W. Shain, et al. (2001). "Axonal outgrowth of hippocampal neurons on micro-scale networks of polylysine-conjugated laminin." Biomaterials **22**(10): 1049-54.

Kang, G. and G. G. Holz (2003). "Amplification of exocytosis by Ca2+-induced Ca2+ release in INS-1 pancreatic beta cells." J Physiol **546**(Pt 1): 175-89.

Kasai, H., H. Takagi, et al. (1996). "Two components of exocytosis and endocytosis in phaeochromocytoma cells studied using caged Ca2+ compounds." J Physiol **494 (Pt 1)**: 53-65.

Kataoka, M., R. Kuwahara, et al. (2000). "Nerve growth factor-induced phosphorylation of SNAP-25 in PC12 cells: a possible involvement in the regulation of SNAP-25 localization." J Neurochem **74**(5): 2058-66.

Kataoka, M., R. Kuwahara, et al. (2006). "Development- and activity-dependent regulation of SNAP-25 phosphorylation in rat brain." Neurosci Lett **407**(3): 258-62.

Katz, B. (1969). "The releaseof neural transmitter substances. ." Liverpool, UK: Liverpool UP.

Kelly, R. B. (1985). "Pathways of protein secretion in eukaryotes." Science **230**(4721): 25-32.

Kennedy, E. D., R. Rizzuto, et al. (1996). "Glucose-stimulated insulin secretion correlates with changes in mitochondrial and cytosolic Ca2+ in aequorin-expressing INS-1 cells." J Clin Invest **98**(11): 2524-38.

Kennedy, R. T., L. Huang, et al. (1993). "Amperometric monitoring of chemical secretions from individual pancreatic beta-cells." Anal Chem **65**(14): 1882-7.

Kennelly, P. J. and E. G. Krebs (1991). "Consensus sequences as substrate specificity determinants for protein kinases and protein phosphatases." J Biol Chem **266**(24): 15555-8.

Klyachko, V. A. and M. B. Jackson (2002). "Capacitance steps and fusion pores of small and large-dense-core vesicles in nerve terminals." Nature **418**(6893): 89-92.

Kullmann, D. M. and S. A. Siegelbaum (1995). "The site of expression of NMDA receptor-dependent LTP: new fuel for an old fire." Neuron **15**(5): 997-1002.

Lando, L. and R. S. Zucker (1994). "Ca2+ cooperativity in neurosecretion measured using photolabile Ca2+ chelators." J Neurophysiol **72**(2): 825-30.

Lawrence, G. W., P. Foran, et al. (1996). "Distinct exocytotic responses of intact and permeabilised chromaffin cells after cleavage of the 25-kDa synaptosomal-associated protein (SNAP-25) or synaptobrevin by botulinum toxin A or B." Eur J Biochem **236**(3): 877-86.

Lawrence, G. W., P. Foran, et al. (1997). "Importance of two adjacent C-terminal sequences of SNAP-25 in exocytosis from intact and permeabilized

chromaffin cells revealed by inhibition with botulinum neurotoxins A and E." Biochemistry **36**(11): 3061-7.

Leszczyszyn, D. J., J. A. Jankowski, et al. (1991). "Secretion of catecholamines from individual adrenal medullary chromaffin cells." J Neurochem **56**(6): 1855-63.

Lin, R. C. and R. H. Scheller (1997). "Structural organization of the synaptic exocytosis core complex." Neuron **19**(5): 1087-94.

Lin, R. C. and R. H. Scheller (2000). "Mechanisms of synaptic vesicle exocytosis." Annu Rev Cell Dev Biol **16**: 19-49.

Link, E., J. Blasi, et al. (1994). "Tetanus and botulinal neurotoxins. Tools to understand exocytosis in neurons." Adv Second Messenger Phosphoprotein Res **29**: 47-58.

Link, E., L. Edelmann, et al. (1992). "Tetanus toxin action: inhibition of neurotransmitter release linked to synaptobrevin proteolysis." Biochem Biophys Res Commun **189**(2): 1017-23.

Liu, Q. Y., M. Coulombe, et al. (2000). "Synaptic connectivity in hippocampal neuronal networks cultured on micropatterned surfaces." Brain Res Dev Brain Res **120**(2): 223-31.

MacDonald, P. E., G. Wang, et al. (2002). "Synaptosome-associated protein of 25 kilodaltons modulates Kv2.1 voltage-dependent K(+) channels in neuroendocrine islet beta-cells through an interaction with the channel N terminus." Mol Endocrinol **16**(11): 2452-61.

Maechler, P., E. D. Kennedy, et al. (1999). "Secretagogues modulate the calcium concentration in the endoplasmic reticulum of insulin-secreting cells. Studies in aequorin-expressing intact and permeabilized ins-1 cells." J Biol Chem **274**(18): 12583-92.

Maertell, A. E. and R. H. Smith (1974-1989). "Critical Stability Constants." Plenum Press **Vol.1-6**.

Malenka, R. C., D. V. Madison, et al. (1986). "Phorbol esters mimic some cholinergic actions in hippocampal pyramidal neurons." J Neurosci **6**(2): 475-80.

Malinow, R., D. V. Madison, et al. (1988). "Persistent protein kinase activity underlying long-term potentiation." Nature **335**(6193): 820-4.

Mennerick, S. and G. Matthews (1996). "Ultrafast exocytosis elicited by calcium current in synaptic terminals of retinal bipolar neurons." Neuron **17**(6): 1241-9.

Mennerick, S., J. Que, et al. (1995). "Passive and synaptic properties of hippocampal neurons grown in microcultures and in mass cultures." J Neurophysiol **73**(1): 320-32.

Mollard, P., E. P. Seward, et al. (1995). "Activation of nicotinic receptors triggers exocytosis from bovine chromaffin cells in the absence of membrane depolarization." Proc Natl Acad Sci U S A **92**(7): 3065-9.

Morgan, A., R. D. Burgoyne, et al. (2005). "Regulation of exocytosis by protein kinase C." Biochem Soc Trans **33**(Pt 6): 1341-4.

Moser, T. and E. Neher (1997). "Rapid exocytosis in single chromaffin cells recorded from mouse adrenal slices." J Neurosci **17**(7): 2314-23.

Muller, D., J. Turnbull, et al. (1988). "Phorbol ester-induced synaptic facilitation is different than long-term potentiation." Proc Natl Acad Sci U S A **85**(18): 6997-7000.

Murthy, V. N., T. J. Sejnowski, et al. (1997). "Heterogeneous release properties of visualized individual hippocampal synapses." Neuron **18**(4): 599-612.

Nagy, G., U. Matti, et al. (2002). "Protein kinase C-dependent phosphorylation of synaptosome-associated protein of 25 kDa at Ser187 potentiates vesicle recruitment." J Neurosci **22**(21): 9278-86.

Neher, E. (1992). "Ion channels for communication between and within cells." Science **256**(5056): 498-502.

Neher, E. (1998). "Vesicle pools and Ca2+ microdomains: new tools for understanding their roles in neurotransmitter release." Neuron **20**(3): 389-99.

Neher, E. and A. Marty (1982). "Discrete changes of cell membrane capacitance observed under conditions of enhanced secretion in bovine adrenal chromaffin cells." Proc Natl Acad Sci U S A **79**(21): 6712-6.

Neher, E. and B. Sakmann (1976). "Single-channel currents recorded from membrane of denervated frog muscle fibres." Nature **260**(5554): 799-802.

Neher, E., B. Sakmann, et al. (1978). "The extracellular patch clamp: a method for resolving currents through individual open channels in biological membranes." Pflugers Arch **375**(2): 219-28.

Neher, E. and R. S. Zucker (1993). "Multiple calcium-dependent processes related to secretion in bovine chromaffin cells." Neuron **10**(1): 21-30.

Newton, A. C. (1995). "Protein kinase C: structure, function, and regulation." J Biol Chem **270**(48): 28495-8.

Nicoletta, J. A., J. J. Ross, et al. (2004). "Munc-18-2 regulates exocytosis of H(+)-ATPase in rat inner medullary collecting duct cells." Am J Physiol Cell Physiol **287**(5): C1366-74.

Nicoll, R. A. and R. C. Malenka (1995). "Contrasting properties of two forms of long-term potentiation in the hippocampus." Nature **377**(6545): 115-8.

Ninomiya, Y., T. Kishimoto, et al. (1997). "Kinetic diversity in the fusion of exocytotic vesicles." Embo J **16**(5): 929-34.

Nishiki, T. and G. J. Augustine (2004). "Dual roles of the C2B domain of synaptotagmin I in synchronizing Ca2+-dependent neurotransmitter release." J Neurosci **24**(39): 8542-50.

Nishiki, T. and G. J. Augustine (2004). "Synaptotagmin I synchronizes transmitter release in mouse hippocampal neurons." J Neurosci **24**(27): 6127-32.

Nishizuka, Y. (1992). "Intracellular signaling by hydrolysis of phospholipids and activation of protein kinase C." Science **258**(5082): 607-14.

Nishizuka, Y. (1995). "Protein kinase C and lipid signaling for sustained cellular responses." Faseb J **9**(7): 484-96.

Oberhauser, A. F., I. M. Robinson, et al. (1996). "Simultaneous capacitance and amperometric measurements of exocytosis: a comparison." Biophys J **71**(2): 1131-9.

Osen-Sand, A., M. Catsicas, et al. (1993). "Inhibition of axonal growth by SNAP-25 antisense oligonucleotides in vitro and in vivo." Nature **364**(6436): 445-8.

Parfitt, K. D. and D. V. Madison (1993). "Phorbol esters enhance synaptic transmission by a presynaptic, calcium-dependent mechanism in rat hippocampus." J Physiol **471**: 245-68.

Pellizzari, R., O. Rossetto, et al. (1999). "Tetanus and botulinum neurotoxins: mechanism of action and therapeutic uses." Philos Trans R Soc Lond B Biol Sci **354**(1381): 259-68.

Pich, E. M. and M. P. Epping-Jordan (1998). "Transgenic mice in drug dependence research." Ann Med **30**(4): 390-6.

Pumplin, D. W., T. S. Reese, et al. (1981). "Are the presynaptic membrane particles the calcium channels?" Proc Natl Acad Sci U S A **78**(11): 7210-3.

Pusch, M. and E. Neher (1988). "Rates of diffusional exchange between small cells and a measuring patch pipette." Pflugers Arch **411**(2): 204-11.

Rettig, J., C. Heinemann, et al. (1997). "Alteration of Ca2+ dependence of neurotransmitter release by disruption of Ca2+ channel/syntaxin interaction." J Neurosci **17**(17): 6647-56.

Rettig, J. and E. Neher (2002). "Emerging roles of presynaptic proteins in Ca++-triggered exocytosis." Science **298**(5594): 781-5.

Rhee, J. S., A. Betz, et al. (2002). "Beta phorbol ester- and diacylglycerol-induced augmentation of transmitter release is mediated by Munc13s and not by PKCs." Cell **108**(1): 121-33.

Rizzoli, S. O. and W. J. Betz (2005). "Synaptic vesicle pools." Nat Rev Neurosci **6**(1): 57-69.

Roberts, W. M., R. A. Jacobs, et al. (1990). "Colocalization of ion channels involved in frequency selectivity and synaptic transmission at presynaptic active zones of hair cells." J Neurosci **10**(11): 3664-84.

Robitaille, R., E. M. Adler, et al. (1990). "Strategic location of calcium channels at transmitter release sites of frog neuromuscular synapses." Neuron **5**(6): 773-9.

Rosenmund, C., J. D. Clements, et al. (1993). "Nonuniform probability of glutamate release at a hippocampal synapse." Science **262**(5134): 754-7.

Sadoul, K., A. Berger, et al. (1997). "SNAP-23 is not cleaved by botulinum neurotoxin E and can replace SNAP-25 in the process of insulin secretion." J Biol Chem **272**(52): 33023-7.

Sakmann, B. (1992). "Elementary steps in synaptic transmission revealed by currents through single ion channels." Science **256**(5056): 503-12.

Scheenen, W. J., C. B. Wollheim, et al. (1998). "Ca2+ depletion from granules inhibits exocytosis. A study with insulin-secreting cells." J Biol Chem **273**(30): 19002-8.

Schiavo, G., F. Benfenati, et al. (1992). "Tetanus and botulinum-B neurotoxins block neurotransmitter release by proteolytic cleavage of synaptobrevin." Nature **359**(6398): 832-5.

Schiavo, G., C. Malizio, et al. (1994). "Botulinum G neurotoxin cleaves VAMP/synaptobrevin at a single Ala-Ala peptide bond." J Biol Chem **269**(32): 20213-6.

Schiavo, G., O. Rossetto, et al. (1993). "Identification of the nerve terminal targets of botulinum neurotoxin serotypes A, D, and E." J Biol Chem **268**(32): 23784-7.

Schiavo, G., C. C. Shone, et al. (1995). "Botulinum neurotoxin type C cleaves a single Lys-Ala bond within the carboxyl-terminal region of syntaxins." J Biol Chem **270**(18): 10566-70.

Schiavo, G., C. C. Shone, et al. (1993). "Botulinum neurotoxin serotype F is a zinc endopeptidase specific for VAMP/synaptobrevin." J Biol Chem **268**(16): 11516-9.

Schulte, M. and R. H. Chow (1996). "A simple method for insulating carbon-fiber microelectrodes using anodic electrophoretic deposition of paint." Anal Chem **68**: 3054-3058.

Shimazaki, Y., T. Nishiki, et al. (1996). "Phosphorylation of 25-kDa synaptosome-associated protein. Possible involvement in protein kinase C-mediated regulation of neurotransmitter release." J Biol Chem **271**(24): 14548-53.

Shoji-Kasai, Y., M. Itakura, et al. (2002). "Protein kinase C-mediated translocation of secretory vesicles to plasma membrane and enhancement of neurotransmitter release from PC12 cells." Eur J Neurosci **15**(8): 1390-4.

Sigworth, F. J. and E. Neher (1980). "Single Na+ channel currents observed in cultured rat muscle cells." Nature **287**(5781): 447-9.

Silinsky, E. M. and T. J. Searl (2003). "Phorbol esters and neurotransmitter release: more than just protein kinase C?" Br J Pharmacol **138**(7): 1191-201.

Smith, C., T. Moser, et al. (1998). "Cytosolic Ca2+ acts by two separate pathways to modulate the supply of release-competent vesicles in chromaffin cells." Neuron **20**(6): 1243-53.

Smith, C. and E. Neher (1997). "Multiple forms of endocytosis in bovine adrenal chromaffin cells." J Cell Biol **139**(4): 885-94.

Smith, P. A., M. R. Duchen, et al. (1995). "A fluorimetric and amperometric study of calcium and secretion in isolated mouse pancreatic beta-cells." Pflugers Arch **430**(5): 808-18.

Sollner, T., M. K. Bennett, et al. (1993). "A protein assembly-disassembly pathway in vitro that may correspond to sequential steps of synaptic vesicle docking, activation, and fusion." Cell **75**(3): 409-18.

Sollner, T., S. W. Whiteheart, et al. (1993). "SNAP receptors implicated in vesicle targeting and fusion." Nature **362**(6418): 318-24.

Sollner, T. H. (2003). "Regulated exocytosis and SNARE function (Review)." Mol Membr Biol **20**(3): 209-20.

Sorensen, J. B., U. Matti, et al. (2002). "The SNARE protein SNAP-25 is linked to fast calcium triggering of exocytosis." Proc Natl Acad Sci U S A **99**(3): 1627-32.

Sorensen, J. B., G. Nagy, et al. (2003). "Differential control of the releasable vesicle pools by SNAP-25 splice variants and SNAP-23." Cell **114**(1): 75-86.

Stevens, C. F. (2003). "Neurotransmitter release at central synapses." Neuron **40**(2): 381-8.

Stevens, C. F. and J. M. Sullivan (1998). "Regulation of the readily releasable vesicle pool by protein kinase C." Neuron **21**(4): 885-93.

Sutton, R. B., D. Fasshauer, et al. (1998). "Crystal structure of a SNARE complex involved in synaptic exocytosis at 2.4 A resolution." Nature **395**(6700): 347-53.

Takahashi, N., T. Kadowaki, et al. (1997). "Multiple exocytotic pathways in pancreatic beta cells." J Cell Biol **138**(1): 55-64.

Thomas-Reetz, A. C. and P. De Camilli (1994). "A role for synaptic vesicles in non-neuronal cells: clues from pancreatic beta cells and from chromaffin cells." Faseb J **8**(2): 209-16.

Thomas, P., J. G. Wong, et al. (1993). "A low affinity Ca2+ receptor controls the final steps in peptide secretion from pituitary melanotrophs." Neuron **11**(1): 93-104.

Thoreson, W. B., K. Rabl, et al. (2004). "A highly Ca2+-sensitive pool of vesicles contributes to linearity at the rod photoreceptor ribbon synapse." Neuron **42**(4): 595-605.

Tong, G. and C. E. Jahr (1994). "Multivesicular release from excitatory synapses of cultured hippocampal neurons." Neuron **12**(1): 51-9.

Tsuboi, T., C. Zhao, et al. (2000). "Simultaneous evanescent wave imaging of insulin vesicle membrane and cargo during a single exocytotic event." Curr Biol **10**(20): 1307-10.

Voets, T. (2000). "Dissection of three Ca2+-dependent steps leading to secretion in chromaffin cells from mouse adrenal slices." Neuron **28**(2): 537-45.

Voets, T., E. Neher, et al. (1999). "Mechanisms underlying phasic and sustained secretion in chromaffin cells from mouse adrenal slices." Neuron **23**(3): 607-15.

Vogel, K. and P. A. Roche (1999). "SNAP-23 and SNAP-25 are palmitoylated in vivo." Biochem Biophys Res Commun **258**(2): 407-10.

Vogt, A. K., L. Lauer, et al. (2003). "Micropatterned substrates for the growth of functional neuronal networks of defined geometry." Biotechnol Prog **19**(5): 1562-8.

von Ruden, L. and E. Neher (1993). "A Ca-dependent early step in the release of catecholamines from adrenal chromaffin cells." Science **262**(5136): 1061-5.

Walch-Solimena, C., J. Blasi, et al. (1995). "The t-SNAREs syntaxin 1 and SNAP-25 are present on organelles that participate in synaptic vesicle recycling." J Cell Biol **128**(4): 637-45.

Wan, Q. F., Y. Dong, et al. (2004). "Protein kinase activation increases insulin secretion by sensitizing the secretory machinery to Ca2+." J Gen Physiol **124**(6): 653-62.

Washbourne, P., P. M. Thompson, et al. (2002). "Genetic ablation of the t-SNARE SNAP-25 distinguishes mechanisms of neuroexocytosis." Nat Neurosci **5**(1): 19-26.

Waters, J. and S. J. Smith (2000). "Phorbol esters potentiate evoked and spontaneous release by different presynaptic mechanisms." J Neurosci **20**(21): 7863-70.

Wei, S., T. Xu, et al. (2000). "Exocytotic mechanism studied by truncated and zero layer mutants of the C-terminus of SNAP-25." Embo J **19**(6): 1279-89.

Wiser, O., M. K. Bennett, et al. (1996). "Functional interaction of syntaxin and SNAP-25 with voltage-sensitive L- and N-type Ca2+ channels." Embo J **15**(16): 4100-10.

Wu, X. S. and L. G. Wu (2001). "Protein kinase c increases the apparent affinity of the release machinery to Ca2+ by enhancing the release machinery downstream of the Ca2+ sensor." J Neurosci **21**(20): 7928-36.

Xu, N. J., Y. X. Yu, et al. (2004). "Inhibition of SNAP-25 phosphorylation at Ser187 is involved in chronic morphine-induced down-regulation of SNARE complex formation." J Biol Chem **279**(39): 40601-8.

Yamamoto, C., M. Higashima, et al. (1987). "Quantal analysis of potentiating action of phorbol ester on synaptic transmission in the hippocampus." Neurosci Res **5**(1): 28-38.

Yamasaki, S., T. Binz, et al. (1994). "Botulinum neurotoxin type G proteolyses the Ala81-Ala82 bond of rat synaptobrevin 2." Biochem Biophys Res Commun **200**(2): 829-35.

Yang, H., H. Liu, et al. (2005). "PKC-induced sensitization of Ca2+-dependent exocytosis is mediated by reducing the Ca2+ cooperativity in pituitary gonadotropes." J Gen Physiol **125**(3): 327-34.

Yang, Y., T. J. Craig, et al. (2007). "Phosphomimetic Mutation of Ser-187 of SNAP-25 Increases both Syntaxin Binding and Highly Ca2+-sensitive Exocytosis." J Gen Physiol **129**(3): 233-44.

Yang, Y. and K. D. Gillis (2004). "A highly Ca2+-sensitive pool of granules is regulated by glucose and protein kinases in insulin-secreting INS-1 cells." J Gen Physiol **124**(6): 641-51.

Yang, Y., S. Udayasankar, et al. (2002). "A highly Ca2+-sensitive pool of vesicles is regulated by protein kinase C in adrenal chromaffin cells." Proc Natl Acad Sci U S A **99**(26): 17060-5.

Yao, Y., A. V. Ferrer-Montiel, et al. (1999). "Activation of store-operated Ca2+ current in Xenopus oocytes requires SNAP-25 but not a diffusible messenger." Cell **98**(4): 475-85.

Zhou, Z. and S. Misler (1996). "Amperometric detection of quantal secretion from patch-clamped rat pancreatic beta-cells." J Biol Chem **271**(1): 270-7.

Zucker, R. S. (1996). "Exocytosis: a molecular and physiological perspective." Neuron **17**(6): 1049-55.

VITA

Yilong Shu was born on April 22, 1977 in Nanchong of Sichuan Province (China). In 1994, he attended Beijing Normal University, the ranked No.1# normal university in China. In 1998, he received his B.S. in biology. After the graduation, he got a faculty position in Beijing Union University and worked there for three years. He joined Interdisciplinary Neuroscience Program (INP) at University of Missouri-Columbia in 2001 and received his Ph.D in neuroscience in May 2007 from Dr. Kevin D. Gillis' laboratory. He will continue his training as a post-doctoral fellow in Dr. Philip Haydon's laboratory in Department of Neuroscience at University of Pennsylvania.

The dissertation was typed by the author.